CLONOTYPIC ANALYSIS OF CMV-SPECIFIC $CD4^+$ T CELLS IN HUMAN AND NONHUMAN PRIMATES

APPROVED BY SUPERVISORY COMMITTEE

_____

Louis J. Picker, M.D., Advisor

_____

Jerry Y. Niederkorn, Ph.D., Chairman

_____

Ellen S. Vitetta, Ph.D.

_____

Nicolai S. C. van Oers, Ph.D.

_____

Richard A. Koup, M.D.

DEDICATION

To
the love and grace of God
that has given me the strength to endure and overcome all the challenges.

And to
my mother and brother, Elda L. Sargon and Andrew Bitmansour
whose love, support, and encouragement made this possible.

ACKNOWLEDGEMENTS

I would like to thank my mentor, Dr. Louis J. Picker, for giving me the opportunity to work in his lab. I am also grateful to learn from Louis because of his knowledge, insight, and brilliant interpretation of data. Thanks for giving me the chance to work on a dissertation project that I found interesting throughout my training.

I would like to express my gratitude to the members of my committee, Drs. Jerry Y. Niederkorn, Ellen S. Vitetta, Nicolai S. C. van Oers, and Richard A. Koup. Your support and guidance have been crucial to the achievement of my educational goals. I am grateful to Dr. Niederkorn for chairing my committee, for his complete support, and for dealing with all of the challenges of an off-campus student. Jerry thanks for always listening and giving me great advice. I would like to thank Dr. van Oers for always challenging me. Nicolai, your questions helped me improve as a scientist and improved my Dissertation. Dr. Koup, thank you for taking the time to come to Dallas to serve on my committee. Rick, your criticism, when I rotated in your lab and as my committee member, has been constructive, compassionate, and appreciated. I am especially indebted to Dr. Vitetta for mentoring me as one of her own students. Dr. Vitetta's advice, support, and care have been crucial in the completion of my journey as a scientist-in-training. Ellen, you answered when I needed a wise and objective advisor. You mediated when I thought the end had come. And finally, you helped me

significantly improve my presentation slides and my Dissertation. I have learned so much from you and am eternally grateful to you. You truly are an amazing mentor.

I am also grateful to Dr. Daniel C. Douek for training me first as a rotation student and then all the way through my graduate career. The hands-on and long distance training that I received from Danny were crucial to my success in my graduate training. Danny, because of you I have learned to produce amazing data with sometimes so very little mRNA, I have textbook standard curves for my TaqMan data, and brilliant sequencing results. Thanks for sharing all of your novel protocols with me and teaching me how to analyze my data.

From UTSW, I would like to thank, Drs. Jennifer L. Klem, Richard H. Scheuermann, and John D. Schatzle. Jennifer, thank you for your tremendous support starting with the Core Course, the second year Immunology Course, Qualifying Exams, every WIPS, and finally my Defense. You have been a friend, a rock, an advisor, a shoulder to cry on, and a kindred spirit. Thanks from the bottom of my heart. To Rich and John, thanks for teaching me the art and science of PCR and cloning so well.

From VGTI, I would like to thank Dr. Michael K. Axthelm, Kristi, Buxton, Dr. Scott G. Hansen, Dr. Ilhem Messaoudi, Dr. Mark K, Slifka, Dr. Andrew Sylwester, Dr. Stanley M. Shiigi, Dr. Dan Cawley, J. M. Walker, J. B. Edgar, Andrew Townsend, Lori Boshears, and Joanne G, Strussenberg. Mike

thanks for being a brilliant vet and scientist, without you the RM cohort would not exist. Kristi thanks for the brilliant viral load data and most importantly your friendship. Scott thanks from the bottom of my heart for your friendship, your advice both scientific and other, for reading my Dissertation, and giving me helpful critique on both my Dissertation and Seminar. Ilhem, thanks for taking the time and helping me with Introduction, Discussion, and Seminar. Your brilliant advice helped me improve my Dissertation and Seminar significantly. I would like to thank Andy for reading my Introduction and for helping me with numerous seminars. Your questions and comments really helped me improve and grow as a scientist. I would like to thank Stan for performing all of the endless cell sorting. Dan thanks for all of your helpful advice and comments on my Introduction. Josh and John, thanks for processing the cells at each time-point and for monitoring the CD4+ T cell responses to CMV. Andrew thanks for helping me with figures, you are a graphics wiz and I am grateful for all of the work that you did for my posters, papers, seminars, and dissertation. Lori thanks for being a wonderful administrator in everyway, from editing my Dissertation to organizing my travel to Dallas every year, and all of the ordering and countless other details that you took care of and made it seem effortless. Last but not least, thank you Joanne for always helping with random equipments and keeping everything in top form. Most of all, thanks for your friendship, all of the fun lunches, and letting me vent in your office.

I would also like to thanks my life-long friend whom I love dearly: Fedra O. Shahbaz, Kathleen Martin, Marlene Bernanrd, PHARM.D., Rhea Ann Dandeneeau, M.S.W., Gavin MacMillan, Melinda Fagan, Ph.D., Jennifer L. Klem, Ph.D., and Paula Harkin. Fedra, I have known you the longest, 25 years. You are my best friend whom I love as dearly as my sister. You are faithful and strong. Your compassion is endless. Your advice is well reasoned and you bestow it with love. Your faith is an awesome witness to God's goodness. I am so blessed to have a friend in you. Kathy, you and I became fast friends in our senior year at Blackford High. How thankful I am to count you among my friends. I love your sense of humor, your passion for the truth, and your love for life. Thanks for your support when I have been down. I know I can always count on you. Marlene and Rhea Ann, my Delta Gamma sisters and more importantly my good friends, since pledging together we gravitated to each other. Our friendship was meant to be. Thanks for all of the fun times at Dee Gee, for the dinners, the study times, the shopping, the get togethers, and your long distance support as I traveled this long and lonely road in my graduate program, miles away from my dear family and friends. How I cherished coming home for Christmas and how I couldn't wait to see you two at our regular dinner hangout, Florentines. Thanks for blessing me with your friendship. Gavin, my favorite Sigma Chi, and my good friend, I have admired your strength, character, and reason. Thank you for keeping me grounded with your sound advice and

extending me your compassion when I needed it the most. Melinda, when I met you, you were a senior graduate student in the Weissman lab when I was about to begin my journey as a graduate student. I have commiserated with you and have relied on your advice through these tough years. Thanks for being my friend, understanding, and cheering me on. Jennifer my dear friend, you and I started our graduate school journey together and from the first day I saw your friendly face I knew we would be friends for life. I am so blessed to call you friend, My dear friend Paula, since the first day I met you at PRC I saw a kindred spirit in you. You impressed me with your confidence, your joy for life, and your uncomplicated friendliness. You have been a steadfast friend, loyal, loving, and supportive. Thanks for all of the heart-to-hearts, the soul cleansing runs, and the much-needed post-run social gatherings. Thank you for being my friend.

Mom and Andrew, you are my family and my best friends. Words cannot describe how much I appreciate you both. You have been supportive in every way possible. Thank you for all of your help, financially and spiritually. Thank you for your love and gentle advice. Thank you for being my rock when I felt weak. Thank you for cheering me on when I felt depleted. Thank you for crying with me, laughing with me, and celebrating with me. I am so blessed to have you as not only my mom and brother, but also as my best friends. Thank you from the bottom of my heart.

CLONOTYPIC ANALYSIS OF CMV-SPECIFIC $CD4^+$ T CELLS IN HUMAN AND NONHUMAN PRIMATES

by

ARLENE DIANA BITMANSOUR

DISSERTATION

Presented to the Faculty of the Graduate School of Biomedical Sciences

The University of Texas Southwestern Medical Center at Dallas

In Partial Fulfillment of the Requirements

For the Degree of

DOCTOR OF PHILOSOPHY

The University of Texas Southwestern Medical Center at Dallas

Dallas, Texas

February, 2005

CLONOTYPIC ANALYSIS OF CMV-SPECIFIC $CD4^+$ T CELLS IN HUMAN AND NONHUMAN PRIMATES

Publication No. _____

Arlene Diana Bitmansour, Ph.D.

The University of Texas Southwestern Medical Center at Dallas, 2005

Supervising Professor: Louis J. Picker, M.D.

Cytomegalovirus (CMV) is a complex pathogen with the ability to persist in a host via mechanisms of immune evasion. CD4+ T cells are known to play a role in maintaining life-long immunity against CMV; however, the cellular requirements for establishing and maintaining protection against CMV disease have not been characterized. The objective of this work was to understand the nature of a protective CD4+ T cell memory response in primates using CMV as a model viral pathogen. First, we characterized the clonotypic hierarchy of an established CMV-specific $CD4^+$ memory T cell response in human subjects and Rhesus macaques (RM). In both we found that long-term $CD4^+$ memory responses to CMV are characterized by highly skewed clonotypic hierarchies, and these hierarchies remained stable over the months examined. We then used the RM model to elucidate the evolution of the CMV-specific $CD4^+$ clonotypic hierarchy during and after primary infection. The clonotypic composition of an

emerging CMV-specific response during a primary infection was strikingly diverse. Third, we reinfected the RM and found that reinfection with CMV recruited new clonotypes into the response, further increasing clonotypic complexity. Taken together, these data indicate the CMV-specific $CD4^+$ T cell response undergoes an evolution during primary and secondary infection and includes the generation of a large initial repertoire, followed by selection of a few dominant clonotypes. In chronic infection, stable oligoclonal hierarchies predominate, suggesting that long-term surveillance for CMV reactivation or reinfection is mediated by a small number of clones, which are maintained at higher frequency. Having found these large single clonotype responses to CMV, we examined T cell receptor (TCR) activation requirements at the level of single clonotypes. We found that single clonotypes have heterogeneous activation thresholds and the activation thresholds for elaborating IL-2 and IFN-γ differed. Finally, we found that the threshold heterogeneity within a clonotype was independent of CD27 expression.

TABLE OF CONTENTS

PUBLICATIONS

Bitmansour, A.D., S. Waldrop, C. Pitcher, E. Khatamzas, F. Kern, V. Maino, and L.J. Picker. 2001. Clonotypic structure of the human $CD4^+$ memory T cell response to cytomegalovirus. *J. Immunol.* 167:1151-1163.

Bitmansour, A.D., D.C. Douek, V.C. Maino, and L.J. Picker. 2002. Direct *ex vivo* analysis of human $CD4^+$ memory T cell activation requirements at the single clonotype level. *J. Immunol.* 169:1207-1218.

FIGURES

ABBREVIATIONS

α	alpha, TCR chain
A	alpha, TCR gene
aa	amino acid
Ag	antigen
AICD	activation induced cell death
APC	antigen presenting cells
AV	TCR alpha variable gene
β	beta, TCR protein chain
B	beta, TCR gene
BMT	bone marrow transplant
BSA	bovine serum albumin
BV	TCR beta variable gene
CCL	constitutive chemokine ligand
CCR	constitutive chemokine receptor
CD25	the alpha chain of the IL-2 receptor
CD62L	L-selectin
CDR	complementarity determining region
CFC	cytokine flow cytometry
CLA	cutaneous lymphocyte-associated antigen

CLP	common lymphocyte progenitor
CMV	cytomegalovirus
CTL	cytotoxic T lymphocytes
D	diversity, gene of TCR
DC	dendritic cells
dPBS	Dulbecco's phosphate buffered saline
EBV	Epstein-Barr virus
EOD	end organ disease
ER	endoplasmic reticulum
EXO-SAP	exonuclease-shrimp alkaline phosphatase
FACS	fluorescence-activated cell sorting
FAM	6-carboxy-fluorescein
FCS	fetal calf serum
FITC	fluorescein isothiocyanate
GB	glycoprotein B
HBSS	Hank's balanced salt solution
HCMV	human cytomegalovirus
HEV	high endothelial venules
HIV	human immunodeficiency virus
HPLC	high-performance liquid chromatography
IFN-γ	interferon-gamma

IL	interleukin
IM	infectious mononucleosis
iNOS	inducible nitric oxide synthase
IPTG	isopropylthio-β-galactoside
J	joining, gene of TCR
L	ligand
LB	Lennox broth
LCMV	lymphocytic choriomeningitis virus
LDA	limiting dilution analysis
MAb	monoclonal antibodies
MAdCAM-1	mucosal cell adhesion molecule-1
MCMV	murine cytomegalovirus
NK cells	natural killer cells
MHC	major histocompatibility complex
PBMC	peripheral blood mononuclear cells
PCC	pigeon cytochrome C
PCR	polymerase chain reaction
PE	phycoerythrin
PerCP	peridinin chlorophyll protein
pi	post infection
PNAd	peripheral lymph node vascular addressin

R	receptor
RACE	rapid amplification of cDNA ends
RCMV	rat cytomegalovirus
RhCMV	Rhesus cytomegalovirus
RM	Rhesus macaque
RT-PCR	reverse transcription-polymerase chain reaction
SA	superantigens
SAIDS	simian acquired immunodeficiency syndrome
SIV	simian immunodeficiency virus
SMART	switching mechanism at 5' end of RNA transcript
TAMRA	6-carboxy-teramethyl-rhodamine
TAP	transporter associated with antigen processing
TAT	tunable activation threshold
TCR	T cell receptor
TdT	terminal deoxynucleotidyl transferase
TNF-α	tumor necrosis factor-alpha
V	variability, gene of TCR

INTRODUCTION

$CD4^+$ T cells play a critical role in immunologic protection against chronic viral pathogens. Our objective was to understand the composition of a protective $CD4^+$ T cell memory response in primates using cytomegalovirus (CMV) as a model viral pathogen. We sought to characterize the most fundamental unit of $CD4^+$ T cell immunity, the TCR-defined clonotype, because we hypothesized that immunologic protection could be defined by the number, frequency, and function of these fundamental units. Therefore, we isolated CMV-responsive $CD4^+$ memory T cells and characterized the clonotypes by examining their number, relative frequency, and activation threshold requirements.

I. T CELL DEVELOPMENT AND REPERTOIRE DIVERSITY

The adaptive arm of the immune system is composed of B and T lymphocytes, which are derived from hematopoietic stem cells (1, 2). In the bone marrow, the common lymphocyte progenitor (CLP) is thought to differentiate into pro-B cells. In contrast, the CLPs that reach the thymus differentiate into T cells. At first, these immature T cells in the thymus lack expression of CD3 (TCR complex), CD4 and CD8 (TCR co-receptors), and are referred to as double-negative T cells. The double-negative T cells differentiate into double-positive T

cells expressing CD3, CD4, and CD8. The double-positive T cells undergo positive selection for major histocompatibility complex (MHC) antigens. Double-positive T cells that do not recognize self-MHC are eliminated. After positive selection on class II or class I antigens, the double-positive T cells lose expression of one of the co-receptors, CD8 or CD4 accordingly, and proceed to negative selection, which eliminates T cells that have a high affinity for self-peptides complexed with self-MHC. The single-positive T cells express CD4 co-receptors, which recognize MHC class II molecules or CD8 co-receptors, which recognize MHC class I molecules. Upon completion of their development program, "naïve", single-positive T cells leave the thymic medulla and enter the peripheral circulation and home to lymphoid tissue (3).

The vertebrate immune system is armed with a diverse TCR repertoire that enables it to mount a response to an array of pathogens. TCR diversity is defined by the hypervariable region of the complementarity determining region (CDR)3. The TCR is a heterodimer comprised of an alpha (α) and beta (β) chain. Each chain has 3 CDR loops known as CDR1, CDR2, and CDR3. The CDR1 and CDR2 loops are encoded in the germline variability (V) segments for the alpha (*A*) and beta (*B*) genes. The center of the antigen-binding site is the CDR3 loop and 3 germline encoded genes, V, diversity (D), and joining (J) contribute to this hypervariable loop. In the beta chain and only 2 germline encoded genes, V and J, contribute to the alpha chain CDR3 loop. The CDR3 is hypervariable due to

the process involved in somatic gene rearrangement (Figure 1). The beta locus rearranges first. One of the two D genes rearranges to join with one of the 13 J genes. This is followed by a joining of one of the ~52 V genes to the rearranged DJ gene. The rearranging process involves N-nucleotide additions by terminal deoxynucleotidyl transferase (TdT) that contributes to additional junctional diversity in the CDR3 loop. Following a productive rearrangement, allelic exclusion ensues so that only one parental beta VDJ gene is rearranged per T cell. The alpha genes then rearrange such that a V to J gene joins to form the rearranged alpha gene. However, since allelic exclusion is "leaky" for the alpha locus, it is possible for a single cell to rearrange the alpha genes on both alleles and express mRNA as well as protein from both rearranged alpha genes (3-6). Because of the □□□□ locus allelic exclusion, T cell repertoire complexity is measured by analyzing the TCR β repertoire complexity based on the CDR3 size heterogeneity within *BV* gene families (7). A TCR-defined clonotype is a clone of $CD4^+$ or $CD8^+$ T cells that express the same TCR and is usually defined by analyzing the TCR *BV* gene sequences.

FIGURE 1. T cell receptor α- and β- chain gene rearrangement

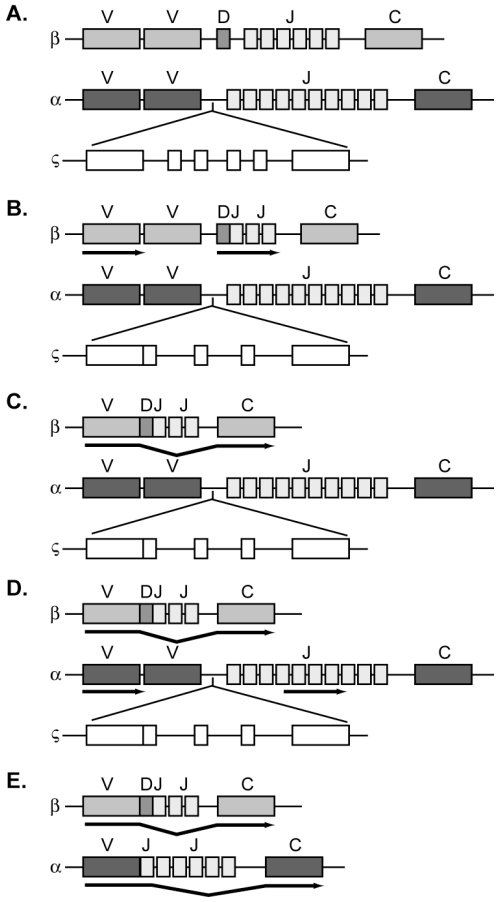

The TCR is a heterodimer comprised of an α and β chain. Each chain has 3 CDR loops known as CDR1, CDR2, and CDR3. The CDR1 and CDR2 loops are encoded in the germline V segments for the α and β chains. The center of the antigen-binding site is the CDR3 loop and 3 germline encoded genes, V, D, and J contribute to this hypervariable loop in the β chain and only 2 germline encoded genes,V and J, contribute to the α chain CDR3 loop. The β chain genes rearrange first. One of the two D genes rearranges to join with one of the 13 J genes **(B)**. This is followed by a joining of one of the ~52 V genes to the rearranged DJ gene **(C)**. The rearranging process involves N-nucleotide additions by terminal deoxynucleotidyl transferase (TdT) that contributes to additional junctional diversity in the CDR3 loop. Following a productive rearrangement, allelic exclusion ensues so that only one β VDJ gene is rearranged per T cell. The α genes then rearrange such that a V to J gene joins to form the rearranged α chain gene **(E)**. Figure modified from *Immunobiology* (3).

The diversity of the T cell repertoire depends upon the TCR structural diversity as well as the functional diversity of the T cells. TCR structural diversity is a result of gene rearrangement, whereas functional diversity is the result of differentiation and maturation of the T cell that begins during positive and negative selection in the thymus and continues in the lymph node as the naïve T cell encounters its cognate antigen in the context of self-MHC (4). Each event in which a T cell samples peptide/MHC complex is influential in shaping the functional characteristic of that T cell.

II. IMMUNODOMINANCE

The recognition of antigens by T cells is dependent upon the TCR. The TCR of $CD8^+$ recognize antigenic ligands of 8-12 amino acids and the TCR of $CD4^+$ T cells recognize antigenic ligands of 12-20 amino acids in the clefts of MHC class I and class II molecules, respectively. The TCR binds to its cognate ligand complexed with self-MHC. The TCR is the product of gene rearrangement, which produces receptors with different ligand-binding sites (3, 8). T cell response complexity can be attributed to epitope complexity and/or clonotypic complexity. Epitope complexity refers to the number of epitopes derived from a pathogen that elicit a T cell response whereas clonotypic

complexity is the number of T cells expressing different TCRs that respond to the same and/or different epitope(s) derived from a pathogen.

The epitope complexity of the T cell response has been studied most extensively in the $CD8^+$ T cell lineage. In a variety of systems it has been shown that virus-specific $CD8^+$ T cells are characterized by immunodominance (9-11), the focusing of the T cell response to a small proportion of the potential immunogenic epitopes on a complex pathogen (12). Some epitopes from a complex pathogen may elicit T cell responses while other potential epitopes from the same pathogen are silent. It is thought that epitope processing, peptide fit into available MHC, and the TCR repertoire contribute to immunodominance (12).

A TCR-defined clonotype is a clone of $CD4^+$ or $CD8^+$ T cells that expresses the same TCR. Therefore, clonotypic complexity refers to the number of TCR-defined clones that respond to a particular pathogen. Pathogen-responsive clonotypes are a cohort of T cells that encompass high, medium, and/or low frequency clonotypes that together comprise a hierarchy of specific T cells that respond to a particular pathogen.

The clonotypic composition and hierarchies of virus-specific T cells have been extensively examined for $CD8^+$ T cells, primarily in the mouse, utilizing T cell lines and clones. The conclusions regarding the clonality of virus-specific $CD8^+$ T cells from these studies varied from being focused and oligoclonal to diverse and polyclonal (10, 11, 13-17). However, because these studies used *in*

vitro-expanded T cell clones or lines, they cannot reliably reflect the physiologic relative frequencies of virus-specific T cells. In contrast, *ex vivo* studies using MHC class I tetramer$^+$ cells have revealed that a small number of virus-specific T cell clones are present at high frequencies and increasing numbers of clones are present at lower and lower frequencies (18-20). Some studies have compared the clonotypic structure of primary vs. secondary T cell responses. Maryanski *et al*. did not find any difference between primary and secondary CD8$^+$ T cell responses and clonotypic structures against mouse tumor cell lines expressing HLA-Cw3 (21). However, McHeyzer-Williams and Davis reported a narrowing in the TCR repertoire during the secondary CD4$^+$ T cell response to pigeon cytochrome C (PCC) (22).

Clonal compositions have also been examined for persistent/chronic viruses such as Epstein-Barr virus (EBV) and cytomegalovirus (CMV). A report examining the clonal composition of an EBV peptide-specific CD8$^+$ cytotoxic T lymphocyte (CTL) response using CTL clones indicated that the response was oligoclonal and that the clonotypes were preserved over a 5 year period (23). Similarly, Callan *et al*. examined two patients with primary EBV infection with acute infectious mononucleosis (IM). CTL clones derived from these patients' PBMC during primary infection were comprised of clonotypes that dominated from the day of diagnosis well into the memory phase 37 months later (13). A third study (24) that examined 3 EBV-infected patients with IM reported

oligoclonal receptor usage among *in vitro*-derived clones specific to an immunodominant epitope similar to the report done by others. However, a 2-year follow-up revealed that the original dominant TCR Vβ were poorly represented, if at all, during the memory phase.

Wills *et al*. first studied the CTL response to the HCMV structural protein, pp65, via limiting dilution assay (LDA) and reported high frequencies of pp65 CTL in all donors dominated by a single *BV* gene rearrangement (11). Weekes and colleagues examined CTL clones from 6 CMV-seropositive subjects and reported that the memory CTL response to 4 pp65 peptides is highly skewed (10). A recent study utilizing MHC class I tetramers and CDR3 size analysis showed that the CTL response to pp65 in CMV-seropositive subjects is highly skewed and sequence analysis of the tetramer-selected populations revealed a single or very limited number of clones, thus confirming the oligoclonality of the response (25).

III. IMMUNOLOGICAL MEMORY

Immunological memory is the ability of the adaptive arm of the immune system to respond more rapidly and more robustly to antigens that it has previously experienced. Although physical barriers provided by skin, epithelial surfaces and the presence of innate immune cells, such as granulocytes and natural killer (NK) cells, provide immediate protection. Ultimately, the adaptive arm of the immune system provides the critical response that mediates lasting

protection against pathogens or viral re-activation in the case of persistent viral infections (26, 27).

The T cell compartment of the adaptive arm of the immune system can be generally divided into two groups: naïve T cells and memory T cells. Naïve T cells are produced in the thymus. Bone marrow-derived progenitors that home to the thymus go through several steps of differentiation (reviewed earlier) to become MHC-restricted naïve T cells. These naïve T cells leave the thymus and enter the peripheral circulation and home to secondary lymphoid tissue. Upon stimulation with antigen in secondary lymphoid tissue, naïve T cells differentiate and undergo clonal expansion and become memory T cells (28).

Naïve and memory T cells differ in their homing capabilities, the sites in which they recirculate, their effector functions and the cytokine they express. They also have different costimulatory requirements (28). Naïve T cells express homing receptors that target them to secondary lymphoid tissues such as lymph nodes, Peyer's patches, and spleen, whereas memory T cells frequently lose expression of these receptors and upregulate a different set of homing receptors that target them to tissue (28, 29). CC chemokine receptor (CCR)7 and L-selectin (CD62L) are expressed by all naïve T cells and only a subset of memory T cells (30). The constitutive chemokines, CC chemokine ligand (CCL)19 and CCL21 are produced by stromal cells in the T cell zone of the spleen and bind the CCR7 receptor. Expression of CCR7 on T cells enables them to migrate to secondary

lymphoid organs where antigens are being presented (31). CD62L, the lymph node homing receptor, is a C-type lectin that recognizes the peripheral lymph node vascular addressin (PNAd) displayed in the high endothelial venules (HEVs) and in Peyer's patches mucosal cell adhesion molecule-1 (MAdCAM-1) (28). Naïve T cells in the blood enter lymphoid tissues through HEVs whereas CD62L-negative T cells enter lymphoid tissues via afferent lymphatics.

Memory T cells circulate through the blood and extravasate through microvascular endothelium (particularly when inflamed) into tertiary sites such as skin, lungs, salivary glands, liver, and the gut to carry out their effector functions (28, 32, 33). For example, memory T cells expressing the cutaneous lymphocyte-associated antigen (CLA) preferentially home to the skin and memory T cells expressing the α4β1 integrin preferentially home to sites of chronic infection (28).

Upon activation in secondary lymphoid tissue, naïve $CD4^+$ T cells express interleukin (IL)-2 but do not express the effector cytokines interferon-gamma (IFN-γ□, tumor necrosis factor-alpha (TNF-α□, or IL-4 (34). When naïve T cells encounter their cognate antigen, they undergo clonal expansion, which requires the secretion of IL-2 by activated T cells. The alpha chain of the IL-2 receptor (IL-2R), CD25, is upregulated and it associates with beta and gamma chains constitutively expressed on T cells to form the high-affinity IL-2R. The binding of IL-2 to the high-affinity IL-2R allows the T cell to progress through the cell

cycle, thus giving rise to thousands of progeny expressing the same TCR (3). Memory T cells efficiently express effector cytokines such as IFN-γ and IL-4/IL-5. The secretion of IFN-γ by memory T cells blocks viral replication and activates macrophages, and the secretion of IL-4 and IL-5 activates B cells. T cell-secreted cytokines mediate many T cell effector functions (3). T cell effector functions also include cytotoxicity via granules and/or ligand/receptor-mediated apoptosis, provide help for B cells, and activate or inhibit antigen presenting cells (APC) via the cytokines, which they secrete.

Naïve and memory T cells also have different requirements for costimulation. When naïve T cells recognize foreign peptide/MHC they require the ligation of CD28 on the T cell by CD80 or CD86 on the APC for triggering whereas memory T cells require little or no costimulation. In the absence of costimulation, antigen recognition by naïve T cells leads to anergy, an inactive state of T cells in which naïve T cells fail to proliferate and differentiate into effector cells. Generally, memory T cells require less costimulation than naïve T cells. The interaction with peptide/MHC is often adequate to induce immunologic action such as cytotoxicity or B cell help (3). However, a caveat to this general statement is the hypothesis that T cells have a spectrum of costimulatory requirements (low to high) (35, 36). At one end of the spectrum the T cells that bind peptide/MHC with high affinity will have little or no requirements for

costimulation and, conversely at the other end of the spectrum, T cells that bind peptide/MHC with low affinity require costimulation.

Naïve T cells are maintained via low level signals delivered through self peptide- self-MHC and IL-7. IL-7 is a potent survival factor as it increases or sustains the expression of the anti-apoptotic protein BCL-2 (37). Recognition of self-peptide-MHC keeps T cells metabolically active enough to avoid passive death (29). Naïve T cells that recognize the foreign peptide-MHC complex form a tight synapse with the APC and get trapped in the T cell zone of the lymph node, and begin the activation and differentiation process (28, 29).

The generation of memory T cells involves four general mechanisms: initiation of the immune response during primary infection, clonal expansion and differentiation of the pathogen-reactive T cells, death of the majority of the expanded T cells, followed by differentiation of the surviving cells into a long-term persistent memory population (37). Initiation of the immune response usually occurs in secondary lymphoid tissue. Upon infection with a viral or microbial pathogen, immature dendritic cells (DC) process antigens and travel to the T cell zones of secondary lymphoid tissue. Dendritic cells are potent activators of naïve T cells and express high levels of MHC class I and class II molecules and a plethora of co-stimulatory (CD80 and CD86) and adhesion molecules (CD11a, CD54, CD58, and CD102).

Dendritic cells process and present peptides derived from proteins complexed with MHC molecules. The antigenic proteins that are synthesized in the DC cytoplasm are degraded to peptides by the proteosome, transported to the lumen of the endoplasmic reticulum (ER), and ultimately bind to the MHC class I molecule and are presented to $CD8^+$ T cells. However, DC can also engulf extra-cellular antigenic proteins into acidic endosomal vesicles for degradation by proteases and presentation via MHC class II to $CD4^+$ T cells (3).

Naïve T cells that encounter their cognate foreign peptide/MHC must rapidly expand and differentiate into effector cells to destroy the invading pathogen. The expansion phase continues until the pathogen is cleared (27, 29). Once the pathogen is cleared, the T cells either undergo clonal deletion, die of neglect, or differentiate further into long-term memory cells (27, 29, 34).

Memory T cells can be generally grouped into two categories, effector memory and central memory cells. In humans, effector memory $CD4^+$ T cells are found predominantly in the blood, spleen, and non-lymphoid tissue, and central memory $CD4^+$ T cells are mainly found in the lymph nodes, spleen, and blood (but not in non-lymphoid tissue) (30, 31, 33, 34). Effector and central memory T cells not only differ in their homing capabilities but also display differences in effector functions. Effector memory T cells have greater capability for cytotoxicity and IL-2 production than central memory T cells (38, 39).

The persistence of long-term $CD8^+$ memory T cells is likely mediated by survival signals received through cytokines such as IL-15 (37). When lymphocytic choriomeningitis virus (LCMV)-immune $CD8^+$ memory T cells were transferred to MHC class I deficient ($\beta_2M^{-/-}$) and MHC class I positive ($\beta_2M^{+/+}$) mice, the $CD8^+$ memory cells persisted in both groups of mice (40). Although the factors responsible for the persistence of $CD4^+$ T cells are not well understood, one study that examined the persistence of $CD4^+$ memory T cells in mice reported that $CD4^+$ memory T cells persisted in MHC class II deficient mice (41). In another study of the homeostasis of $CD4^+$ memory T cells it was reported that IL-7 contributed to the maintenance of $CD4^+$ memory T cells (42).

IV. ACTIVATION THRESHOLD REQUIREMENTS

Activation threshold is the strength, duration, and quality of the stimulus required to activate a T cell to produce cytokines, upregulate cell surface molecules, and/or to proliferate. Grossman and Singer have proposed "the tunable activation threshold (TAT) model" to explain T cell adaptability to stimulation that can differ in quality and quantity and the ability of T cells to adjust their response level to stimuli (35, 36, 43). The TAT model proposes that the adaptation of a particular T cell reflects the interaction history of that cell. This interaction history begins in the thymus where positively selected T cells with a spectrum of appropriate affinities for self-MHC which at the high end would

require a lower stimulus and, conversely at the low end, a higher stimulus for activation. A T cell may encounter a stimulus that does not result in activation, but this event is instrumental in tuning the cell for a particular activation threshold. The next stimulus must exceed the activation threshold that was set by the previous event to elicit a full response. Stimuli that do not exceed the activation threshold contribute to a background level that in turn will affect the activation threshold of the stimulated T cell (35, 36).

Naïve T cells interact with self-peptide-MHC complexes in the thymus to obtain survival signals. These interactions do not trigger full activation and clonal expansion of the naïve T cells. However, the opposite is true when naïve T cells encounter their cognate foreign peptide presented by self-MHC in the lymph node. The activation of naïve T cells by foreign peptide-MHC is influenced by the functional avidity and that, in turn, depends upon the affinity of the TCR and the peptide-MHC complex, the density of the TCR and MHC molecules on the cell surface, the presence of the co-receptors and co-stimulatory molecules, and the downstream signaling cascade (44).

Studies have established that exogenous co-stimulation via CD28 and CD49d monoclonal antibodies (MAbs) increases the observed frequencies of human antigen-specific $CD4^+$ memory T cells by up to 3-fold, but does not stimulate the T cells in the absence of antigen (45). Studies using different APCs to examine $CD4^+$ T cell responses to superantigens (SA) have found that $CD4^+$ T

cells have hierarchical thresholds when responding to SA in the presence of different APCs. B cells and macrophages as compared to endothelial cells stimulated T cell activation at lower concentrations of antigen (46). Therefore, co-stimulation can act to lower the activation thresholds of T cells such that triggering is achieved at lower concentrations of antigen. Studies from our lab have also shown that stimulation of T cells with antigen and exogenous co-stimulation sequentially increase response frequencies suggesting the possibility that T cells have heterogeneous triggering thresholds. However, it is possible that the differences in response frequencies may be due to heterogeneous TCR affinities for peptide (45).

V. CYTOMEGALOVIRUS AND THE IMMUNOLOGY OF CMV INFECTION

CMV is a ubiquitous beta herpesvirus that establishes a lifelong infection in its host. Infection rates are dependent on socioeconomic background. Greater than 90% of people from third world countries are CMV-seropositive as opposed to 40-60% of people living in areas with better hygiene (47, 48). The beta herpesvirus classification is based on the biological properties of host specificity, length of the replication cycle, and cytopathic effects (49).

CMV is species-specific (49, 50) and human CMV (HCMV) has the largest genome among the herpesvirus group, with ~230 kilobase pairs. HCMV

encodes over 200 proteins of greater than 100 amino acids (51). Although primary infection of HCMV is usually asymptomatic, some rare cases of severe post-primary infection illness include mononucleosis type syndrome, hepatitis, Guillain-Barré syndrome, and interstitial pneumonia (51). HCMV infections of immunocompromised hosts such as neonates, transplant recipients, or HIV-1^{-} infected individuals, can result in pneumonitis, hepatitis, gastrointestinal tract disease, and retinitis (51).

When CMV infects a cell it can lead to the characteristic enlargement of the cell with intranuclear inclusions, which is why the term cytomegalic inclusion disease was used to characterize the disease before the etiologic agent was found (50). The virus is spread by close/intimate contact as the virus tends to be present and is shed in oropharyngeal secretions, urine, cervical and vaginal secretions, spermatic fluids, breast milk, tears, feces, and blood. Viral shedding can occur for months to years after exposure. Oral and respiratory spread are the most common routes of viral transmission during childhood and probably adulthood (50). CMV is highly pathogenic when unrestrained and can cause tissue destruction via its cytopathic effects. CMV end organ disease (EOD) consists of an inflammatory response, viral cytolysis, and vasculitis leading to organ dysfunction (50).

CMV has a tropism for the salivary gland and replicates in epithelial cells, endothelial cells, fibroblasts, macrophages, placental trophoblasts, and rarely, in T cells (51). CMV appears to employ several persistence strategies that include

broad cell tropism, differential patterns of gene expression in different cell types, novel patterns of gene expression, distinct genome structures during persistence, and expression of viral gene products that can modulate host immune responses (47, 48, 52-55).

CMV has a long evolutionary relationship with its mammalian hosts and has achieved enormous success (e.g., ubiquity) by striking a balance with the host in which its pathogenicity is restrained by host immunity, but its manipulation of the immune system prevents its elimination. Like most persistent viruses, CMV has achieved this biological balance with its host by modulating the host immune response to evade adaptive immunity. CMV has several gene products that mediate immune evasion. These gene products include: US2, which targets the MHC class I heavy chain, the MHC class II DR, and DM α chain for degradation; US3, which retains class I molecules in the ER; US6, which inhibits transporter associated with antigen processing (TAP); US11, which targets MHC class I heavy chains for degradation; UL18, which inhibits NK cell lysis; and IE/E product, that interferes with MHC class II upregulation (26).

The immunological mechanisms that serve to restrain the virus are poorly understood. However, it is known that large immunologic resources are devoted to CMV. For example, in humans, 5-10-fold higher $CD4^+$ memory T cell frequencies are devoted to CMV when compared to $CD4^+$ memory T cell frequencies to non-persistent viruses (45, 56-59). One can speculate that devoting

a large proportion of the memory T cell compartment to CMV, while innocuous in immunocompetent individuals, may prove to be detrimental in cases of immunodeficiency because it leaves the host with a memory repertoire that can respond to CMV but not other potential pathogens.

VI. $CD4^+$ T CELL RESPONSES TO VIRAL PATHOGENS

A. Evolution of the $CD4^+$ T cell response to viral antigens

Viral infection of a host usually occurs at respiratory, gut, or genital surfaces (60). However, viruses can enter through breaches in skin caused by animal bites, insect bites, or contaminated needles. The virus then enters the blood and travels to the spleen. Viruses that enter through the respiratory, gut, or genital surfaces are engulfed by the local DC present at the site of infection and are transported to the draining lymph node. The up take of antigen initiates activation of these DCs. Activated DCs up-regulate CCR7, which enables them to migrate to the lymph nodes. Once the DCs reach the lymph nodes they express processed foreign peptide-MHC and the necessary co-stimulatory molecules to activate the resident naïve T cells (27, 29, 61).

Viral infection induces a burst of activation among the responsive T cells that results in the generation of an antigen-specific memory T cell repertoire, which then expands to clear the viral infection (43, 61, 62). The burst of T cell activation is characterized by transient exposure of the TCR and CD28 to foreign

peptide-MHC and CD80/CD86. The ensuing signaling cascade causes the up-regulation of CD25 and CD154, which interact with IL-2 and CD40 to provide the additional co-stimulatory signals that are required to induce activation, differentiation, and proliferation of T cells (63).

Although transient exposure to antigen alone is sufficient to induce a $CD4^+$ T cell response, the functional qualities of the effector memory cells in question depend upon the exposure strength and duration of the antigen and the co-stimulatory molecules involved (34). $CD4^+$ T cells depend on the interaction of TCR with peptide-MHC in conjunction with the ligation of co-stimulatory molecules with their receptors. Whitmire and colleagues (63) showed that mice deficient in CD28 and CD154 co-stimulatory molecules have severely compromised virus-specific $CD4^+$ T cell responses. CD28 is a regulator of $CD4^+$ T cell activation and it interacts with CD80 and CD86 expressed on activated APCs. CD154 is up-regulated on activated T cells. Mice deficient in CD154 have reduced $CD4^+$ T cell responses to the virus.

Various mechanisms control clonal expansion and contraction of T cells. High-affinity T cells synthesize both pro-apoptotic Fas and FasL and anti-apoptotic Bcl-2 and Bcl-X_L. Bcl-2 and Bcl-X_L prevent cells from apoptotic death during clonal expansion. After the expansion phase, the antigen-specific T cell pool undergoes a silencing, neglect, or death phase, and the number and frequency of the antigen-specific T cells is typically reduced by ~90% (34, 61).

The silencing phase of the T cell response is due to the apoptotic death of highly activated T cells expressing Fas and FasL, which mediate this activation-induced cell death (AICD) and antigenic neglect (64). Also, IFN-γ plays a role in controlling the magnitude of the $CD4^+$ T cell expansion by rendering $CD4^+$ T cells susceptible to AICD via caspase-8-dependent apoptosis (65).

The reduction of activated T cells at the end of a primary infection may be due to death or homing of T cells to nonlymphoid tissues. When parental T cells were transferred to irradiated H2-heterozygous mice, large numbers of activated donor-derived effector cells appeared in the thoracic duct lymph by 3-4 days post-transfer. These effector cells were then transferred to syngeneic (donor) mice and the cells homed to the spleen and lymph nodes but then disappeared via two mechanisms. First, many of the activated T cells left the spleen and localized in nonlymphoid tissues, notably the lungs, liver, and gut. Second, the majority of these T cells died within five days and only a few survived to become memory cells (29, 66-68).

Additionally, the generation of memory $CD4^+$ T cells in the mouse was examined by performing immunohistology of the whole body (32). The naïve $CD4^+$ T cells were found primarily in secondary lymphoid tissue. After exposure to ovalbumin peptide, the $CD4^+$ T cells proliferated in secondary lymphoid tissue and then migrated to the lung, liver, gut, and salivary glands, and then disappeared from these organs between 3 to 11 days. However, if ovalbumin

peptide was injected along with lipopolysaccharide, memory T cells survived for months post-exposure (32). The important caveat to these results is that these studies were performed using non-persistent antigens that are readily cleared, whereas viruses that persist induce memory $CD4^+$ T cells that persist for many years (57). For example, adult human subjects with persistent CMV infection that are clinically asymptomatic have high frequencies of CMV-specific $CD4^+$ T cells. The CMV responses are stable for more than two years and without any evidence of CMV re-infection or CMV replication (45, 56, 57).

Although memory T cells can exist for years after initial infection, the impact of future viral infections on their stability is not known. Varga and colleagues (69) examined the relative stability of LCMV-specific CD4+ T cell memory under conditions of CD8+ T cell memory loss due to heterologous virus infections. In this study it was apparent that the $CD4^+$ and $CD8^+$ pools of memory cells were independently regulated and the reduction of memory T cells due to multiple heterologous virus infection (Pichinde virus, vaccinia virus, murine CMV [MCMV]) appeared to be specific to $CD8^+$ T cells and the $CD4^+$ T cell memory pool remained unchanged (69). Therefore, in this mouse model it did not appear that $CD4^+$ memory T cells were susceptible to the same level of attrition as $CD8^+$ memory T cells after successive viral infections. In humans, the estimated half-lives of vaccinia-specific $CD4^+$ and $CD8^+$ T cell responses have been reported to be 8-15 years. The vaccinia-specific $CD4^+$ T cells were better

maintained than vaccinia-specific $CD8^+$ T cells (70). Whether the differences in attrition between $CD4^+$ and $CD8^+$ memory T cells are due to independent regulation, differences in clonal expansion and activation bursts, and/or different niches in immunological space remain to be answered.

B. $CD4^+$ T cell mechanisms for anti-viral responses

Experiments in animals have revealed three general mechanisms by which $CD4^+$ T cells play a critical role in response to persistent viral pathogens. First, $CD4^+$ T cells can have direct antiviral effects via elaboration of cytokines such as IFN-γ and TNF-α (71). IFN-γ is a potent activator of inducible nitric oxide synthase (iNOS). TNF-α can synergize with type I IFNs to inhibit viral replication via activation of iNOS and iNOS-dependent pathways of macrophage antiviral defense (63, 72). IFN-γ and TNF-α can also interfere with the intracellular replication of the virus (72).

Second, $CD4^+$ T cells secrete IL-2, which facilitates $CD8^+$ T cell activation and expansion, hence playing a key role in maintaining CTL function during the chronic phase of viral infections (53, 63, 73-76). Also, a small subset of $CD4^+$ CTL can mediate direct MHC class II-restricted killing via perforin and Fas/FasL-mediated pathways (77, 78).

Third, $CD4^+$ T cells express CD154 and provide help for humoral responses by direct cell-to-cell interaction with CD40 expressed on B cells. Also,

$CD4^+$ T cell help is required for the production of high affinity anti-viral antibodies (28, 63, 74). Although CMV-specific antibodies appear to play a role in limiting virus dissemination during episodes of virus recurrence, studies in B cell-deficient mice have shown that CMV-specific antibodies are not required for controlling primary CMV viremia, since CMV was cleared from the salivary glands of both mutant (B cell-deficient) and wild-type mice (79, 80).

C. Evidence that $CD4^+$ T cells contribute to the control of CMV

$CD4^+$ T cells contribute to the immune response and control of CMV. Numerous studies have shown a high steady state frequency of CMV-specific $CD4^+$ T cells in progressive human immunodeficiency virus (HIV)-1 infection. It has been reported that CMV-induced EOD generally occurs when $CD4^+$ T cell counts fall below 50 cells/μl (57, 59, 81, 82).

CMV seropositive BMT recipients suffer a risk of CMV reactivation that can cause morbidity and mortality. In immunotherapy trials, CMV-specific $CD8^+$ CTL clones were isolated from bone marrow donors, propagated *in vitro*, and adoptively transferred to immunodeficient BMT recipients. The persistence of the CMV-specific $CD8^+$ CTL clones depended upon the presence of CMV-specific $CD4^+$ T cells (83, 84). Also, adoptive transfer experiments were performed in stem cell transplant recipients. The subjects in this study were viremic and lacked a CMV-specific $CD4^+$ T cell response. Adoptive transfer of

CMV-specific $CD4^+$ T cells to these subjects resulted in a decrease in the viral load within two weeks as well as the expansion of CMV lower matrix protein (pp65)-specific $CD8^+$ T cells within 2 months of therapy, suggesting that CMV-specific $CD4^+$ T cells play a role in mediating protection against CMV-disease (85).

VII. RHESUS MACAQUE MODEL

Rhesus CMV (RhCMV) infects *Macaca mulatta* (RM). The RhCMV genome is ~221 kilobase pairs. HCMV and RhCMV are structurally similar, encoding immunomodulatory genes, structural proteins, and enzymes required for replication. The RhCMV genome contains 230 open reading frames (ORFs) that are collinearly arranged with HCMV, MCMV, and rat CMV (RCMV). There are 138 ORFs in RhCMV encoding gene products that are homologous to HCMV proteins (54). The RhCMV immune evasion genes homologous to the HCMV immune evasion genes have been identified and include Rh182 (US2, targets class I heavy chain, class II DR, and DM α chain for degradation), Rh184 (US3, retains class I in the ER), and Rh189 (US11, targets class I heavy chain for degradation) (54).

RhCMV infection is similar to HCMV infection since almost 100% of captive RM in the Oregon National Primate Center are CMV-seropositive by the time they are one year old, and the infection is asymptomatic. Healthy RM adults

tend to shed virus in their urine, saliva, semen, cervical secretions, and breast milk for months to years. As in humans infected by HIV-1, simian immunodeficiency virus (SIV)-infected RMs can display disseminated CMV disease including orchitis, encephalitis, and respiratory tract disease (54).

To study the development of primary T cell responses to CMV and the mechanisms involved in immunological control of the virus, an animal model is necessary. MCMV infection in mice has been used to study T cell immunity as well as T cell memory; however, MCMV is evolutionarily distant from HCMV with an average divergence score of 0.7 for 4 gene sets (86). Primate CMVs are closely related and RhCMV is more closely related to HCMV with an average divergence score of 0.25 for the same 4 gene sets (86).

One of the first studies that used the RM model examined 13 animals that were experimentally infected with SIV/Delta, a strain of SIV isolated from a RM with simian acquired immunodeficiency syndrome (SAIDS) at the Tulane National Primate Research Center (87, 88). All infected animals died and autopsies were performed to locate CMV intranuclear and intracytoplasmic inclusions and cytomegaly. Changes in the brain, lung, lymph node, liver, spleen, small intestine, testicle, nerves, and arteries were attributed to disseminated CMV infection. The pathogenesis of disseminated RhCMV infection observed in these SIV-immunodeficient RMs was similar to that of disseminated HCMV infection in humans infected with HIV-1. Based on this study, it was apparent that the RM

would be a good model for studying the pathogenesis, treatment, and prevention of CMV infections in HIV-1 infected human beings (88).

In another study (89), lesions characteristic of CMV-associated disease were found in SIV-infected RMs that were also infected with RhCMV. 64% of the RMs had productive RhCMV infections defined by immunohistochemistry of the gastrointestinal tract, hepatobiliary system, testicles, and lungs. This study showed that the incidence of productive RhCMV infection in the SIV-infected RMs appeared to be comparable to HCMV infection in HIV-1-infected humans (89).

In a separate study (52), RMs were experimentally infected with RhCMV to investigate the early stages of viral infection in vivo. The tissues positive for RhCMV DNA were similar to those identified for HCMV DNA during disseminated HCMV infection. Eight of nine animals developed antiviral antibodies. None of the healthy hosts displayed clinical signs of disease even though the virus displayed persistent gene expression (52).

Kaur and colleagues (53) compared SIV-infected RMs with CMV disease to SIV-infected RMs that did not develop CMV disease and found that animals with CMV disease had significantly higher plasma SIV RNA and CMV DNA. Over the course of CMV disease in SIV-infected RMs, a significant decline in anti-CMV antibodies and CMV-specific $CD4^+$ and $CD8^+$ T cells was observed.

The reduction of the anti-CMV antibodies and the CMV-specific $CD8^+$ T cells correlated with a decline in CMV-specific $CD4^+$ T cells (53).

The homology between HCMV and RhCMV genomes (54), infection patterns (52, 53, 88, 89), induction of humoral (53) and cellular immune responses (90 and L. Picker unpublished data) indicate that the RM is an ideal model for investigating the development of a primary $CD4^+$ T cell response and the generation of long-term memory T cells.

Although many studies have defined $CD4^+$ T cell responses to persistent viral pathogens such as CMV, the correlates of protection are not well defined. It is not known whether the and frequency of CMV-specific $CD4^+$ T cells emerging at the end of a primary infection changes over time? The composition of the CMV-specific $CD4^+$ TCR BV-defined clonotypes is not known. It is unclear whether re-exposure to CMV changes the frequency and relative hierarchy of CMV-specific clonotypes. The clonotypic structure of a primary and memory $CD4^+$ T cell response has not been characterized. To answer these questions we have chosen the RhCMV/RM model to study these parameters.

MATERIALS AND METHODS

Human

I. Cell preparation and antigen stimulation

PBMCs were isolated from heparinized or citrated venous blood by density gradient sedimentation using Ficoll-Hypaque (Histopaque-1077, Sigma Chemical Co., St. Louis, MO). Cells were then washed twice in Hank's Balanced Salt Solution (HBSS; Ca^{++}/Mg^{++}-free, Cellgro/Mediatech, Fisher Scientific, Federal Way, WA) and resuspended in RPMI 1640 media (Hyclone Labs, Logan, UT) supplemented with 10% heat inactivated fetal calf serum (FCS; Hyclone), 2 mM L-glutamine (Sigma), 1 mM sodium pyruvate (Sigma) and 50 μM 2-mercaptoethanol (Sigma). Cytokine flow cytometry (CFC) was performed as follows: PBMCs were placed in 17x100 mm polypropylene tissue culture tubes (Sarstedt, Newton, NC) at 1 x 10^6 cells/ml complete media (1-10 ml/tube) with appropriately titered "whole" CMV viral preparations (~40 μl prep./ml), CMV pp65 15 mer peptide(s) or no Antigen as a negative control with or without the co-stimulatory MAbs CD28 and CD49d (1 μg/ml each). These MAbs provide exogenous co-stimulation to allow the total cohort of Antigen-specific cells to respond in this assay. The cultures were incubated at a 5° slant at 37ºC in a humidified 5% CO_2 atmosphere for 6 hours with the final 5 hours including 10

μg/ml of Brefeldin A (Sigma). After incubation, cells were harvested by washing in cold (4ºC) Dulbecco's phosphate-buffered saline (dPBS; Invitrogen, Carlsbad, CA) with 0.1% bovine serum albumin (BSA; Roche Molecular Biochemicals, Indianapolis, IN), and processed for immediate staining. Antigen stimulation for surface IFN-γ capture was performed similarly except Brefeldin A was not included. The cultures were incubated for a total of 5 hours and harvested cells were labeled with IFN-γ capture reagent, and then incubated an additional 45 minutes at 37ºC, according to the manufacturer's instructions (Miltenyi Biotech, Auburn, CA).

II. Immunofluorescent staining and flow cytometric analysis and sorting

For the analysis of intracellular cytokine, stimulated cells were first stained on the cell surface with directly conjugated TCR-Vβ or CD3 MAbs (30 minutes at 4ºC), washed once with cold dPBS/BSA prior to resuspension in fixation/permeabilization solution (Becton Dickinson Biosciences [BD Biosciences], San Jose, CA) at 2 x 10^6 cells/ml, and incubated for 10 minutes at room temperature in the dark. Fixed and permeabilized cells were washed twice with cold dPBS/BSA, and then incubated on ice in the dark with directly conjugated cytokine, CD69 and CD4 MAbs for 30 minutes. For cell surface immunofluorescent analysis using the unconjugated IgM MAb 2H4 (anti-CCR7), freshly isolated cells (1 x10^6/test) were stained as follows (with washing between

each step): 1) incubation with MAb 2H4 x 30 minutes, 2) incubation with FITC-conjugated goat anti-mouse IgM x 30 minutes, 3) second stage blocking with 0.5 ml 10% normal mouse serum x 10 minutes, and 4) incubation with directly conjugated MAbs. All steps were performed at 0-4ºC, and included 5 mM sodium azide. Steps 1 through 3 were excluded in those cell surface analyses using only directly conjugated MAbs. After the last incubation with MAbs, stained cells were washed, resuspended in 1% paraformaldehyde in dPBS (for analysis) or dPBS/BSA (for sorting), and then kept in the dark at 4ºC until analysis or sorting on the flow cytometer.

Five or six parameter flow cytometric analysis was performed on a two-laser FACSCalibur instrument using FITC, phycoerythrin (PE), and peridinin chlorophyl protein (PerCP), and allophycocyanin as the 4 fluorescent parameters. List mode multiparameter data files (each file with forward scatter, orthogonal scatter, and 3-4 fluorescent parameters and including 30-250,000 events after gating on $CD4^+$ small T cells) were analyzed using the PAINT-A-GATE^{Plus} software program (BD Biosciences). In some instances, live gating on TCR-$V\beta^+$, $CD4^+$ or IFN-γ^+/$CD69^+$, $CD4^+$ T cell subsets (with collection up to 10,000 gated events) was performed to enhance quantification of small populations.

Five parameter fluorescence-activated cell sorting (FACS) was performed using a two laser FACSVantage SE flow cytometer (BD Biosciences). Viable CMV-responsive cells (required for RT-PCR) were sorted on the basis of their

surface expression of CD4 (FITC), CD69 (allophycocyanin), and surface IFN-γ (PE) capture. For PCR analysis, cells can be analyzed after fixation/permeabilization, and cells were therefore sorted on the basis of their intracellular expression of IFN-γ (FITC), CD69 (PE), and CD4 (allophycocyanin). Sorted populations were used immediately for RT-PCR, or stored at –80ºC for PCR analysis.

III. Antigens and antibodies

CMV Antigen preparations were obtained from Microbix Biosystems, Inc. (Toronto, Canada). CMV pp65 peptides (consecutive 15 mers overlapping by 11 amino acids (aa) spanning the whole molecule; consecutive 12 mers or 9 mer overlapping by a single amino acid spanning regions of interest) were custom synthesized by Dr. Dieter Stoll (Natural and Medical Sciences Institute of the University of Tuebingen, Tuebingen, Germany) based on the pp65 sequence of CMV strain AD169. Peptide sequences were confirmed by electrospray mass spectroscopy. Optimal 15 mers and all 12 mers and 9 mers were subjected to high-performance liquid chromatography (HPLC) purification (resulting in an average purity of 95%). MAbs SK3 (CD4; PerCP-conjugated, allophycocyanin-conjugated), SK7 (CD3; PerCP, allophycocyanin); L78 (CD69; PE, PerCP, allophycocyanin), L293 (CD28; unconjugated), L25.3 (CD49d; unconjugated), 25723.11 (anti-IFN-γ; FITC, allophycocyanin), 5344.111 (anti-IL-2; FITC, PE,

allphycocyanin), IgG1 and IgG2 isotype-matched controls and streptavidin-allophycocyanin were obtained from BD Biosciences. TCR Vβ-2 and -17 MAbs (PE and biotin) were obtained from Coulter/Immunotech (Hialeah, FL). The anti-IFN-γ MAb (PE) used for surface IFN-γ staining was obtained from Miltenyi Biotech. FITC-conjugated goat anti-mouse IgM was obtained from Kirkegaard & Perry Labs (Gaithersburg, MD).

IV. TCR BV CDR3 size analysis and clonotype characterization

Total RNA was isolated by TRIzol reagent, according to the manufacturer's instructions (Invitrogen). RT-PCR mix (RT-PCR buffer with 1.5 mM $MgCl_2$; Roche Molecular Biochemicals), 0.2 mM dNTP mix (Roche), 5.0 μCi (α-^{32}P) dCTP (Amersham Pharmacia Biotech, Inc., Piscataway, NJ), 5 mM DTT (Roche), 10 units RNAguard (Amersham Pharmacia), 0.5 μM 5' primer, 0.5 μM 3' primer, and 1.0 μl Titan enzyme mix (AMV and Expand High Fidelity PCR-System; Roche) was added to either total RNA, and reverse transcription was carried out at 50°C for 30 minutes followed by 5 minutes of inactivation at 95°C. This was in turn followed by 35 cycles of PCR (denaturation at 94°C for 0.5 minutes, annealing at 60°C for 0.5 minutes, and extension at 68°C for 0.5 minutes) with a final extension at 68°C for 2 minutes. BV and AV PCR were carried out using 5' and 3' TCRB and TCRA primers from Manfras *et al*. (91).

Six μl of the final RT-PCR reaction volume was added to 4 μl of

formamide/dye stop solution (Amersham Biosciences), heated at 95°C for 2 minutes, and applied to a 4% acrylamide sequencing gel (Zaxis, Hudson, OH). Autoradiography was performed on dried gels. The DNA from the dominant bands was eluted from the dry gel by precisely cutting and placing the dried gel band in a microfuge tube. One hundred μl water was added to each tube and the tubes were heated at 100ºC for 10 minutes, and then microcentrifuged at 13,000 x *g* for 5 minutes. The supernatant was removed and 20 μl from each eluted DNA sample was used in separate PCR reactions using the appropriate BV- and BC-specific primers (91). The PCR products were purified on a 2% agarose gel. Each band was cut out of the agarose gel, DNA was extracted (Concert Matrix Gel Extraction System, Invitrogen), cloned into pGEM vector (Promega, Madison, WI), and JM109 High Efficiency Competent Cells (Promega) were transformed. White colonies were picked, plasmid DNA was isolated (Promega), and submitted for sequencing. Analysis of sequence data was performed using MacVector software (Accelrys Inc., Madison, WI).

V. Clonotype-specific real-time PCR

Clonotype-specific primer pairs and probes were designed for real-time PCR such that the primers and probes span the TCRBVDJ junctional region (Table 1). The standard series for each clonotype was made up from the plasmid DNA originally used to sequence the clonotype and was analyzed and validated

over a range of 10^7 to 10^3 copies per reaction. Sorted CMV-responsive and -nonresponsive $CD4^+$ T cells were aliquoted in microfuge tubes and pelleted by centrifugation at 13,000 x *g* for 3 minutes. Fifty μl of 10 mM Tris-HCl, pH 7.4, containing PCR Grade Proteinase K (Roche; 50 μg/ml) was added to the cell pellets and the lysate was incubated for 4 hours at 56°C. The Proteinase K was then inactivated at 95°C for 10 minutes. For real-time PCR, 5.0 μl of cell lysate or clonotype standard was combined with PCR mix containing PCR buffer (20 mM Tris-HCl, pH 8.0, and 50 mM KCl), 0.2 mM dNTP mix (Invitrogen), 1.5 mM $MgCl_2$, 0.5 μM 5' primer, 0.5 μM 3' primer, 6.25μM probe, and 2.5 units Platinum *Taq* DNA Polymerase (Invitrogen). The PCR protocol included denaturation at 94°C for 2 minutes, 40 cycles of PCR (denaturation at 94°C for 0.25 minutes, annealing and extension at 60°C for 1 minute). Real time PCR data was analyzed using ABI 7700 Sequence Detection System software (version 1.6.3).

TABLE 1 Human TCR BV and clonotype-specific PCR primers

	5' Primer	3' Primer
CB	AATGGGAAGGAGGTGCACAG	CB ATAGAGGATGGTGGCAGAC
VB		CB
5.1	GATGAATGTGAGCACCTTGGAG	AGATCTCTGCTTCTGATGGCTC
7	CCTGAATGCCCCAACAGC	AGATCTCTGCTTCTGATGGCTC
12	CTCTGGAGTCCGCTACCAGT	AGATCTCTGCTTCTGATGGCTC
17	ACTGTGACATCGGCCCAAAA	TGTGCACCTCCTTCCCATTCA
18	GGATCCAGCAGGTAGTGCG	AGATCTCTGCTTCTGATGGCTC
7	CCTGAATGCCCCAACAGCTCTC	TGTGCACCTCCTTCCCATTCA
16	AGAGTCTAAACAGGATGAGTCC	TGTGCACCTCCTTCCCATTCA
17	ACTGTGACATCGGCCCAAAA	TGTGCACCTCCTTCCCATTCA
1	CACAACAGTTCCCTGACTTGCA	TGTGCACCTCCTTCCCATTCA
8	TCTGGTACAGACAGACCATGAT	TGTGCACCTCCTTCCCATTCA
13.1	GACCAAGGAGAAGTCCCCAA	TGTGCACCTCCTTCCCATTCA
2	ATACGAGCAAGGCGTCGAGAAG	TGTGCACCTCCTTCCCATTCA
5.1	GAGTGAGACACAGAGAAACAAA	TGTGCACCTCCTTCCCATTCA
22	AAGTGATCTTGCGCTGTGTCCCCA	TGTGCACCTCCTTCCCATTCA
VB		CDR3
5.1	TCCCTGGTCGATTCTCAGGGCG	GTTGGCCCCAGCCTCCTGTCCC
12	TGGATGCTGGAATCACCCAGAGCC	GCCCGAAGTACTGGGTCCTTAGGTC
17	GGTACAGCGTCTCTCGGGAG	GAACTCCCTGTCCCAAGA
7	CTTAAACCTTCACCTACACGCC	GTATCTGTTCTCCGAATCGATC
16	CCCCAGCCACAGCGTAATAGAG	TGCCATTGTACCCTGCCTGAGG
17	CTGAAGGGTACAGCGTCTCT	TGTAGCCATAGTTATCCCGG
8	TCTGGTACAGACAGACCATGAT	GTCTCTTGGAGCCCTGTCCCGC
13.1	TGCACAAGACCCAGGCATGG	TGCTGGGGCTGATTACCCTG
VB		JB
18	GGATCCAGCAGGTAGTGCG	1.3 CAACTTCCCTCTCCAAAATAT
18	GGATCCAGCAGGTAGTGCG	2.3 AGCACTGTCAGCCGGGTG
1	CACAACAGTTCCCTGACTTGCA	2.7 ACCGTGAGCCTGGTGTCC

Rhesus macaque

I. Animals

All animals used in this study were colony-bred RM (*Macaca mulatta*) of Indian origin maintained and used in accordance with guidelines of the Animal Care and Use Committee at the Oregon National Primate Research Center (ONPRC) and the *National Institutes of Health Guide for the Care and Use of Laboratory Animals*. Healthy animals were selected and screened for titers of RhCMV antibody. Four RhCMV-seronegative animals were chosen for the RhCMV Primary Infection Cohort. The other animals in this study were RhCMV-seropositive and were chosen by age and $CD4^+$ T cell response to RhCMV. Animals were anesthetized with ketamine hydrochloride for blood drawing and bronchioalveolar lavage.

II. Cell preparation and antigen stimulation

PBMCs were isolated from citrated venous blood by density gradient sedimentation using Ficoll-Hypaque (Histopaque-1077, Sigma Chemical Co.). Cells were then washed twice in Hank's Balanced Salt Solution (HBSS; Ca^{++}/Mg^{++}-free, Cellgro/Mediatech, Fisher Scientific) and resuspended in RPMI 1640 media (Hyclone Labs) supplemented with 10% heat inactivated FCS (Hyclone), 2 mM L-glutamine (Sigma), 1 mM Sodium Pyruvate (Sigma) and 50

μM 2-mercaptoethanol (Sigma). Antigen stimulations were performed as follows: PBMCs were placed in 17x100 mm polypropylene tissue culture tubes (Falcon, Franklin Lakes, NJ) at 1 x 10^6 cells/ml complete media (1-10 ml/tube) with appropriately titered "whole" RhCMV viral preparations or no Antigen as a negative control and the co-stimulatory MAbs CD28 and CD49d (0.5 μg/ml each). The cultures were incubated at a 5° slant at 37°C in a humidified 5% CO_2 atmosphere for 48 hr. After incubation, cells were harvested by washing in cold (4°C) Dulbecco's phosphate-buffered saline (dPBS; Invitrogen) with 0.1% BSA (Roche Biochemicals), and processed for immediate staining.

III. Antigens and antibodies

RhCMV (Cercopithecine Herpesvirus 8) Antigen preparations were prepared from 68.1 strain (ATCC VR-677)-infected monolayers of primary RM fibroblasts. After a 90-100% cytopathic effect was reached, infected cells were scraped off the flasks. Cells and media were clarified by centrifugation at 3840 x *g* for 10 minutes. Cell pellets were resuspended in media, freeze-thawed 3 times, sonicated for 10 cycles (30 seconds/cycle) and then clarified by centrifugation at 3840 x *g* for 10 minutes. Supernatants from both original culture media and lysed cell pellets were combined and the virus was pelleted at 12,400 x *g* for 1 hour. Viral pellets were resuspended in medium (2% of original culture volume) and titered in the CFC assay.

MAbs L200 (CD4; allophycocyanin-conjugated), SP34 (CD3; True Red); L78 (CD69; PE), L293 (CD28; unconjugated), L25.3 (CD49d; unconjugated), (anti TNF-α; FITC, allophycocyanin), (CD25; FITC), IgG1 and IgG2 isotype-matched controls and streptavidin-allophycocyanin were obtained from BD Biosciences.

IV. Immunofluorescent staining, flow cytometric analysis, and sorting

Stimulated cells were stained on the cell surface for CD4, CD25, and CD69 (30 minutes at 4°C). 0.5 million of the stimulated cells and 1 million of the control cells were also stained with CD3 in a separate tube for FACSCalibur analysis. The $CD4^+/CD25^+/CD69^+$ cells and the $CD4^+/CD25^-/CD69^-$ cells were sorted into 0.5 ml Sarstedt tubes containing 100 μl of RNAlater (Ambion Inc., Austin, TX). Post-sorting, the tubes were centrifuged at 13,000 x *g* for 8 minutes and stored at -80°C overnight. For PCR analysis, cells can be analyzed after fixation/permeabilization, and cells were therefore sorted on the basis of intracellular expression of □□□□α (FITC), CD69 (PE), and surface CD4 (allophycocyanin). Sorted populations were stored at –80ºC for PCR analysis.

V. RhCMV quantification via real time PCR

Purified DNA was analyzed in duplicate for each sample using real-time quantitative PCR. A fluorescently labeled probe and forward and reverse primers

to the RhCMV IE2 sequence were designed using Primer Express software (Applied Biosystems, Foster City, CA) .

PROBE: (6FAM-ACTCCGAAGACCACAAGGACCCACG-TAMRA)

FORWARD PRIMER: (GGGCATCCTCAGGATCACA)

REVERSE PRIMER; (CGACACCAAGAGGGTATGGG)

The 5' end of the probe sequence was labeled with the reporter dye FAM (6-carboxy-fluorescein) and the 3' end with the quencher dye TAMRA (6-carboxy-tetramethyl-rhodamine). Each 25 μL reaction contained TaqMan Universal PCR Mastermix (Applied Biosystems), 100 pmol of each forward and reverse primers, 5 pmol probe, and 10 μL of purified DNA. The RhCMV IE2 gene was cloned and analyzed over a range of 25-1,000,000 copies to create a standard curve of known IE2 copies for each assay. Since one-quarter of each sample was assayed per reaction and results were reported normalized to the entire sample, the lower limit of detection for the assay was one hundred copies of IE2. Reaction parameters were one cycle of two minutes at 50°C, one cycle of ten minutes at 95°C, and 40 cycles of 15 seconds at 95°C followed by one minute at 60°C.

VI. TCRBV CDR3 size analysis using ^{32}P

The cells were processed and the mRNA was purified using the Oligotex Direct mRNA minikit (Qiagen, Valencia, CA) per manufacturer's protocol. Superscript One-Step RT-PCR *Taq* mix (2X Reaction Mix with 2.4 mM $MgSO_4$

and 0.4 mM of each dNTP; Invitrogen), 0.5 μl α-^{32}P dCTP (Amersham), 10 units RNAguard (Amersham Pharmacia), 0.5 μM 5' primer (BV, Table 2), 0.5 μM 3' primer (BC, Table 2), and 0.5 μl RT/Platinum *Taq* mix (SuperScript II RT and Platinum *Taq*; Invitrogen) was added to mRNA, and reverse transcription was carried out at 50°C for 30 minutes followed by 2 minutes of inactivation at 94°C. This was in turn followed by 35 cycles of PCR (denaturation at 94°C for 0.5 minutes, annealing at 55°C for 0.5 minutes, and extension at 72°C for 1 minute) with a final extension at 72°C for 10 minutes. 5 μl of PCR products, mixed with 2 μl of 95% (v/v) formamide/10 mM EDTA, were electrophoresed on a 5% acrylamide sequencing gel and visualized via a phosphorimager screen and a Typhoon 8600 phosphorimager (Molecular Dynamics Division of Amersham).

TABLE 2. RM TCRB primers modified from Chen *et al.* (92)

RM BV Primers (5')	RM BJ Primers (3')	RM BC Primer (3')
BV1 - GCACAACAGTTCCCTGACTTGCAC	BJ1.1 - ACAAGGCACCAGACTCACAG	GTGCTGACCCCACTGTGCACCTC
BV2 - CATCAACCATCCAAACCTGACCT	BJ1.2 - CCTTCGGTTCAGGGACCA	
BV3 - GTCTCTAGAGAGAAGAAGGAGCGC	BJ1.3 - GAGGGAAGTCGGCTCACTG	**RM BC Primer (5')**
BV4 - ACATATGAGAGTGGATTTGTCATT	BJ1.4 - AGTGGAACCCAGCTCTCTG	CCATCAGAAGCAGAGATCTC
BV5 - TGTCTACTGGTACCAGCAGG	BJ1.5 - GAUGGCACUCGACUCUCCG	
BV6 - AGGACTGAGGGATCCGTCTC	BJ1.6 - AACGGGACCAGGCTCACTG	**RM BC RUNOFF Primer (3')**
BV7 - CCTGAATGCTCCAAGAGCTCTC	BJ2.1 - ACACGGCTCACCGTGCTA	CACGTGGTCGGGGTAGAAGCC
BV8 - ATTTACTTTAACAACAAGTCTCCG	BJ2.2 - TCTAGGCTGACCGTGCTGG	
BV9 - TCTCCAGACAAAGCTCATTT	BJ2.3 - CACCCGGCTGACAGTGCT	
BV10 - CCCAAAACTCATCCTGTACC	BJ2.4 - GCGCCGGGACCCGGCTCT	
BV11 - TCAACAGTCTCCAGAATAAGGA	BJ2.5 - ACGCGGCTCCTGGTGCT	
BV12 - AAAGGAGAAGTCTCAGAT	BJ2.6 - GCAGCCGGCTGACCGTGCT	
BV13.1 - ACCCAGGCATGGGGCTGA	BJ2.7 - GGGCACCAGGCTCACAGT	
BV13.2 - ACGTGTCACCAGACTTGGA		
BV14 - GTCTCTCGAAAAGAGAAGAGGAA		
BV15 - GGGTACAGTGTCTCTAGAGA		
BV16 - CAGGATGAGTCCGGTATGCC		
BV17 - GATGAGTCAGGAATGCCAAAGGAA		
BV18 - CAGATAGTAAATGACATTCA		
BV19- AACAGCTTTCTATCTCTGTGC		
BV20 - CAATGCCCCAAGAACCTACC		
BV21 - TCACAGTTGCCTAAGGATCG		
BV22 - GGAAGCATCCCTGATCGATT		
BV23 - AGTCTGAAATATTTGAAGATC		
BV24 - ACAATGAAGCAGACACCCCT		

VII. TCRBV CDR3 size analysis via fluorescent runoff reactions

The cells were processed and the mRNA was purified using the Oligotex Direct mRNA minikit (Qiagen) according to the manufacturer's protocol. Superscript One-Step RT-PCR *Taq* mix (2X Reaction Mix with 2.4 mM $MgSO_4$ and 0.4 mM of each dNTP; Invitrogen), 10 units RNAguard (Amersham Pharmacia), 0.5 μM 5' primer (BV, Table 2), 0.5 μM 3' primer (BC, Table 2), and 0.5 μl RT/Platinum *Taq* mix (SuperScript II RT and Platinum *Taq*; Invitrogen) was added to mRNA, and reverse transcription was carried out at 50°C for 30 minutes followed by 2 minutes of inactivation at 94°C. This was in turn followed by 35 cycles of PCR (denaturation at 94°C for 0.5 minutes, annealing at 55°C for 0.5 minutes, and extension at 72°C for 1 minute) with a final extension at 72°C for 10 minutes. The PCR products were visualized on a 1.8% agarose gel by SyberGreen (Molecular Probes, Eugene, OR) staining. Runoff reactions were performed as previously described (93). Two microliters of the BV-BC PCR products were fluorescently labeled by 10 cycles of runoff elongation using a labeled 3' primer (Table 1). Runoff elongation products, mixed with the same volume of 95% (v/v) formamide/10 mM EDTA, were electrophoresed on a 6% acrylamide sequencing gel (FMC Bioproducts, Rockland, ME) loaded on an automated ABI 377 DNA sequencer (Applied Biosystems). CDR3 size analysis was performed using Immunoscope™ software

(Pasteur Institute, France).

VIII. Identification of TCRB sequences

Identification of TCRB sequences were performed as previously described (94).

A. mRNA purification and RACE-PCR

The sorted cells were processed and the mRNA was purified using the Oligotex Direct mRNA minikit (Qiagen) per manufacturer's protocol. Three microliters of purified mRNA was used to synthesize 5' cDNA using the switching mechanism at 5' end of RNA transcript (SMART)^{TM} rapid amplification of cDNA ends (RACE) cDNA Amplification Kit (Clontech BD Biosciences) according to the manufactures protocol. We designed a 3' gene-specific primer in the RM TCR BC region for PCR amplification of TCR SMART cDNA (see Figure 2.2, page 71).

3' gene-specific primer RM BC:

(5'AGGTCGCTGTGTTTGAGCCATCAGAAGCA3')

Depending upon the number of sorted cells, 5-15 μl of SMART cDNA was used for RACE-PCR. A 50 μl volume of 5 μl 10X Advantage 2 PCR Buffer, 5 μl 10X universal primer mix (UMP), 1 μl 3' TCR gene-specific primer, 1 μl dNTP (10 mM), 1 μl 50X Advantage 2 Polymerase Mix, and PCR-Grade Water

was added to volume. A touch-down PCR protocol was used for amplification as follows. Cycle 1: 95°C for 30 seconds; cycle 2-6: 95°C for 5 seconds, 72°C for 2 minutes; cycles 7-11: 95°C for 5 seconds, 70°C for 10 seconds, 72°C for 2 minutes; cycles 12-37: 95°C for 5 seconds, 68°C for 10 seconds, 72°C for 2 minutes. The RACE-PCR products were resolved on a 1.8% agarose gel. A band between 500-700 base pairs was cut and the DNA was eluted using the Wizard PCR prep DNA Purification System (Promega) per manufacturer's protocol. DNA elution volume was 25-30 μl.

B. Cloning and colony-PCR

The pGEM T Easy Vector Kit (Promega) was used for TA cloning. Five microliters of eluted DNA was added to 7.5 μl 2X ligation buffer, 1 μl pGEM T Easy Vector, and 1.5 μl DNA ligase. The reaction was incubated at 4°C overnight. Five microliters of the ligation reaction was added to 50 μl JM109 High Efficiency Competent Cells (Promega) and transformation was performed according to the manufacturer's protocol. After 1.5 hours of growth at 37°C in a shaker incubator, 100-500 μl of transformation mixture was plated on Lennox broth (LB) ampicillin plates that were prepared with 4 μl isopropylthio-β-galactoside (IPTG) (Invitrogen) and 40 μl (X-GAL) (Invitrogen). The plated were incubated at 37°C overnight. White colonies containing the TCR/pGEM clones were picked for colony PCR. The colony PCR mix was prepared with

HiFi Platinum *Taq* (Invitrogen) as follows: 5 μl 10X HiFi PCR Buffer, 2 μl $MgSO_4$, 1 μl dNTP mix (10 mM), 1 μl M13F primer (25 μM), 1 μl M13R primer (25 μM), 0.25 μl HiFi *Taq*, 39.75 μl PCR-grade water. Fifty microliters of PCR mix was added to 0.2 ml PCR tubes and a sterile pipet tip was used to pick each white colony from the plate and swirled in the 50 μl PCR mix to dislodge the picked cells. The tip was then used to make a replica imprint of the picked colony on a new LB/ampicillin plate. The plate was incubated at 37°C overnight and then stored at 4°C. The colony PCR cycles consisted of 35 cycles of 95°C for 30 seconds, 57°C for 30 seconds, and 68°C for 3 minutes.

C. EXO-SAP treatment and sequencing

Five microliters of colony PCR reaction was treated with 2 μl exonuclease I and shrimp alkaline phosphatase (EXO-SAP) (Amersham Biosciences) and incubated at 37°C for 15 minutes followed by deactivation at 80°C for 15 minutes. The DNA concentration was determined by optical density at 260 nm and the cleaned-up PCR product was submitted to the DNA sequencing core at the ONPRC for sequencing. MacVector software (Accelrys) was used to analyze the sequences.

D. Clonotype-specific real-time PCR

Clonotype-specific primer pairs and probes were designed for real-time

PCR such that the primers and probes span the TCRBVDJ junctional region (Table 1). The standard series for each clonotype was prepared from the plasmid DNA originally used to sequence the clonotype and was analyzed and validated over a range of 10^7 to 10^3 copies per reaction. Sorted CMV-responsive and -nonresponsive $CD4^+$ T cells were aliquoted in microfuge tubes and pelleted by centrifugation at 13,000 x *g* for 3 minutes. 50 μl of 10 mM Tris-HCl, pH 7.4, containing PCR Grade Proteinase K (Roche; 50 μg/ml) was added to the cell pellets and the lysate was incubated for 4 hours at 56°C. The Proteinase K was then inactivated at 95°C for 10 minutes. For real-time PCR, 5.0 μl of cell lysate or clonotype standard was combined with PCR mix containing PCR buffer (20 mM Tris-HCl, pH 8.0, and 50 mM KCl), 0.2 mM dNTP mix (Invitrogen), 1.5 mM $MgCl_2$, 0.5 μM 5' primer, 0.5 μM 3' primer, 6.25μM probe, and 2.5 units Platinum *Taq* DNA Polymerase (Invitrogen). The PCR protocol included denaturation at 94°C for 2 minutes, 40 cycles of PCR (denaturation at 94°C for 0.25 minutes, annealing and extension at 60°C for 1 minute. Real time PCR data were analyzed using ABI 7700 Sequence Detection System software (version 1.6.3).

CHAPTER I

CLONOTYPIC STRUCTURE OF THE HUMAN CD4$^+$ T CELL MEMORY RESPONSE TO CMV

OBJECTIVE

The clonotypic composition and hierarchies of virus-specific T cells have been extensively examined for CD8$^+$ T cells (12, 95, 96). The studies that utilized mouse T cell lines and clones have varied conclusions regarding the clonality of virus-specific CD8$^+$ T cells. Some studies found oligoclonal hierarchies whereas other studies found polyclonal hierarchies (10, 11, 13-17). However, because these studies used *in vitro*-expanded T cell clones or lines, they cannot reliably reflect the physiologic relative frequencies of virus-specific T cells because T cell clones and lines are stimulated repeatedly as they are propagated *in vitro*. In contrast, *ex vivo* studies using MHC class I tetramer-positive cells found a small number of virus-specific T cell clones present at high frequencies with increasing numbers of clones present at lower and lower frequencies (18-20, 97). Some studies have compared the clonotypic hierarchies during primary versus secondary T cell responses. Maryanski *et al*. did not find any difference between

primary and secondary $CD8^+$ T cell responses and clonotypic structures to mouse tumor cell lines expressing HLA-Cw3 (21). However, McHeyzer-Williams and Davis reported a narrowing in the TCR repertoire during the secondary $CD4^+$ T cell response to pigeon cytochrome C (PCC) (22).

To understand the essential components of a protective $CD4^+$ T cell response to CMV, we started by analyzing 4 healthy CMV-seropositive human subjects. In these subjects, we determined the Vβ response complexity (clonality) and the number and frequency of the clonotypes (hierarchy) that contributed to the $CD4^+$ memory T cell response to CMV.

RESULTS

A. Determination of TCR-Vβ usage among CMV-specific $CD4^+$ memory T cells by CFC

In the mid-1990s Picker *et al*. (98) developed an *in vitro* assay to quantify antigen-responsive T cells by short-term (6 hours) activation. This assay, termed CFC, is used to detect antigen-specific T cells directly without long-term culture, thus avoiding either antigen-induced proliferation or cell death. Briefly, PBMCs from HCMV-seropositive adults are activated *in vitro* for six hours with HCMV antigen and exogenous costimulation (CD28 and CD49d MAbs) in the presence of a secretion inhibitor (Brefeldin A) and stained for intracellular CD4, CD69, and IFN-γ. The antigen-responsive $CD4^+$ T cells will stain positively for CD69 and

IFN-γ. First, we set out to characterize the clonotypic heterogeneity of the $CD4^+$ T cell response to HCMV. To achieve this goal we examined the TCR-Vβ usage by HCMV-responsive $CD4^+$ T cells as a first step. The TCR-Vβ usage by HCMV-reactive $CD4^+$ T cells was determined by utilizing TCR-Vβ family and subfamily MAbs. Figure 1.1 is an example of this analysis, depicting the HCMV-responsive $CD4^+$ memory T cells. The top two dot plots depict the $CD4^+$ T cell response to HCMV within the overall $CD3^+$ T cell population. The total HCMV-specific $CD4^+$ memory T cell response was 1.09%. The remaining dot plots show the distribution of the response among representative Vβ families and subfamilies. Even though TCR down-regulation diminishes the surface expression of TCR-Vβ, there is sufficient cell surface TCR-Vβ staining to depict the distribution of the response. The results in this figure depict a typical $CD4^+$ memory T cell response to HCMV. Note that the fraction of the total response attributable to each Vβ family ranges from <1% - 25% of the total response.

FIGURE 1.1 Determination of TCR-Vβ usage among CMV-specific CD4$^+$ memory T cells by CFC

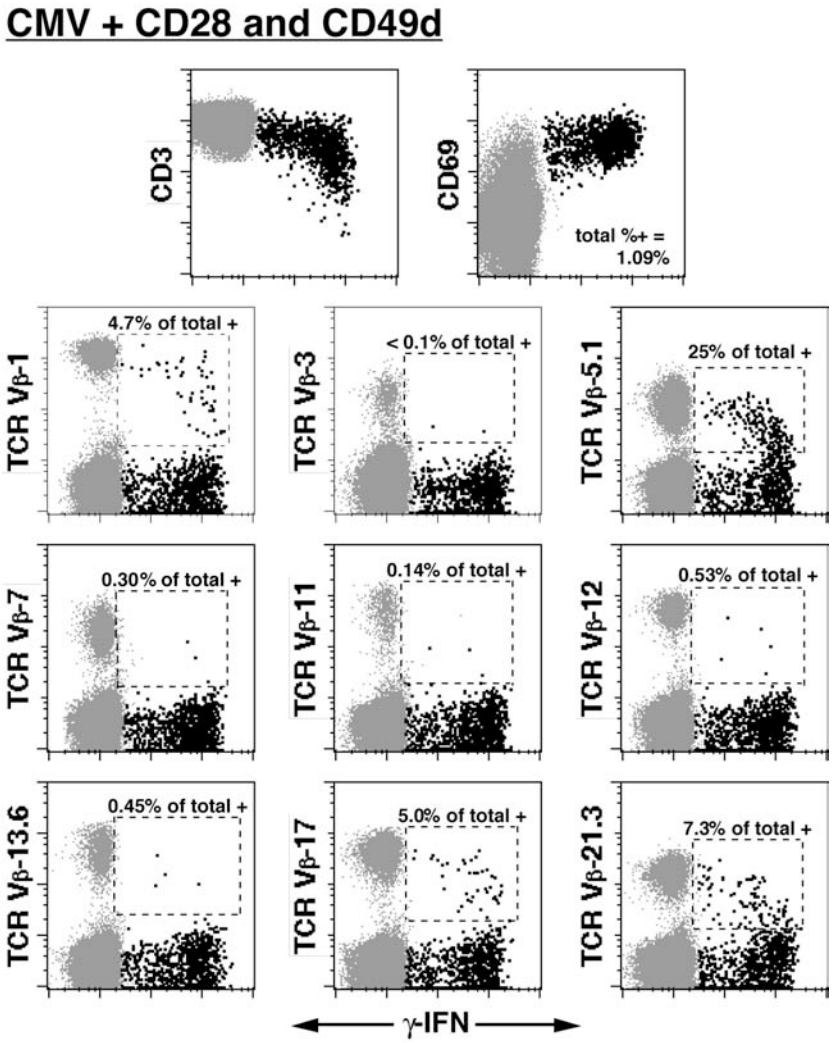

PBMCs from a CMV-seropositive 44-year-old female were stimulated with CMV and CD28/CD49d for a total of 6 hours with the addition of Brefeldin A for the last 5 hours and stained on the cell surface for CD3 or TCR-Vβ and intracellularly for CD69 and IFN-γ. One hundred thousand events gated on CD4$^+$ small lymphocytes are shown. The CMV responding population, CD69$^+$ and IFN-γ$^+$, are highlighted in black. The top two dot plots demonstrate the CD4$^+$ T cell response as a function of CD3. The remaining dot plots show the distribution of the CD4$^+$ T cell response among representative Vβ families and subfamilies.

B. TCR-Vβ usage among CMV-specific CD4$^+$ memory T cells is focused

We performed the same analysis on four additional CMV-seropositive individuals (Figure 1.2). The figure shows the percent of CMV-responsive (bottom panels) or -nonresponsive CD4$^+$ T cell population that stains for TCR-Vβ. The panel of TCR-Vβ MAbs used in these experiments covered 62-73% of the total CD4$^+$ Vβ repertoire (determined by adding the percent of each Vβ-defined population). This analysis shows that for all subjects, 1-3 TCR-Vβ families and subfamilies dominate the CD4$^+$ T cell response to HCMV, accounting for 74% of the total response. Among non-CMV-responding CD4$^+$ T cells (Figure 1.2, top bar graph panels, the Vβ distribution is relatively homogeneous, reflecting the representation of each Vβ in the overall population. We were able to re-examine two of the subjects two additional times over a 20-25 month period after the first analysis (Figure 1.3). In both subjects, the Vβ distribution of the HCMV response was stable despite the fact that one of the subjects examined had an ~4-fold increase in the overall frequency of the HCMV-responsive CD4$^+$ T cells over this time period.

FIGURE 1.2 TCR-Vβ usage among CMV-specific CD4⁺ memory T cells is highly skewed

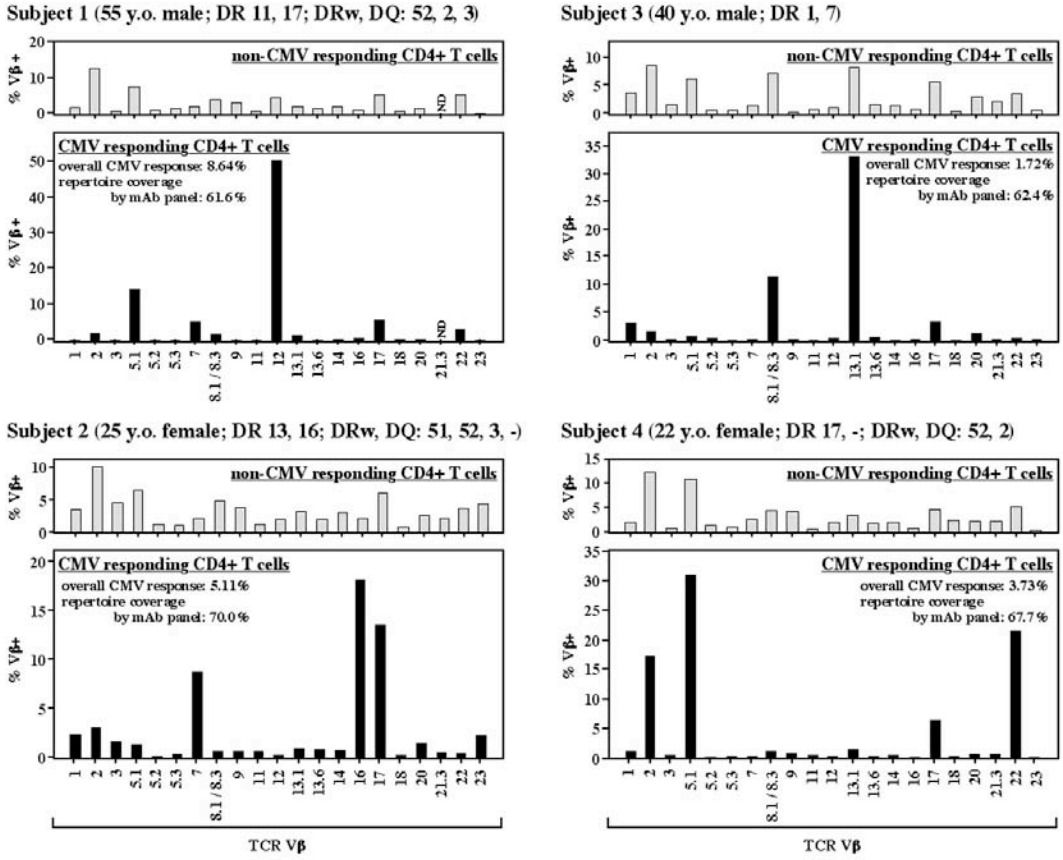

The contribution of individual TCR-Vβ families or subfamilies to the total CMV-specific CD4⁺ memory T cell response is shown in the bottom bar graphs for 4 additional subjects. The top bar graphs show the TCR-Vβ distribution among CMV-nonresponsive CD4⁺ T cells. The TCR-Vβ families and subfamilies analyzed here represent all those to which MAbs are available. The percent of the CD4⁺ T cell repertoire covered by this panel were calculated for each subject by determining the sum of the %+ for all MAbs in
this panel. ND, no data.

FIGURE 1.3 Patterns of TCR-Vβ usage among CMV-specific CD4$^+$ T cells are stable over time

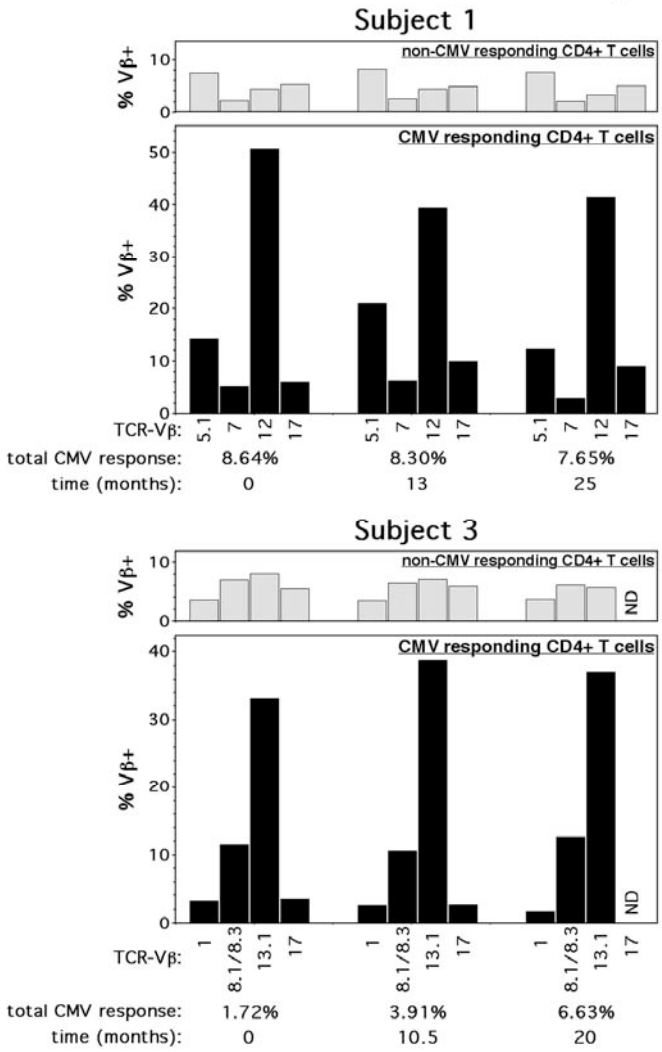

The CFC assay was used to evaluate the relative contribution of dominant and subdominant Vβ families and subfamilies to the overall CMV-specific CD4$^+$ T cell response at the time intervals shown (bottom bar graphs). The top bar graphs shows the same dominant and subdominant Vβ families and subfamilies in the non-CMV-responsive CD4$^+$ T cell fraction.

C. Molecular characterization of the clonotypic content of the HCMV-responsive TCR-Vβ families and subfamilies

The focusing of the $CD4^+$ memory T cells in these subjects to a few Vβ families and subfamilies suggested that only a few clonotypes were responsible for eliciting the total $CD4^+$ T cell response to HCMV. Therefore, we further characterized each responsive Vβ family and subfamily via molecular analysis of the clonotypes that participated in the HCMV response. To analyze the clonotypic content of the HCMV-responsive Vβ families and subfamilies, viable $CD4^+$ T cells needed to be isolated by FACS and the RNA purified for CDR3 size analysis via RT-PCR (7). The amplified products would then be cloned and sequenced. Since we had determined the TCR-Vβ usage in each subject via the CFC assay by staining with the panel of TCR-Vβ MAbs, we could focus the clonotype analysis on the $CD4^+$ Vβ families and subfamilies that were major contributors to the HCMV response. We could not use the CFC assay to isolate the HCMV-responsive $CD4^+$ T cells by FACS because the permeabilization with detergent and fixation with paraformaldehyde required for staining intracellular cytokines in the CFC assay would result in the loss and chemical modification of RNA (99), effectively preventing RT-PCR amplification of TCR BV mRNA. Analysis of specific TCR BV rearrangements at the DNA level (DNA is preserved during intracellular staining) is, of course, prevented by the fact that the

TCR BC gene is spliced onto the VDJ gene at the mRNA level. Therefore, we searched for surrogate cell surface molecules that would identify HCMV-responsive $CD4^+$ memory T cells and allow viable sorting of this population. Our first approach was based on co-expression of CD69 and CD154, these are "effector" molecules that are rapidly upregulated on the cell surface following TCR signaling. Figure 1.4 shows a comparison of intracellular staining of activated $CD4^+$ T cells that express IL-2, and IFN-γ, with CD154. We found that 72% of $CD69^+$/IFN-γ^+ cells also expressed CD154 and 93% of $CD69^+$/IFN-γ^+ cells also expressed CD154. These results show that the CMV-responsive $CD4^+$ T cell populations delineated by CD4/CD69/CD154 and CD4/CD69/IFN-γ are largely overlapping. Therefore, CD4/CD69/CD154 can be used as surrogate markers to cluster and sort the HCMV-responsive populations. Later, a kit became available through Miltenyi Biotech that allowed the capture of secreted IFN-γ on the cell surface. The capture of IFN-γ on the cell surface in combination with staining for CD69 and CD4 results in clustering anywhere from 50-100% of the responding cells as identified by our CFC assay (data not shown).

The first approach was used on subjects 1-3 and the second approach was used on subject 4. PBMCs from all 4 subjects were stimulated with HCMV plus CD28/CD49d MAbs. HCMV-responsive (+) and HCMV-nonresponsive (-) $CD4^+$ T cells were isolated using FACS (Figure 1.4C). The RNA was extracted from the FACS-isolated cell populations and used for CDR3 size analysis via RT-PCR.

FIGURE 1.4 Viable cell sorting using surface expression of CD69 and either CD40L or surface capture IFN-γ

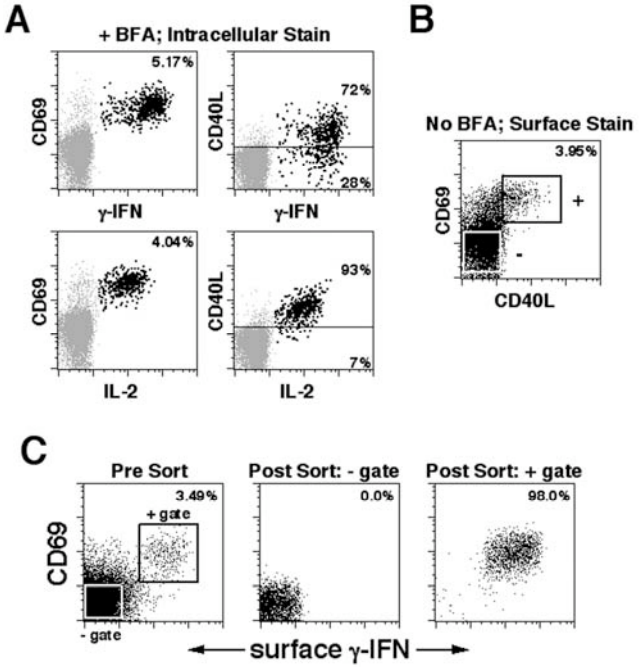

A. PBMCs from subject 1 were stimulated with CMV and CD28/CD49d for a total of 6 hours with the addition of Brefeldin A for the last 5 hours and stained intracellularly for IFN-γ or IL-2, CD69, CD40L, and CD4. Ten thousand events gated on $CD4^+$ small lymphocytes are shown with the CMV-responding cells highlighted in black. The total %+ for IFN-γ and IL-2 are indicated in the dot plots.

B. PBMCs from subject 1 were stimulated with CMV and CD28/CD49d in the absence of Brefeldin A and stained on the surface for CD4, CD69, and CD40L. Ten thousand events gated on $CD4^+$ small lymphocytes are shown with the sort gates for CMV-responsive and non-CMV-responsive delineated by positive (+) and negative (-) respectively. Total % responding is indicated in the dot plot.

C. PBMCs from subject 4 were stimulated with CMV and CD28/CD49d in the absence of Brefeldin A and stained on the surface for CD4, CD69, and IFN-γ capture. The left dot plot shows ten thousand events gated on $CD4^+$ small lymphocytes with the sort gates for CMV-responsive and CMV-nonresponsive delineated by + and - respectively. Total % responding is indicated in the dot plot. The middle dot plots shows the negative sort (3000 events) and the right dot plot shows the positive sort (1400 events) with the %+ indicated in the dot plot.

Our previous analysis utilizing the CFC assay along with TCR-Vβ staining revealed the responsive $CD4^+$ Vβ for each subject. Therefore, we were able to focus the CDR3 size analysis on the responsive BV families and subfamilies. The RT-PCR products were resolved on a 4% denaturing polyacrylamide sequencing gel. Typically, the RT-PCR products for a particular BV family or subfamily of a polyclonal population consists of 6-8 bands with a Gaussian distribution when a minimum 100,000 cells are used for CDR3 size analysis. Figure 1.5 depicts the CDR3 size analysis we performed on the HCMV-responsive and -nonresponsive $CD4^+$ T cell populations. The limited number of sorted cells (4,000-30,000) did not permit classic Gaussian distribution of the BV families. However, in the CMV-nonresponsive (-) lanes, multiple bands, a smear of bands, or no bands were visible, and in the CMV-responsive population, 1-2 bands were visible for each BV analyzed.

Each band on a CDR3 size analysis gel represents BV CDR3 regions identical in length. Any particular band may represent more than one clonotype with identical CDR3 lengths yet different sequences. Therefore, we cut each dominant band from the (+) lanes (see arrows with lower case letters in Figure 1.5), eluted, cloned, and sequenced the DNA.

FIGURE 1.5 CDR3 size analysis of sorted CMV-responsive and -nonresponsive CD4⁺ T cells

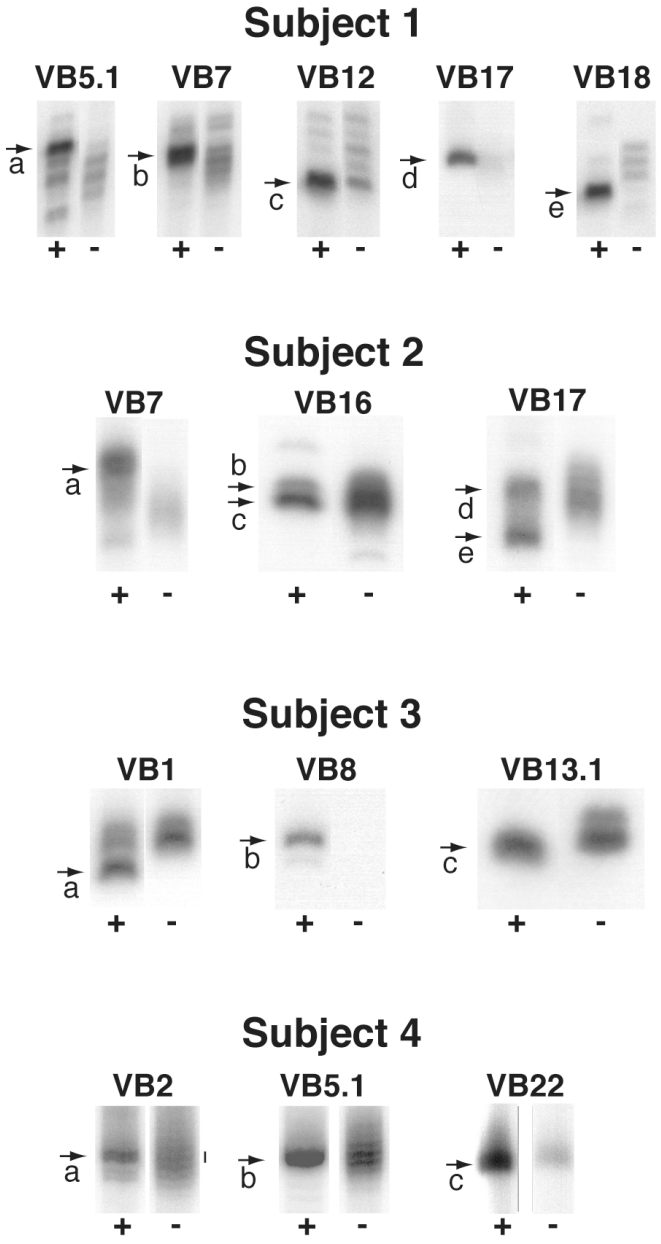

PBMCs from subjects 1-4 were stimulated with CMV and CD28/CD49d. The CMV-responsive and –nonresponsive $CD4^+$ T cells were sorted and the RNA was isolated for CDR3 size analysis. The arrows and small case letters designate dominant bands from CMV-responsive TCR-Vβ that were cloned and sequenced.

Figure 1.6A and B depicts the sequencing results. We examined 5 BV families and subfamilies by CDR3 analysis for subject 1. In subject 1, the CFC assay showed that Vβ 12 had a dominant response contributing ~50% of the total $CD4^+$ T cell response to HCMV (Figure 1.2). Sequence analysis of BV12 revealed one sequence and hence one clonotype that was responsible for ~50% of the total $CD4^+$ memory T cell response to HCMV. We also examined BV5.1, BV7, and BV□7 (subdominant responses) and one minor response, BV18. BV5.1, BV17 were also comprised of a single clonotype. However, sequence analysis of BV7 revealed 5 different sequences and sequence analysis of BV18 revealed 2 different sequences.

FIGURE 1.6A Sequence analysis of dominant bands derived from the CMV-responsive CD4⁺ T cells from subjects 1-2

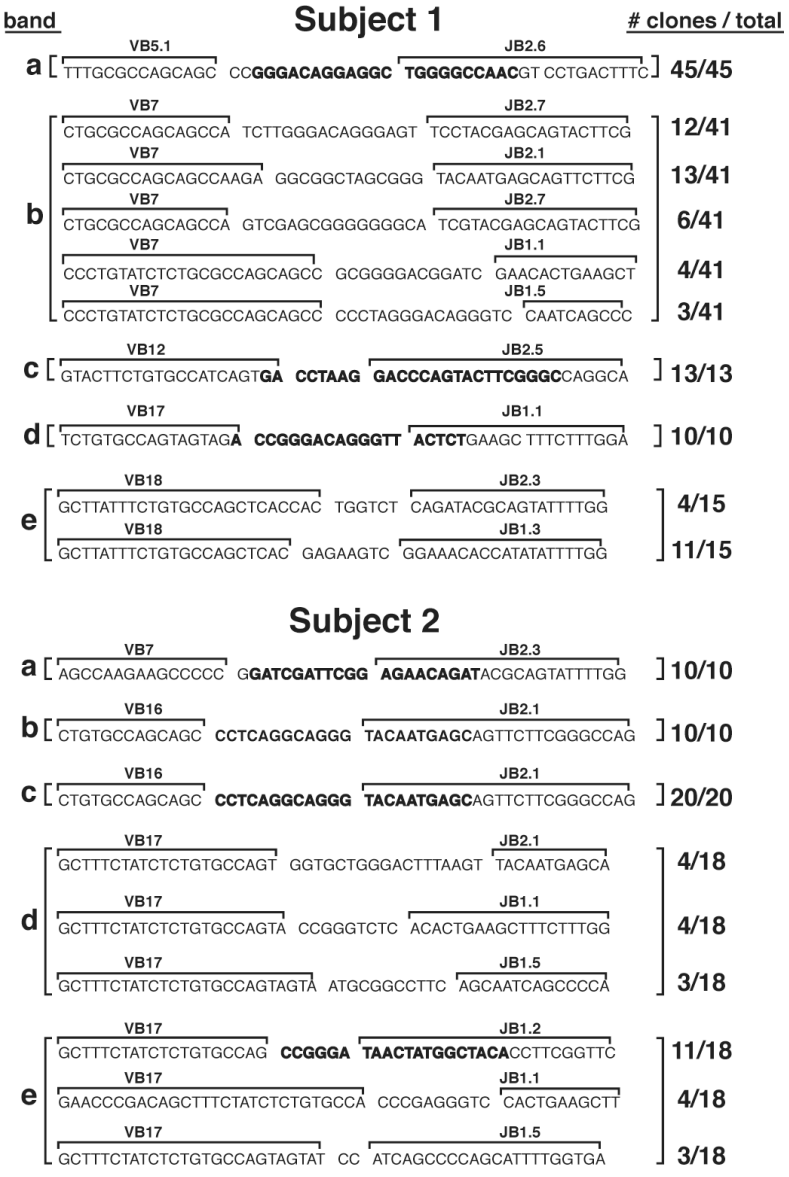

The small case letters on the left correspond to the designated bands in Figure 1.5. Only sequences that were identified in three or more clones are listed with the number of clones containing the indicated sequence and the total number of clones analyzed for that band designated on the right. The bolded sequence indicates the clonotype-specific 3' primer designed to anneal in the CDR3 region.

FIGURE 1.6B Sequence analysis of dominant bands derived from the CMV-responsive CD4⁺ T cells from subjects 3-4

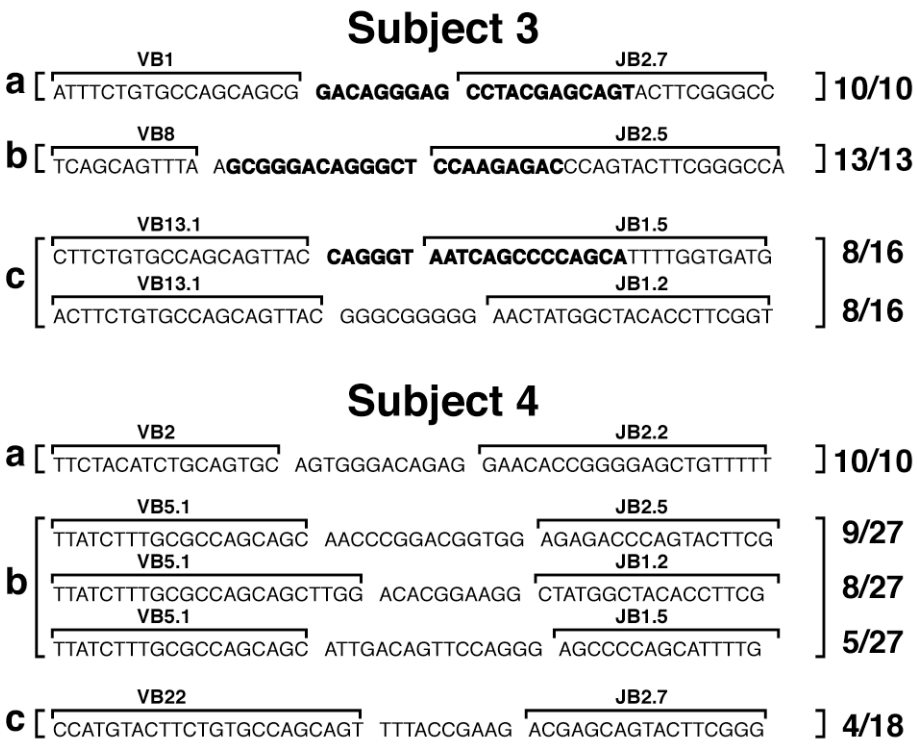

The small case letters on the left correspond to the designated bands in Figure 1.5. Only sequences that were identified in three or more clones are listed with the number of clones containing the indicated sequence and the total number of clones analyzed for that band designated on the right. The bolded sequence indicates the clonotype-specific 3' primer designed to anneal in the CDR3 region.

The dominant Vβ response for subject 2 was Vβ16 and sequence analysis revealed one sequence. The BV16 band appeared as a doublet on the gel. When DNA polymerase enzyme mixes (such as *Pwo* and *Taq*) are used for PCR amplification, around 1/3 of the PCR products will retain additional "A" nucleotide(s) added by *Taq*, whereas *Pwo* will chew off the additional "A(s)" from the remaining PCR products amplified by *Taq*. Therefore, when resolved on a 5% polyacrylamide sequencing gel, these PCR products will appear as doublets, differing in size by 1-2 nucleotides (but identical when sequenced), whereas the BV bands in a given lane will differ in size by 3 nucleotides (1 amino acid) in the CDR3 region. We sequenced the subdominant responses, BV7 and BV17, for subject 2. BV7 was composed of a single sequence whereas BV17 was composed of six different sequences.

The dominant Vβ response for subject 3 was Vβ13.1 and sequence analysis revealed two sequences. However, the subdominant BV1 and BV8 were each composed of a single clone. The dominant Vβ response for subject 4 was Vβ5.1 and sequence analysis revealed three sequences. Similar to subject 3, the subdominant BV2 and BV22 were each composed of a single clone.

Subject 4 had a Vβ5.1 dominant response and sequence analysis revealed that this Vβ was comprised of 3 sequences. The subdominant response from Vβ2 was comprised of a single sequence whereas the subdominant response from and Vβ22 had multiple sequences with one sequence being repeated 4 times.

D. Confirmation of the CMV specificity of the identified CD4$^+$ T cell clonotypes

Because we used surrogate cell surface markers or cell surface IFN-γ capture to isolate the CMV-responsive cells for CDR3 size analysis and sequencing of clonotypes, we needed to confirm the CMV specificity of the identified clonotypes. The sequence results would afford us the opportunity to design clonotype-specific PCR primers in the BV and CDR3 region so that we could amplify rearranged TCR DNA rather than having to perform RT-PCR. Therefore, since the fixation and permeabilization process in the CFC assay does not alter genomic DNA we could isolate CD4$^+$ CMV-responsive and CMV-nonresponsive T cells based on the expression of CD69 and IFN-γ.

We designed clonotype-specific primers such that the 5' primer would anneal in the BV region of the rearranged TCR gene and the 3' primer would anneal in the CDR3 region of the rearranged TCR gene, thus making the primer pair clonotype-specific. Each primer pair was analyzed for specificity (Figure 1.7) to ensure that the primer pair only amplified DNA from the subject it was designed for. Control primers in the BC region were used to show that equivalent DNA was used in each PCR reaction.

FIGURE 1.7 The clonotype-specific primers amplify product from genomic DNA only in the subjects in which the clonotypes originated

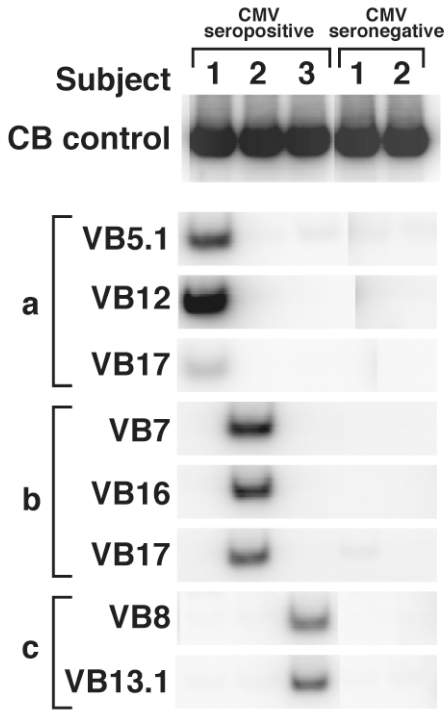

PBMCs from CMV-seropositive subjects 1-3 and two CMV seronegative controls were lysed and genomic DNA (1 μg/reaction) was PCR amplified using the clonotype specific primers. TCR BC amplification was used to control for equivalent DNA from positive and negative fractions per reaction.

To confirm the CMV specificity of the clonotypes, we used our conventional CFC assay and sorted the CMV-responsive and CMV-nonresponsive $CD4^+$ T cells based on the expression of CD69 and IFN-γ (Figure 1.8A). We then performed PCR (Figure 1.8B) using the clonotype-specific primers and found the clonotypes exclusively enriched in the CMV-responsive fraction except for subject 1, BV12BJ2.5, and subject 3, BV13.1BJ1.5, where there was a marked enrichment of the clonotype in the CMV-responsive fraction and a faint band in the CMV-nonresponsive fraction. To measure the difference in quantity of subject 1, clonotype BV12BJ2.5, between the two fractions we used quantitative PCR.

We also evaluated the CMV specificity of three additional minor or subdominant clonotypes from subject 1, BV18BJ1.3, BV19BJ2.3, and from subject 3, BV1BJ2.7. Instead of clonotype-specific primers we used BV/BJ primers and amplified DNA from the $CD69^+/IFN\text{-}\gamma^+$ fraction and $CD69^-/IFN\text{-}\gamma^-$ fraction. Both fractions yielded similar bands. The DNA from the bands was eluted, cloned, and sequenced. The sequences from the BV/BJ band of the $CD69^+/IFN^-\gamma^+$ fraction were identical to those identified originally (Figure 1.6). The sequences from the BV/BJ band of the $CD69^-/IFN\text{-}\gamma^-$ fraction were diverse and different than those identified originally.

FIGURE 1.8 Semiquantitative PCR reveals enrichment of clonotype in CD4$^+$ T cells producing IFN-γ after stimulation with CMV and CD28/CD49d

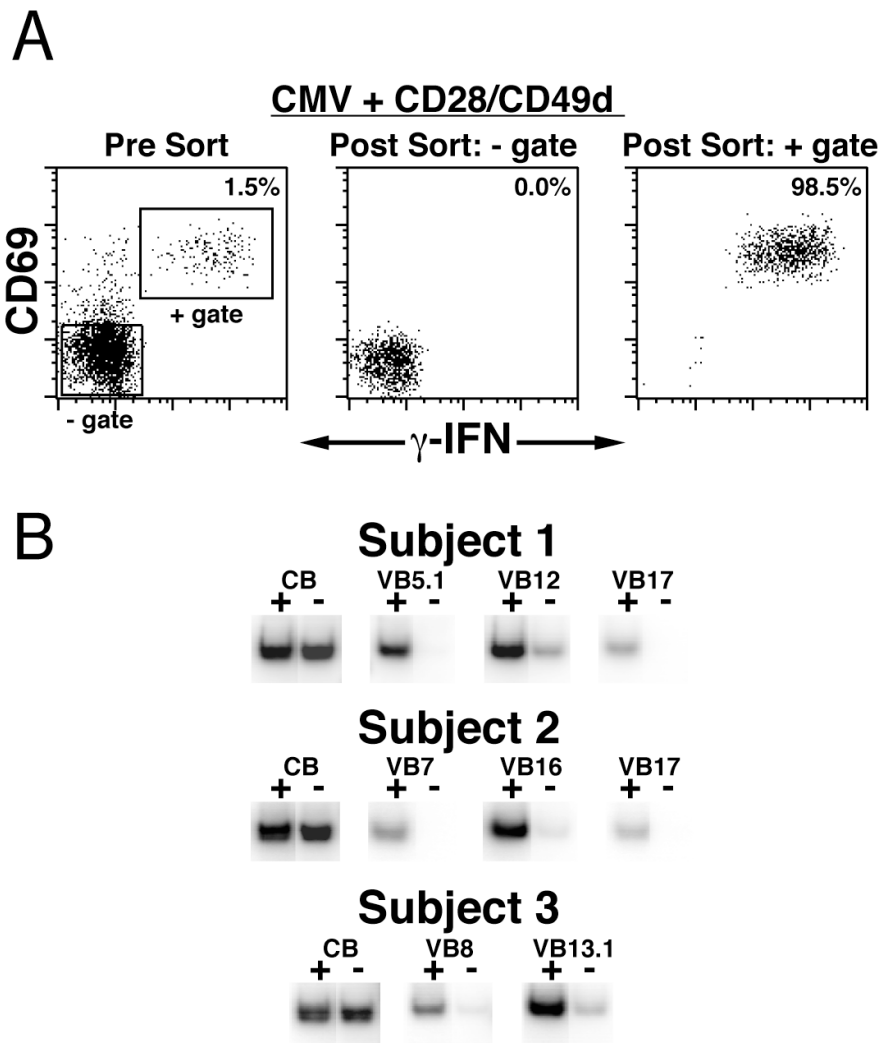

A. PBMCs from CMV-seropositive subject 2 were stimulated with CMV and CD28/CD49d in the presence of Brefeldin A and stained intracellularly for CD4, CD69, and IFN-γ and sorted into CMV-responsive fraction (CD4$^+$/CD69$^+$/IFN-γ$^+$) and CMV-nonresponsive fraction (CD4$^+$/CD69$^-$/IFN-γ$^-$). The dot plots gated on CD4$^+$ small lymphocytes show the pre-sort, negative gate post-sort, and positive gate post sort with 3000, 1000, and 811 events, respectively.

B. The cells from each fraction were lysed and genomic DNA was subjected to semiquantitative PCR for clonotype. TCR BC amplification was used to control for equivalent DNA from positive and negative fractions per reaction.

Taken together, these two approaches provide compelling evidence that the clonotypes identified on the basis of CD69/CD154 or CD69/ surface IFN-γ sorts were CMV-specific. We confirmed this by directly comparing the frequency of the dominant (BV12BJ2.5) clonotype on subject 1 at two different time-points by FACS versus quantitative clonotype PCR. At the first time-point, data from quantitative PCR revealed that BV12BJ2.5 comprised 1.54% of total PBMC and hence ~4.5% of $CD4^+$ T cells. This corresponded with the FACS data in which the $V\beta12^+$ cells had a 4% estimated frequency in the $CD4^+$ T cell population. The data from the second time-point from real-time quantitative PCR revealed that BV12BJ2.5 comprised 1.73% of total PBMCs, also corresponding with the FACS data.

E. The CMV-specific clonotype response to immunodominant epitopes within CMV matrix phosphoprotein pp65

Each $CD4^+$ T cell clonotype probably responds to a single CMV epitope; however, a single epitope may be recognized by more than one clonotype. Therefore, the actual complexity of the CMV-specific $CD4^+$ T cell response might be even less than suggested by the number of CMV-responsive clonotypes. Identification of every epitope that is responsible for eliciting the clonotype response is difficult due to the vast number of possible epitopes within the CMV genome. Since pp65 is a common target of $CD4^+$ T cells, we examined the $CD4^+$

T cell response against pp65 in our 4 subjects. We could detect $CD4^+$ T cell responses against pp65 in all four subjects (Table 1.1). The $CD4^+$ T cell responses to pp65 in subjects 2 and 3 were minor, 0.50% and 0.35%, respectively. However, the $CD4^+$ T cell responses to pp65 in subjects 1 and 4 were large, 2.96% and 1.95%, respectively, thus accounting for 38% and 31% of the total CMV response. Most of the pp65 response in subject 1 and 4 was attributable to single epitopes, amino acids 489-503 for subject 1 and amino acids 509-523 for subject 4.

TABLE 1.1 Contribution of pp65 epitopes to the CMV-specific $CD4^+$ T cell response

	Response to		
Subject	Whole CMV[a] (%)	pp65 protein or total pp65 15mer mix[a,b] (%)	Single pp65 15mer peptides[a,c] (%)
1	7.86	2.96	aa (489–503) –2.74 (509–523) –0.56
2	8.87	0.50	(509–523) –0.35 (417–431) –0.08 (177–191) –0.04
3	3.90	0.35	(507–521) –0.22 (285–299) –0.09
4	6.42	1.95	(509–523) –1.49

a. The percentage of $CD69^+$/IFN-γ^+ within the antigen/peptide stimulated $CD4^+$ T cells; the % $CD69^+$/IFN-γ^+ within the $CD4^+$ T cell subset of control (no antigen)-stimulated cultures.
b. The total pp65 response was determined using purified pp65 protein in subject 2 and the pp65 peptide mix (138 15mers overlapping by 11 aa) in subjects 1, 3, and 4.
c. Determined using overlapping pools of pp65 15mer peptides followed by analysis of all candidate single peptides. Responses observed to adjacent overlapping peptides were considered a single response, with the 15mer peptide providing the highest response considered the "optimal" epitope. All such optimal epitopes are listed.

We used our CFC assay to determine the likelihood of the two identified epitopes, $pp65^{489-503}$ and $pp65^{509-523}$, as targets for the major clonotypes. As shown in Figure 1.9, three of four Vβ families and subfamilies from subject 1 had substantial responses to $pp65^{489-503}$. Interestingly, the dominant family, Vβ12, did not respond to this epitope. In contrast, the response to epitope $pp65^{509-523}$ in subject 4 was exclusively from the dominant Vβ2 family, and the other 3 Vβ families did not contribute.

FIGURE 1.9 Flow cytometric analysis of TCR-Vβ family involvement in subject 1 and 4's $CD4^+$ T cell response to a single immunodominant peptide from CMV pp65 lower matrix phosphoprotein

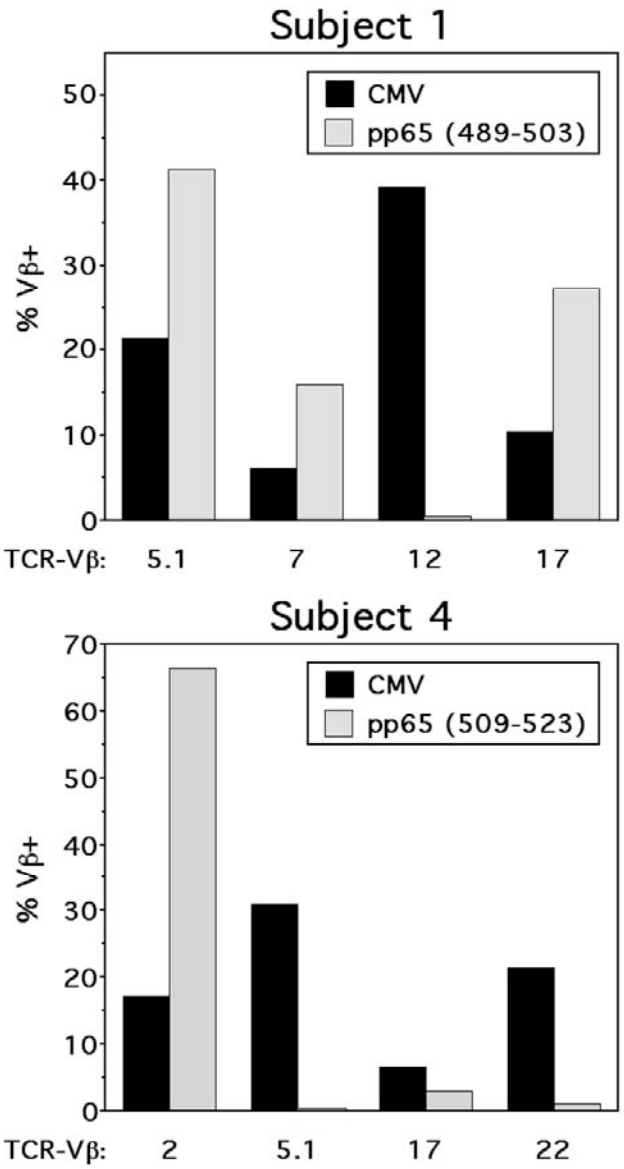

PBMCs from subject 1 and 4 were stimulated with CMV or the subject's specific pp65 immunodominant peptide and CD28/CD49d. The bar graphs depict the % response of each TCR-Vβ to CMV and the immunodominant pp65 peptide.

To confirm that the epitope responses by the Vβ families and subfamilies in subject 1 and 4 were indeed the same clonotypes that we had identified as HCMV-responsive, we stimulated PBMC from subjects 1 and 4 with the appropriate pp65 peptide, isolated the peptide- responsive and peptide-nonresponsive cells using CD154 and CD69 sorting, purified RNA, and performed RT-PCR for CDR3 size analysis. Since Vβ12 did not contribute to the $pp65^{489-503}$ response, it follows that the clonotype would be isolated in the peptide-nonresponsive lane. Indeed, sequence analysis revealed that the BV12BJ2.5 clonotype in the HCMV-nonresponsive lane (Figure 1.10A) is identical to the BV12BJ2.5 clonotype we had identified (Figure 1.6). The largest response to $pp65^{489-503}$ was from Vβ5.1, and sequence analysis revealed an identical sequence as the one identified previously (Figure 1.6). The same was true for BV7 as the 3 sequences identified as $pp65^{489-503}$-responsive were also identical to previously identified sequences in response to HCMV. Additionally, we confirmed the results for subject 1 by stimulating PBMCs from subject 1 with $pp65^{489-503}$ and CD28/CD49d in the presence of Brefeldin A and stained intracellularly for CD4, CD69, and IFN-γ and sorted into $pp65^{489-503}$ -responsive and $pp65^{489-503}$ -nonresponsive fractions. (Figure 1.10B). In subject 4 the $pp65^{509-523}$-responsive cells yielded a single sequence that was identical to the BV2BJ2.2 sequence that was identified with HCMV stimulation (Figure 1.6).

FIGURE 1.10 Molecular analysis of TCR-Vβ-defined clonotype in subject 1 and 4's CD4⁺ T cell response to a single immunodominant peptide from CMV pp65 lower matrix phosphoprotein

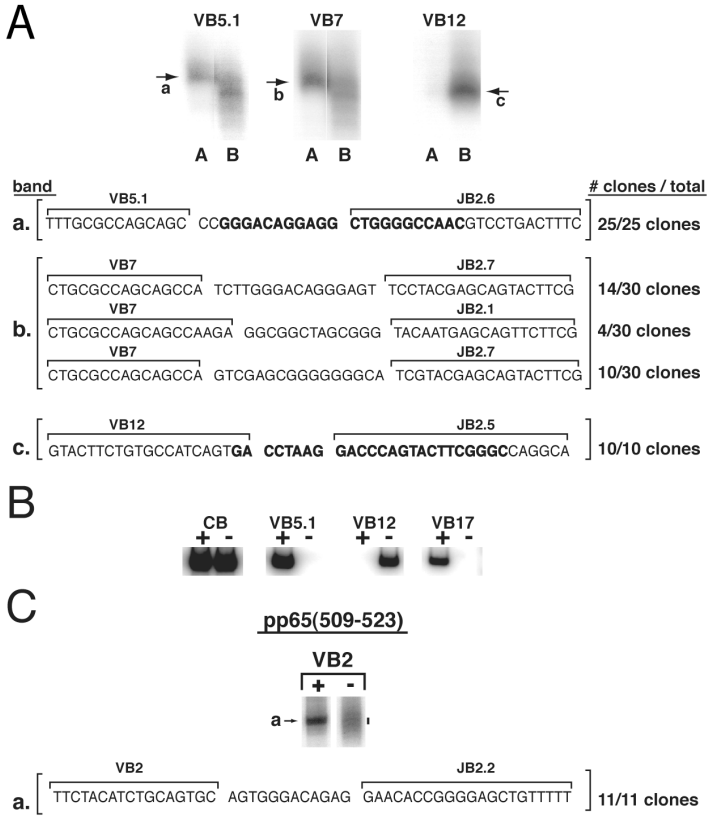

A. PBMCs from subject 1 were stimulated with $pp65^{489\text{-}503}$ and CD28/CD49d and stained on the cell surface for CD4, CD69, and CD40L and sorted. The CMV-responsive and -nonresponsive $CD4^+$ T cells were subjected to RT-PCR CDR3 size analysis. The arrows and small case letters designate bands that were cloned and sequenced.

B. PBMCs from subject 1 were stimulated with $pp65^{489\text{-}503}$ and CD28/CD49d in the presence of Brefeldin A and stained intracellularly for CD4, CD69, and IFN-γ and sorted into $pp65^{489\text{-}503}$ -responsive and $pp65^{489\text{-}503}$ -nonresponsive fractions. The cells from each fraction were lysed and the genomic DNA was PCR amplified with clonotype specific primers.

C. PBMCs from subject 4 were stimulated with $pp65^{509\text{-}523}$ and CD28/CD49d and the cell surface stained for CD4, CD69, and IFN-γ surface capture and sorted into $pp65^{509\text{-}52}$-responsive and $pp65^{509\text{-}52}$-nonresponsive fractions. The isolated RNA from these fractions was subjected to RT-PCR CDR3 size analysis for TCR BV2. The dominant band was cloned and sequenced.

SUMMARY

The goal of this study was to identify, quantify, and confirm the specificity of clonotypes comprising the $CD4^+$ memory T cell response to HCMV using freshly isolated PBMC from HCMV-seropositive subjects. Since *in vitro*-expanded clones or cell lines are subject to differential proliferation and thus lose physiologic significance for conclusions regarding clonality, it was important for us to use fresh PBMCs. In all subjects examined, we found that the $CD4^+$ memory T cell response to HCMV is dominated by 1-3 large clonotypes (each ≥10% of the total response) with multiple subdominant (3-10% of the response) and minor (<3% of the response) clonotypes. The CMV specificity of these clonotypes was confirmed.

We also investigated immunodominant responses to HCMV matrix protein pp65 in two subjects. In subject 1 the response to the immunodominant pp65 peptide was mediated by two subdominant (BV5.1BJ2.6; BV17BJ1.1) and minor (BV7) clonotypes, whereas in subject 4 the response to the immunodominant pp65 peptide was mediated by a single dominant clonotype (BV2BJ2.2).

In conclusion we found that the HCMV-specific $CD4^+$ clonotypic structure in these subjects is highly skewed, implying that long-term control of HCMV probably rests with a handful of clones.

CHAPTER II

CLONOTYPIC STRUCTURE OF THE PRIMARY CD4$^+$ T CELL RESPONSE TO RHCMV IN RHESUS MACAQUES

OBJECTIVE

We have embarked on studies to characterize CD4$^+$ T cell responses to a persistent viral pathogen, CMV. We started our investigation by studying memory CD4$^+$ T cell responses to HCMV in human subjects. We found that the CD4$^+$ memory T cell response to HCMV has a highly skewed clonotypic structure and is dominated by 1-3 large clonotypes and multiple subdominant and minor clonotypes. The results from our first study showed the nature of the CD4$^+$ T cell response long after primary infection. We were interested in understanding how this pattern develops, and hence sought to examine the clonotypic structure, and the number and frequency of CMV-specific CD4$^+$ clonotypes after primary infection. It is unknown whether the CMV-specific CD4$^+$ clonotypes are skewed from the beginning or whether the CD4$^+$ clonotypic structure gets skewed over time such that only a handful of clones are maintained for long-term memory and

control of virus. Do the dominant clonotypes observed in a memory response start out as dominant clonotypes or is there a shift in the size of the clones as some clones are selected for long-term memory?

To study the development of primary T cell responses to CMV and the mechanisms involved in immunological control of the virus, an animal model is necessary. We chose RM as a model to investigate a primary $CD4^+$ T cell response to CMV and the generation of long-term persistent memory T cells. Primate CMVs are closely related, and RhCMV infection is similar to HCMV infection in that almost 100% of captive RMs are CMV-seropositive by the time they are one year old, and the infection is asymptomatic.

The general goal of this project was to study the development of a $CD4^+$ T cell response against a persistent viral pathogen during primary infection and in the setting of a long-term persistent infection. Specifically, we were interested in characterizing the number and frequency of $CD4^+$ clonotypes that develop during a primary response and compare the clonotypic structure of the primary response to the clonotypic structure of a memory response. We also studied the effect of reinfection on these clonotypes.

RESULTS

A. Detection of RhCMV-specific CD4$^+$ T cell responses in a naturally infected Rhesus macaque using the CFC assay

Virtually 100% of captive RMs are infected with RhCMV, and we investigated whether we could detect CD4$^+$ T cell responses to RhCMV utilizing our CFC assay (98). PBMCs from a seven-year-old RM from the colony were stimulated *in vitro* with RhCMV lysate and exogenous costimulation (CD28 and CD49d MAbs) for six hours. The cells were stained for CD3 and CD4 on the cell surface and intracytoplasmic CD69 and TNF-α. Figure 2.1 shows the RhCMV-specific CD4$^+$ T cell response. When PBMCs from this animal were incubated with costimulatory antibodies alone, the CD4$^+$ T cells did not express CD69 or TNF-α, and did not display TCR/CD3 down-regulation. This shows that costimulation alone does not result in activation of CD4$^+$ T cells. In contrast, the activated CD4$^+$ T cells display the characteristic TCR/CD3 down-regulation and express CD69 and TNF-α. The total RhCMV-specific CD4$^+$ T cell response in this animal was 6.54%, which is similar to the frequencies of HCMV-specific CD4$^+$ T cell response observed in humans (45, 57, 100).

FIGURE 2.1 Detection of RhCMV-specific $CD4^+$ T cell responses in a naturally infected RM

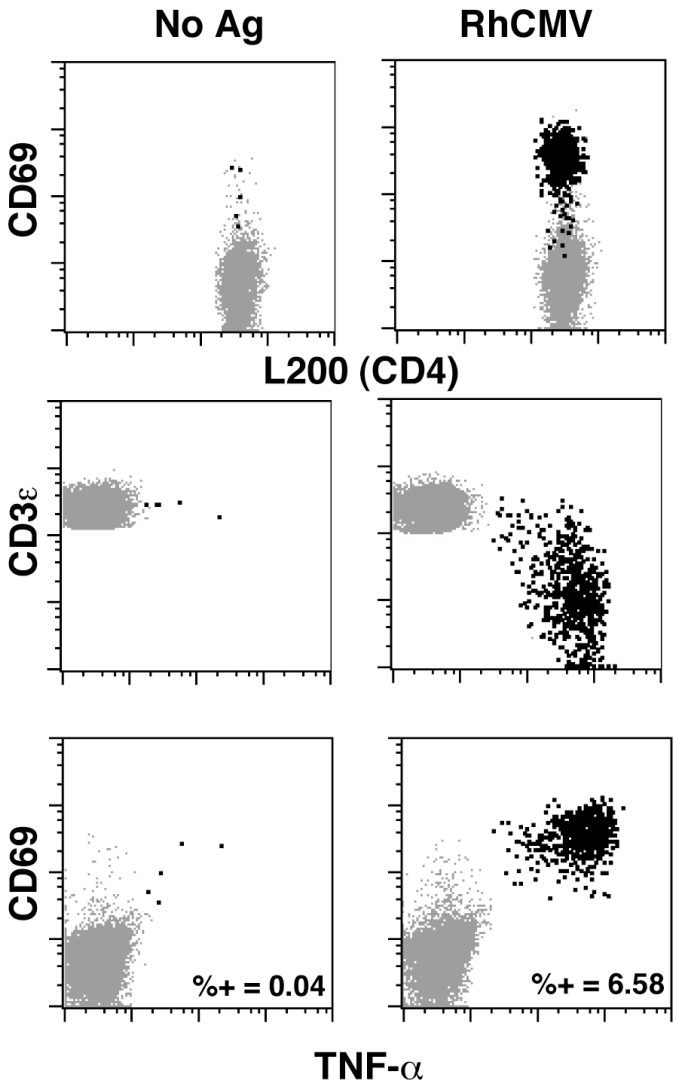

PBMCs from RhCMV seropositive RM were stimulated in vitro with RhCMV preparation and CD28/CD49d or CD28/CD49d alone for 6 hours and in the presence of Brefeldin A for the last five hours. The cells were stained with CD3 and CD4 on the cell surface and for CD69 and TNF-α after fixation and permeabilization. The panels are gated on $CD3^+/CD4^+$ small lymphocytes, with the responding cells highlighted in black and the non-responding cells colored gray. The total $CD4^+$ T cell response to RhCMV in this RM is 6.54%.

B. Development of stimulation and staining protocol to isolate RhCMV-specific CD4$^+$ T cells using FACS

We needed to develop a stimulation and staining protocol for RMs to isolate viable RhCMV-specific CD4$^+$ T cells for mRNA purification and CDR3 size analysis. In the human studies, we described two techniques for sorting viable antigen-specific CD4$^+$ T cells: sorting by coordinate surface staining of CD4, CD69, and CD154 or surface IFN-γ capture. Neither one of these techniques worked in the RMs because the human CD154 and the surface IFN-γ capture antibodies do not cross-react with the RM antigens. Therefore, we embarked on developing a stimulation protocol that would allow us to use other activation markers to cluster viable antigen-responsive CD4$^+$ T cells. We performed a series of simulations and examined the levels of CD25 (IL-2Rα) in conjunction with CD4 and CD69 after different lengths of stimulation. We found that after 48 hours of stimulation with RhCMV lysate and exogenous costimulation there wasan up-regulation of CD69 and CD25 and down-regulation of surface CD3 (Figure 2.2A). Importantly, the 48 hour culture allows for maximal antigen-induced expression of these activation antigens without sufficient time for significant proliferation and the potential for unequal expansion of clonotypes.

FIGURE 2.2 Isolation of viable RhCMV-specific CD4$^+$ T cells for clonotype analysis

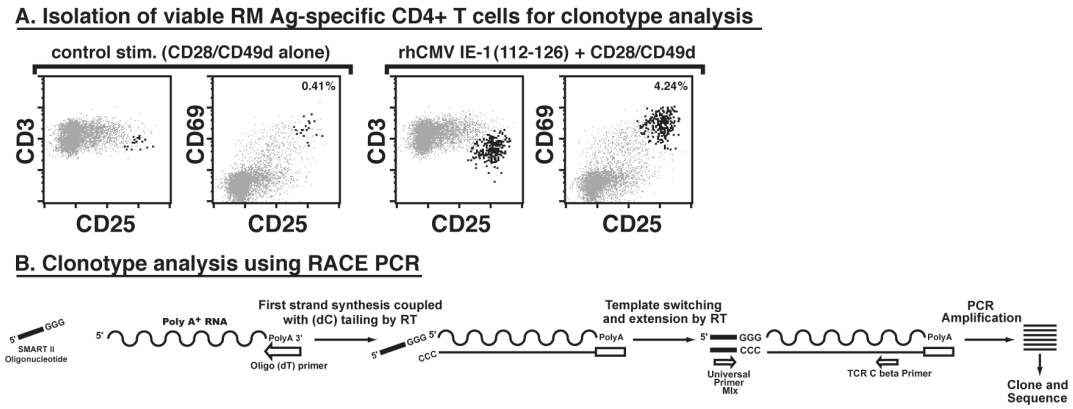

PBMCs from RhCMV seropositive RM were stimulated in vitro with RhCMV preparation and CD28/CD49d for 48 hours. Non-permeabilized cells were stained with CD3, CD4, CD25, and CD69. The panels are gated on CD3$^+$/CD4$^+$ small lymphocytes, with the responding cells highlighted in black and the non-responding cells colored gray. The RhCMV-responsive cells were sorted by FACS. mRNA was isolated from the sorted cells and used to make TCR gene-specific cDNA in a RACE reaction and the cDNA was PCR amplified. The PCR products were gel purified, TA cloned, and submitted for sequencing.

C. CDR3 size analysis via BV RT-PCR: fluorescence verses radioactive

Our next goal was to analyze the clonotypic content of RhCMV-specific $CD4^+$ T cells. Even though genomic DNA sequences for the RM TCR genes aren't available in public databases, a panel of 25 TCR BV primers have been designed based on cDNA sequences (92), allowing us to use these primers and perform CDR3 size analysis via PCR amplification and primer extension in run-off reactions. First, we optimized and/or redesigned the BV primers (Material and Methods, Table 2) and the PCR reaction using total RNA purified from 50 million RM neonate thymocytes. After several attempts we were able to redesign and optimize the 25 TCR BV primers so that they amplified RM neonate thymocyte cDNA. However, the amount of amplified product for each BV primer varied, probably due to variable amplification efficiency.

Next, we stimulated PBMCs from an RhCMV-seropositive RMs for 48 hours with RhCMV and exogenous costimulation, stained with CD4, CD25, and CD69, sorted the RhCMV-responsive and -nonresponsive cells, and purified RNA from the sorted populations, PCR reactions were set up for each BV primer (25 total) and 1 μl of each PCR reaction was used in a run-off reaction that included a 3' fluorescent primer. 1.5 μl of the run-off reaction was loaded onto a 377 DNA sequencer (Applied Biosystems). The data from each fluorescent band within a BV family or subfamily is analyzed via the immunoscope software, and depicted

as peaks. The bands of a BV family or subfamily in a normal T cell repertoire appear as peaks with a Gaussian distribution, each peak representing a CDR3 region with a specific length and each peak differing in size by 3 nucleotides (1 amino acid) from its neighboring peak. The size of each peak is representative of the amount of product, and the most abundant CDR3 regions are the peaks in the middle. For antigen-specific T cells with a focused response, instead of a Gaussian distribution of peaks for a given BV family or subfamily, a single peak may be apparent, which would mean that one or few clonotypes with the same size CDR3 region are responding to the antigen.

We performed the CDR3 size analysis on the sorted population and did not detect many BV families or subfamilies (data not shown). We decided to check the results by performing the same analysis using radioactivity and autoradiography. Even though more responsive BV families and subfamilies are detectable with radioactive CDR3 size analysis due to enhanced sensitivity of radioactivity, we still were not satisfied that the CMV-responsive TCR BV analysis was exhaustive of the whole repertoire because CDR3 size analysis via BV RT-PCR has some limitations. The BV primers are not comprehensive, there is a potential for cross-reactive amplification, and the efficiency of each primer pair is not similar. Therefore, we decided to pursue a different technique for clonotype analysis.

D. Clonotype analysis via RACE-PCR

RACE allows the comprehensive amplification of the gene(s) of interest in an anchored RT-PCR using a modified version of the SMART procedure and a gene-specific TCRB primer at the 3' end of the gene (94). This technique would allow us to analyze the clonotypic content of responsive BV families and subfamilies with similar efficiency and without any cross-reactivity. PBMCs from RhCMV-seropositive RMs were stimulated using our 48 hour stimulation procedure, the antigen-specific $CD4^+$ T cells were sorted based on coordinate expression of CD4, CD25, and CD69, and mRNA was extracted using the Qiagen Oligotex kit. Anchored RT-PCR using a modified version of the SMART procedure and a gene-specific TCRB primer at the 3' end of the gene was performed and the PCR product was ligated into the pGEM T Easy vector and used to transform bacteria. Colonies were picked, amplified, and submitted for sequencing (Figure 2.2B).

E. Using RACE-PCR to determine the TCR BV diversity in the $CD4^+$ T cell response to RhCMV in six healthy, middle-aged and old RhCMV-seropositive RMs with a persistent RhCMV infection

We sought to examine the complexity of the RhCMV-specific $CD4^+$ T cell response in RMs with a persistent RhCMV infection. PBMCs from persistently infected RMs with robust CMV-specific $CD4^+$ T cell responses (Table 2.1) were

stimulated in our 48-hour assay, stained, and sorted. mRNA was isolated from RhCMV-responsive cells and used to make TCR gene-specific cDNA in a RACE reaction and the cDNA was PCR amplified. The PCR products were gel-purified, TA-cloned, and submitted for sequencing. The sequence results (Table 2.2) for the old and middle-aged RM depict a very similar CMV-specific $CD4^+$ memory T cell clonotypic structure that is oligoclonal with 1-2 clonotypes dominating the response. The evaluation of the 4 middle-aged RMs at the second time-point revealed that the oligoclonal hierarchy is stable.

TABLE 2.1 RhCMV-specific CD4$^+$ T cell responses in four middle-aged and two aged RhCMV-seropositive RM with a persistent RhCMV infection

RM	Age (years)	RhCMV-Specific Response (% of CD4+ T Cells)
19145	8	5.17
19279	8	4.93
18290	9	4.22
20027	6	2.83
04507	33	2.54
08919	25	5.31

TABLE 2.2 Determination the TCR BV diversity in the CD4$^+$ T cell response to RhCMV in RM with a persistent RhCMV infection

MIDDLE-AGE RM

	TIMEPOINT #1				TIMEPOINT #2			
19145	TCRBV	CDR3	TCRBJ	%freq	TCRBV	CDR3	TCRBJ	%freq
	2.2	CSAISRTAQETQY	2.5	47	2.2	CSAISRTAQETQY	2.5	42
	13.3	CASSVSTGGQSAQLF	2.2	45	4.1	CSVEGTGDTQY	2.4	20
	4.1	CSVEGTGDTQY	2.4	7	5.1	CASSLVGSAGTTAQLF	2.2	17
	12.3	CASRSPTNEKLF	1.4	1	12.3	CASRSPTNEKLF	1.4	11
					13.3	CASSVSTGGQSAQLF	2.2	4
					2.2	CSARSGGDTAQLF	2.2	2
					5.1	CASSPAGGSFEQY	2.7	2
					22.1	CASSPRTGFDYT	1.2	2
19279	2.2	CSATPGANTAQLF	2.2	67	2.2	CSATPGANTAQLF	2.2	77
	13.3	CASRLERDNYDYT	1.2	21	13.3	CASRLERDNYDYT	1.2	7
	2.2	CSARVLEGTGHYT	1.2	3	2.2	CSARVLEGTGHYT	1.2	5
	10.1	CASSTSWGGARYNEQF	2.1	3	10.1	CASSTSWGGARYNEQF	2.1	3
	1.1	CASSPDRVNDYT	1.2	2	1.1	CASSPDRVNDYT	1.2	3
	2.2	CSARTGTVAQY	2.3	2	23.1	CASSRPGGGLQETQY	2.5	3
	13.3	CASRRQGGQETQY	2.5	2	2.2	CSARETGGLNEQF	2.1	2
18290	2.2	CSARETAREQY	2.7	77	2.2	CSARETAREQY	2.7	60
	14.1	CASRLGGTYTKNYNEQF	2.1	10	19.1	CASSQSGQTNEKLF	1.4	35
	19.1	CASSQSGQTNEKLF	1.4	10	9.2	CASSQDFRPDSPLH	1.6	2
	12.3	CASSESGVSTDPQY	2.3	3	9.2	CASSRPSGGASQNTQY	2.4	2
20027	14.1	CASSTQMRWGNQNTQY	2.4	55	14.1	CASSTQMRWGNQNTQY	2.4	76
	6.1	CASSSYSGWRSYEQY	2.7	16	2.2	CSAGNRNTQY	2.4	11
	2.2	CSAGNRNTQY	2.4	9	2.2	CSARDRGFGDYT	1.2	11
	6.5	CASSPRVSGASVLT	2.6	6	6.8	CASSLGGSRQNTQY	2.4	2
	2.2	CSARDRGFGDYT	1.2	3				
	7.1	CASSQPGRGYDYT	1.2	2				
	14.1	CASSIGTGDTAQLF	2.2	2				
	4 SINGLE CLONOTYPES							

OLD RM (NECROPSY)

04507	13.3	CASSEVGRGGSQNTQY	2.4	54
	21.2	CASSSLGVSYEQY	2.7	28
	9.2	CASSQDLPTGQYEQY	2.7	17
	22.1	CASATGGNQETQY	2.5	1
08919	7.1	CASSQDSVTDPQY	2.3	43
	19.1	CASSPYRPDDPGTNSNQ	1.5	22
	13.3	CASSVPGHSSYEQY	2.7	9
	9.2	CASSSGGSFPAQY	2.5	6
	6.1	CASSQTRPGQGEAF	1.1	6
	13.3	CASSEKVGWGGNRIEQY	2.7	4
	13.3	CASRDRVRWGTGAETQY	2.5	4
	4 SINGLE CLONOTYPES			

Two time points were analyzed for the 4 middle-aged RM and the two aged RM were analyzed at necropsy. For the 4 middle-aged RM, the percent frequency of identical clonotypes at each time point are highlighted with the same color. Percent frequency is calculated as follows: (number of clonotype / number of sequences examined) x 100.). In all 6 RM studied, the RhCMV-specific CD4$^+$ memory T cell population was oligoclonal, containing a 1-3 dominant and a total of 4-11 different TCRB CDR3 sequences.

F. Confirmation of the CMV-specificity of the clonotypes found by RACE-PCR

Because we used surrogate cell surface markers to isolate the CMV-responsive cells for RACE-PCR and sequence analysis, we needed to confirm the CMV-specificity of the identified clonotypes. The sequence results allowed us to design clonotype-specific PCR primers to amplify rearranged TCR DNA. Therefore, since the fixation and permeabilization process in the CFC assay does not alter genomic DNA, we could isolate $CD4^+$ CMV-responsive and CMV-nonresponsive cells based on the expression of CD69 and TNF-α.

We designed clonotype-specific primers such that the 5' primer would anneal in the BV region of the rearranged TCR gene, and the 3' primer would anneal in the CDR3 region of the rearranged TCR gene, thus making the primer pair clonotype-specific. Each primer pair was analyzed for specificity (Figure 2.3A) to ensure that the primer pair only amplifies DNA from the RM it was designed for. Control primers in the BC region were used to show that equivalent DNA was used in each PCR reaction.

To confirm the CMV specificity of the clonotypes, we used our conventional CFC assay and sorted the CMV-responsive and CMV-nonresponsive $CD4^+$ T cells based on the expression of CD69 and TNF-α.

FIGURE 2.3 Confirmation of the CMV-specificity of the clonotypes found by RACE-PCR

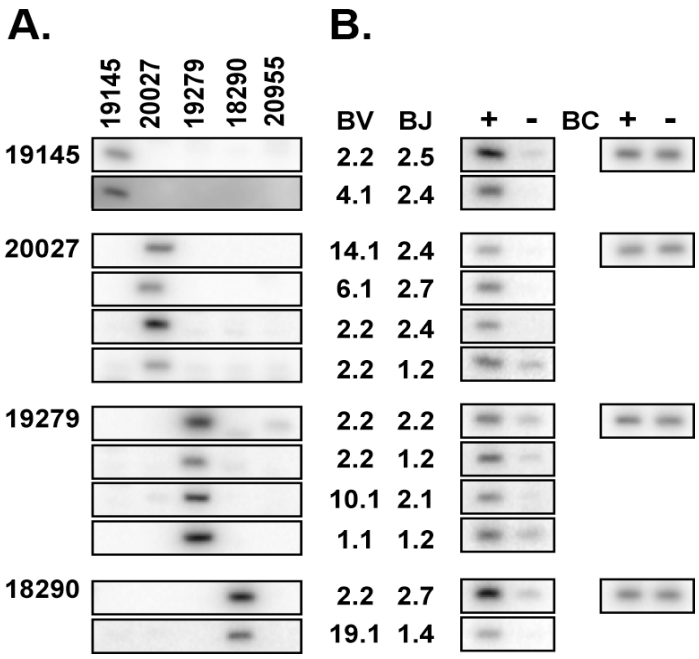

A. Clonotype-specific primers were designed such that the 5' primer would anneal in the BV region of the rearranged TCR gene and the 3' primer would anneal in the CDR3 region of the rearranged TCR gene thus making the primer pair clonotype-specific. Each primer pair only amplified target DNA in the appropriate RM, confirming the specificity of the reaction.

B. To check the RhCMV-specificity of the clonotypes PBMCs from RhCMV seropositive RMs were stimulated in vitro with RhCMV preparation and CD28/CD49d for 6 hours and in the presence of Brefeldin A for the last five hours and sorted into CMV-responsive fraction ($CD4^+/CD69^+/TNF\text{-}\alpha^+$) and CMV-nonresponsive fraction ($CD4^+/CD69^-/$ $TNF\text{-}\alpha^-$). The cells from each fraction were lysed and genomic DNA was subjected to semiquantitative PCR using the clonotype-specific primers. TCR BC was used to control for equivalent DNA from positive and negative fractions in each reaction. The clonotypes highly were enriched in the CMV-responsive fraction for each RM thus confirming the CMV specificity of the clonotypes found by RACE-PCR.

We then performed PCR using the clonotype-specific primers and found the clonotypes highly enriched in the CMV-responsive fraction (Figure 2.3B), thus confirming the CMV specificity of the clonotypes identified via RACE-PCR.

G. Description of primary RhCMV infection RM cohort

We selected a group of 4 CMV-seronegative RMs to infect with RhCMV and study the $CD4^+$ T cell clonotypic structure-post primary infection. The 68-1 strain of RhCMV was used to infect our primary infection cohort. A real-time quantitative PCR assay was used to detect and quantify RhCMV in samples collected weekly, including blood (PBMC), lung lavage, and buccal swabs (saliva). Cell-associated virus was detected in blood (Figure 2.4) at day 42 post-infection (pi) in 3 of 4 animals, and in lung lavage (Figure 2.5) virus was detected by day 28 pi for 2 animals, and day 42 pi and 56 pi for the other 2 animals. In 3 of 4 animals virus detection was declining by day 56 pi, with the fourth animal displaying persistent viral replication through day 182 pi. The buccal swab (Figure 2.6) for one animal was positive for virus at day 21pi and for the other 3 animals at day 42 pi. All 4 animals' buccal swabs remained virus-positive from day 70 pi through all the days we examined.

FIGURE 2.4 RhCMV viral load in blood

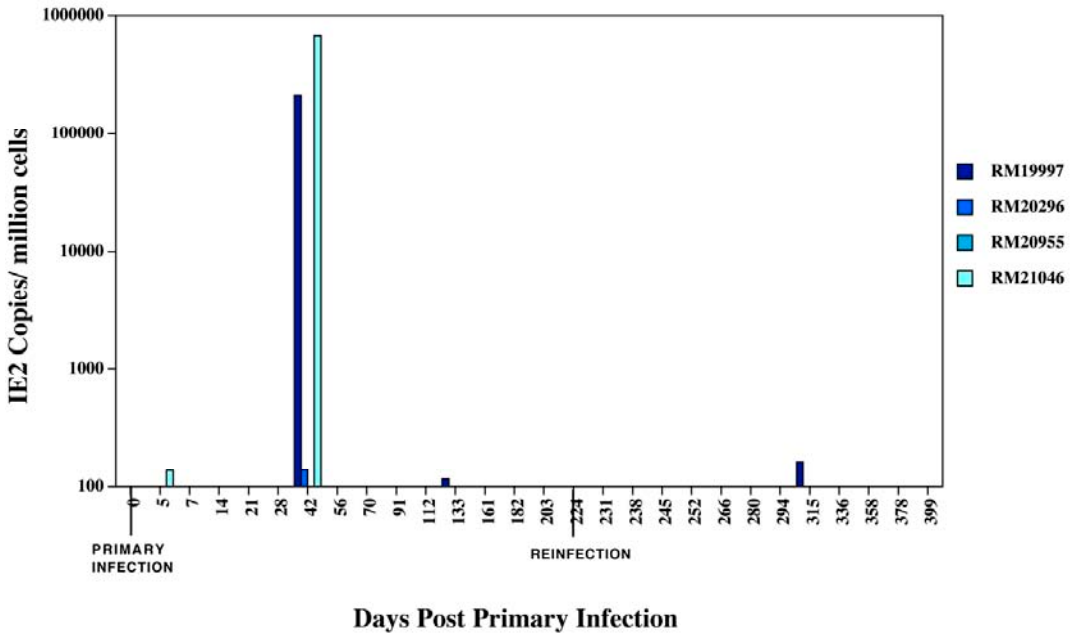

A real time quantitative PCR assay was used to detect cell associated RhCMV copies in PBMC. The number of viral copies per one million cells are graphed for each time point.

FIGURE 2.5 RhCMV viral load in lung

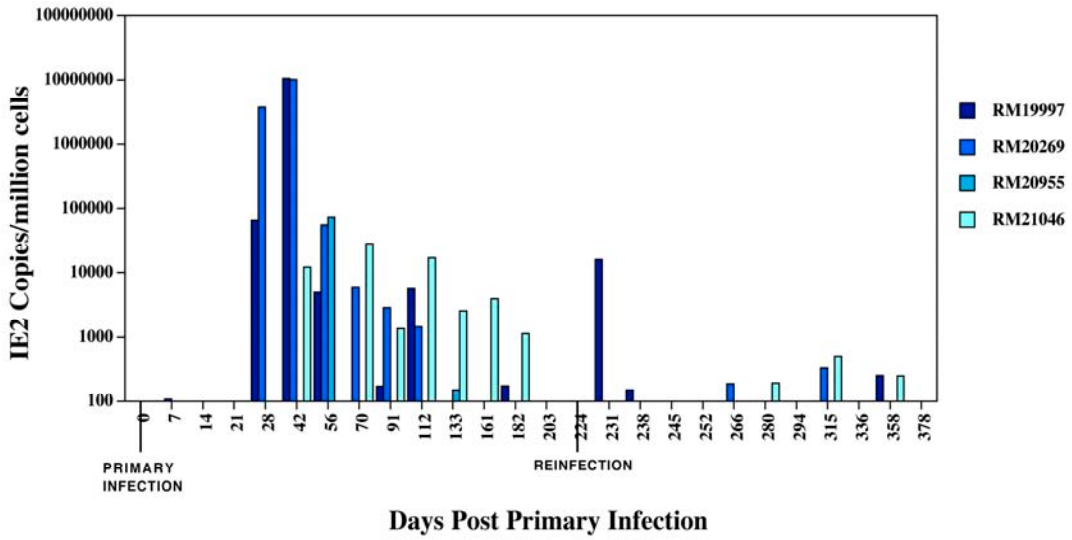

A real time quantitative PCR assay was used to detect cell associated RhCMV copies in lung lavage cells. The number of viral copies per one million cells are graphed for each time point.

FIGURE 2.6 RhCMV viral load in buccal swab samples

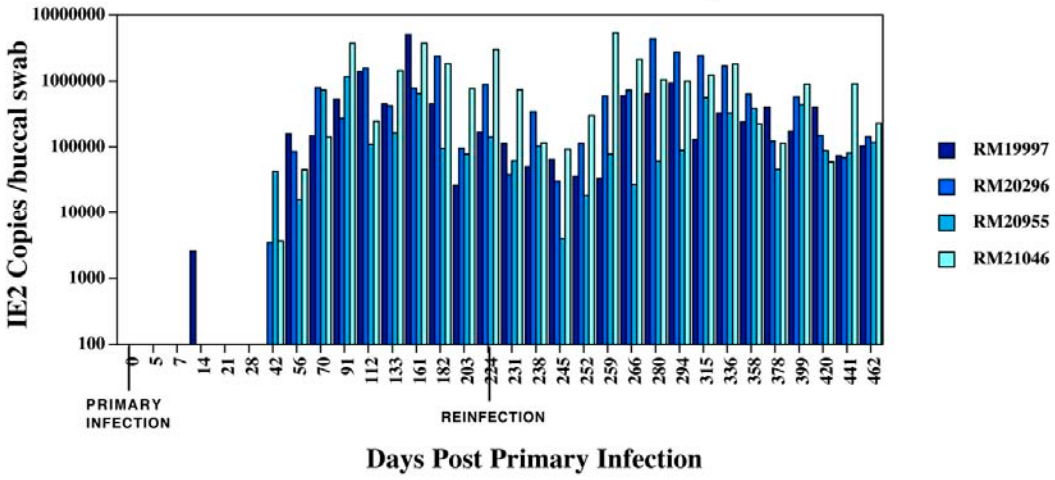

A real time quantitative PCR assay was used to detect cell free RhCMV copies in buccal swab samples. The number of viral copies per buccal swab are graphed for each time point.

FIGURE 2.7 RM1997 RhCMV-specific $CD4^+$ T cell responses in PBMC

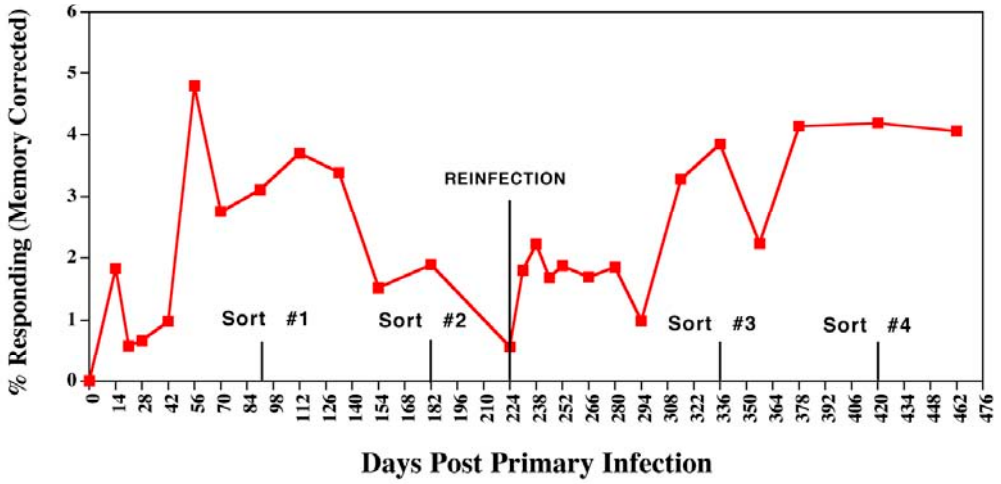

PBMCs from RhCMV seropositive RM were stimulated in vitro with RhCMV and CD28/CD49d in the presence of Brefeldin A. The cells were stained for CD3 and CD4 on the cell surface and intracellular CD69 and TNF-α. The percent response in $CD3^+/CD4^+$ small lymphocytes was determined by the coordinate expression of intracytoplasmic CD69 and TNF-α. The percent response is reported after memory correction (percent response / percent memory).

FIGURE 2.8 RM20296 RhCMV-specific $CD4^+$ T cell responses in PBMC

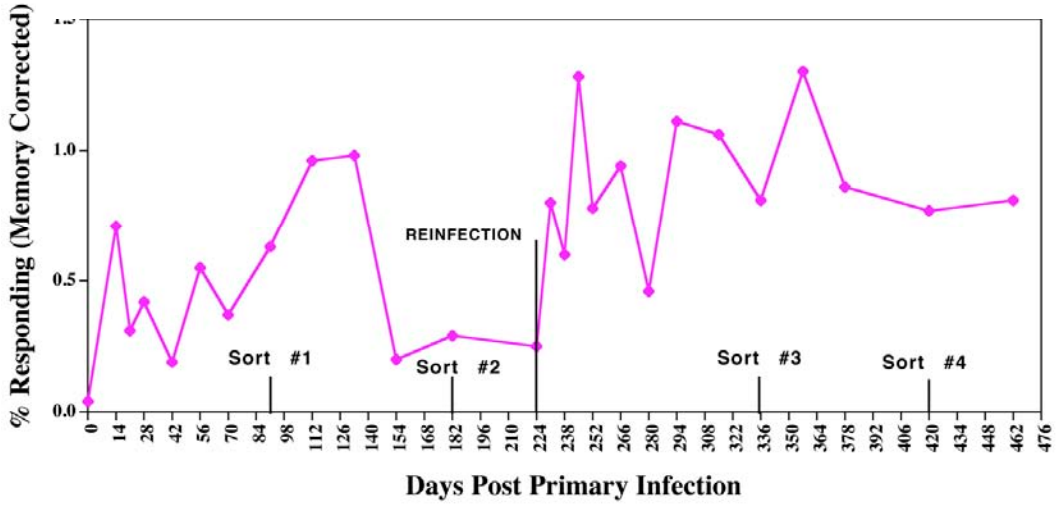

PBMCs from RhCMV seropositive RM were stimulated in vitro with RhCMV and CD28/CD49d in the presence of Brefeldin A. The cells were stained for CD3 and CD4 on the cell surface and intracellular CD69 and TNF-α. The percent response in $CD3^+/CD4^+$ small lymphocytes was determined by the coordinate expression of intracytoplasmic CD69 and TNF-α. The percent response is reported after memory correction (percent response / percent memory).

FIGURE 2.9 RM20955 RhCMV-specific CD4⁺ T cell responses in PBMC

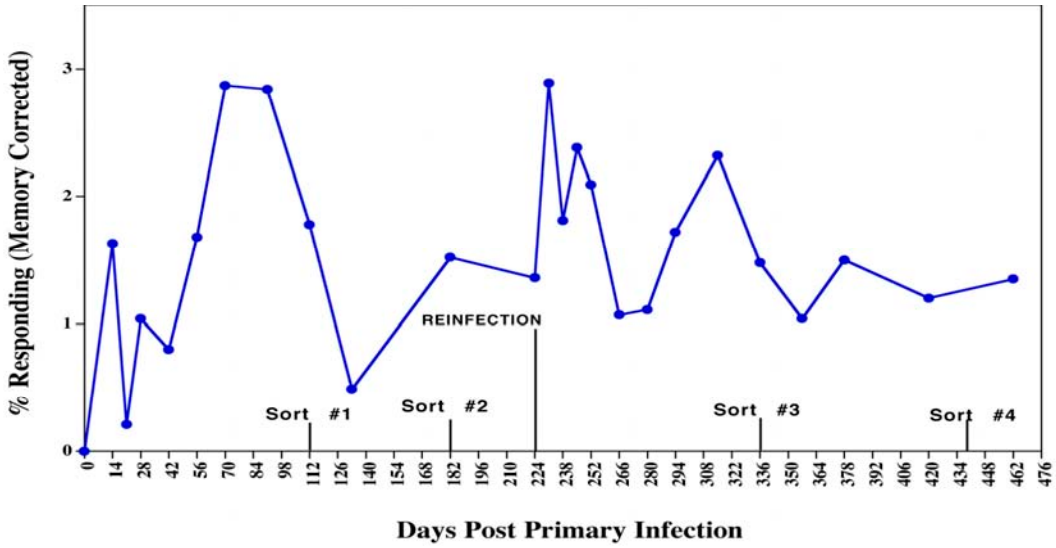

PBMCs from RhCMV seropositive RM were stimulated in vitro with RhCMV and CD28/CD49d in the presence of Brefeldin A. The cells were stained for CD3 and CD4 on the cell surface and intracellular CD69 and TNF-α. The percent response in $CD3^+/CD4^+$ small lymphocytes was determined by the coordinate expression of intracytoplasmic CD69 and TNF-α. The percent response is reported after memory correction (percent response / percent memory).

FIGURE 2.10 RM21046 RhCMV-specific CD4$^+$ T cell responses in PBMC

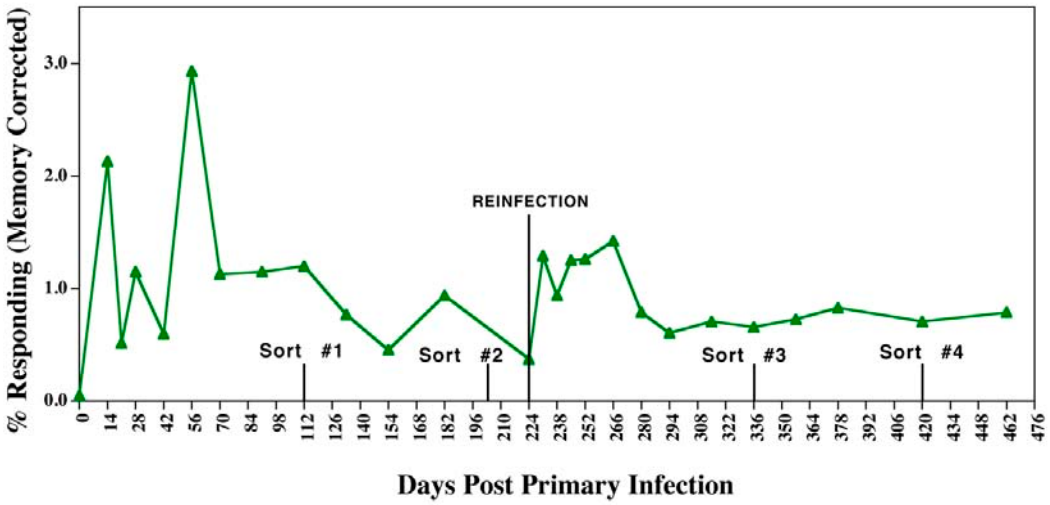

PBMCs from RhCMV seropositive RM were stimulated in vitro with RhCMV and CD28/CD49d in the presence of Brefeldin A. The cells were stained for CD3 and CD4 on the cell surface and intracellular CD69 and TNF-α. The percent response in CD3$^+$/CD4$^+$ small lymphocytes was determined by the coordinate expression of intracytoplasmic CD69 and TNF-α. The percent response is reported after memory correction (percent response / percent memory).

FIGURE 2.11 RM1997 RhCMV-specific $CD4^+$ T cell responses in lung

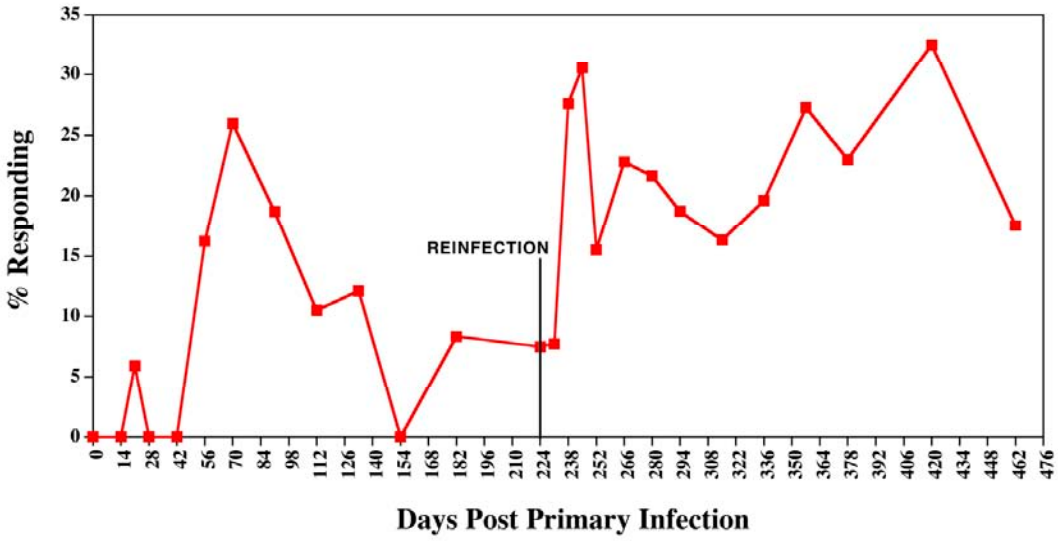

Lung cells from RhCMV seropositive RM were stimulated in vitro with RhCMV and CD28/CD49d in the presence of Brefeldin A. The cells were stained for CD3 and CD4 on the cell surface and intracellular CD69 and TNF-α. The percent response in $CD3^+/CD4^+$ small lymphocytes was determined by the coordinate expression of intracytoplasmic CD69 and TNF-α.

FIGURE 2.12 RM20296 RhCMV-specific $CD4^+$ T cell responses in lung

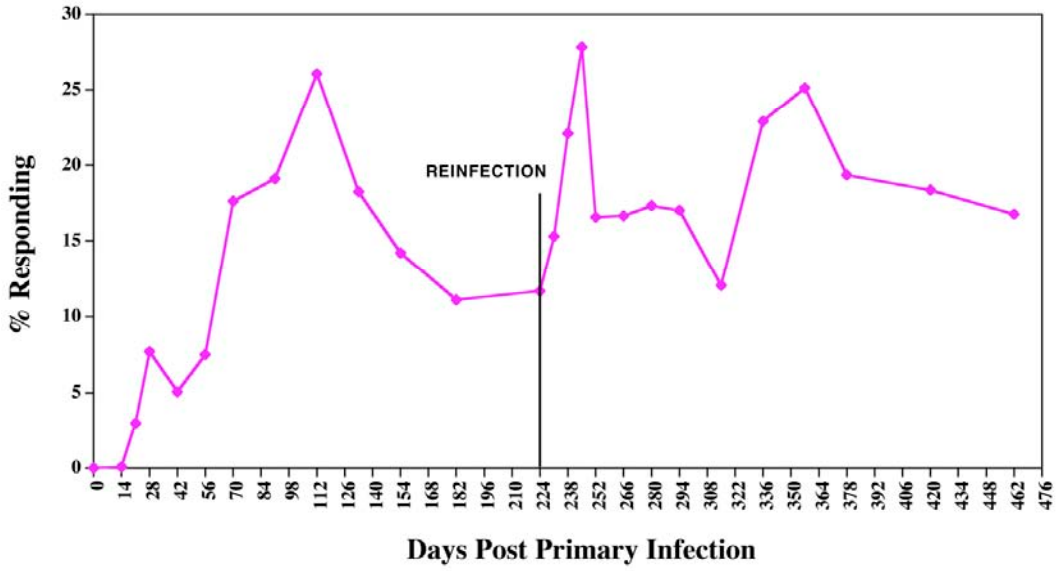

Lung cells from RhCMV seropositive RM were stimulated in vitro with RhCMV and CD28/CD49d in the presence of Brefeldin A. The cells were stained for CD3 and CD4 on the cell surface and intracellular CD69 and TNF-α. The percent response in $CD3^+/CD4^+$ small lymphocytes was determined by the coordinate expression of intracytoplasmic CD69 and TNF-α.

FIGURE 2.13 RM20955 RhCMV-specific $CD4^+$ T cell responses in lung

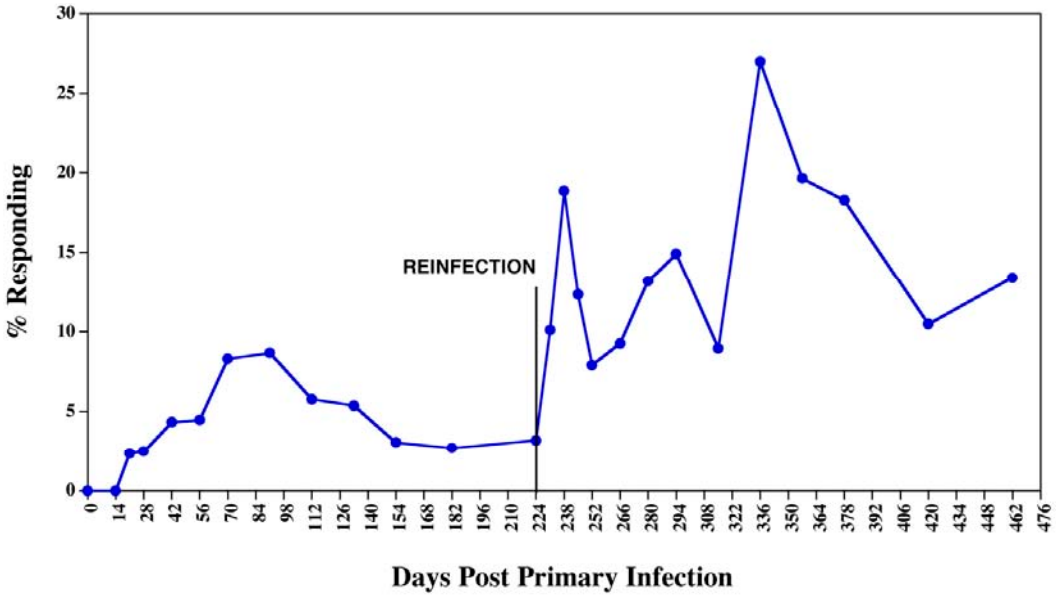

Lung cells from RhCMV seropositive RM were stimulated in vitro with RhCMV and CD28/CD49d in the presence of Brefeldin A. The cells were stained for CD3 and CD4 on the cell surface and intracellular CD69 and TNF-α. The percent response in $CD3^+/CD4^+$ small lymphocytes was determined by the coordinate expression of intracytoplasmic CD69 and TNF-α.

FIGURE 2.14 RM21046 RhCMV-specific $CD4^+$ T cell responses in lung

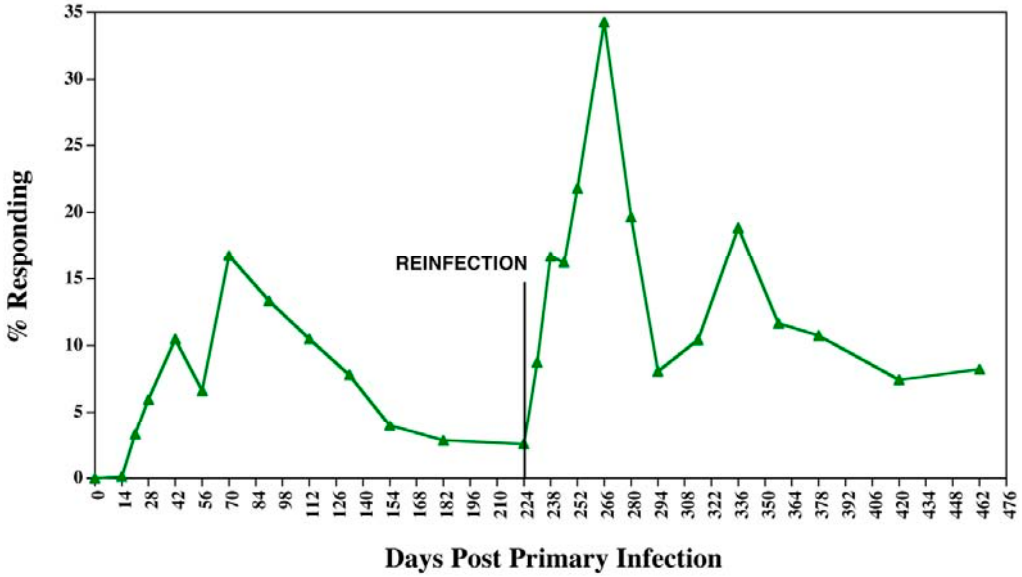

Lung cells from RhCMV seropositive RM were stimulated in vitro with RhCMV and CD28/CD49d in the presence of Brefeldin A. The cells were stained for CD3 and CD4 on the cell surface and intracellular CD69 and TNF-α. The percent response in $CD3^+/CD4^+$ small lymphocytes was determined by the coordinate expression of intracytoplasmic CD69 and TNF-α.

Additionally, we followed the generation of the $CD4^+$ T cell response to RhCMV in these four RMs. Blood and lung lavage samples were collected weekly following infection. CMV-specific $CD4^+$ T cells were present by day 14 pi in both blood and lung (Figures 2.7 –2.14). CMV-specific $CD4^+$ T cell responses in blood appeared to fluctuate between 1-5% of memory cells, and in the lung lavage the CMV-specific $CD4^+$ T cell responses peaked up to 25% between day 60 pi and day 90 pi and then returned to ~5% by day 182 pi. The 4 RMs were reinfected on day 224 pi and a boost in the $CD4^+$ T cell response was apparent in all 4 animals. The response boost was more impressive in the lung compared to blood. In the lung the response boost was higher than the peak response after primary infection and 3 of 4 animals had 30-35% $CD4^+$ T cell response frequencies. The fourth, RM20295, had ~20% response frequency after reinfection, which was lower than the response boost in the other three RM, but impressive when compared to its peak response (~7%) after primary infection. In PBMCs, the RhCMV-specific primary response frequencies of $CD4^+$ T cells was biphasic and after reaching the second peak, the frequencies oscillated and plateaued. After reinfection, the RhCMV-specific primary response frequencies of $CD4^+$ T cells was also biphasic with a higher peak and appeared to oscillate and level off at a higher plateau.

We also examined Ki67 expression in CMV-specific $CD4^+$ T cells (Figure 2.15). Proliferating cells in the late G1, S, and G2/M phases of the cell cycle

expressed Ki67 antigen. During the acute phase of the reinfection, the majority of CMV-specific $CD4^+$ T cells were undergoing proliferation. This will be further discussed in conjunction with the TCR BV clonotype analysis.

H. Using RACE-PCR to determine TCR BV diversity in the $CD4^+$ T cells response after primary infection with RhCMV

We used RACE-PCR to study the clonotypic complexity of the primary response. PBMC from primary infected RMs were stimulated in our 48 hour assay, stained, and sorted. mRNA was isolated from RhCMV-responsive cells and used to make TCR gene-specific cDNA in a RACE reaction; the cDNA was PCR-amplified. The PCR products were gel-purified, TA-cloned, and submitted for sequencing. The RACE-PCR analysis was performed on day 112 pi and day 182 pi for three of four RMs and the fourth, RM21046, was analyzed on day 112 pi and day 203 pi. Sequence analysis of this cohort on day 112 pi revealed 22 to 28 RhCMV-responsive clonotypes per RM (Table 2.3A & B).

FIGURE 2.15 RM19997 proliferative status of CMV-specific CD4$^+$ T cells

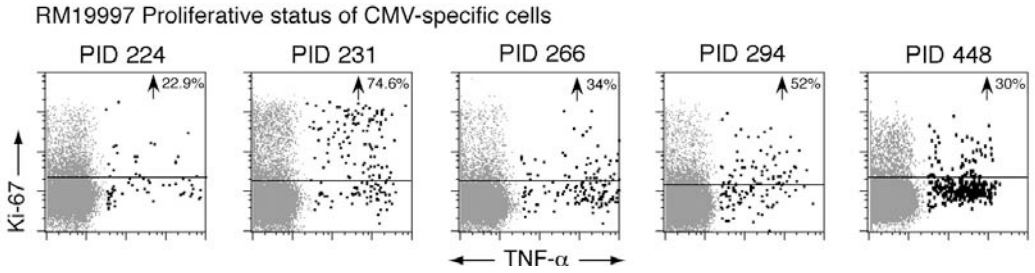

PBMCs from RhCMV seropositive RM were stimulated in vitro with RhCMV preparation and CD28/CD49d for 6 hours and in the presence of Brefeldin A for the last five hours. The cells were stained for CD3 and CD4 on the cell surface and for Ki-67 and TNF-□ after fixation and permeabilization. The panels are gated on CD3$^+$/CD4$^+$ small lymphocytes, with the responding cells highlighted in black and the non-responding cells colored gray. The percentage of proliferating cells measured by the cell cycle marker Ki-67 is indicated in the upper right corner of each panel.

TABLE 2.3A Determination of TCR BV diversity in the developing CD4$^+$ T cell response against RhCMV after primary infection and reinfection (RM19997 and RM20296)

PRIMARY INFECTION						REINFECTION					
TIMEPOINT #1				TIMEPOINT #2		TIMEPOINT #3				TIMEPOINT #4	
TCRBV	CDR3	TCRBJ	%freq	TCRBV	CDR3	TCRBJ	%freq	TCRBV	CDR3	TCRBJ	%freq
RM19997											
8.1	CASSSAGTLYDYT	1.2	31	22.1	CASSEGTATNEKLF	1.4	27	8.1	CASSSAGTLYDYT	1.2	36	6.2	CASSQFRGEENQPQY	1.5	31
22.1	CASSEGTATNEKLF	1.4	10	2.2	CSARAPGGTTDPQY	2.3	23	2.2	CSVPGLGGNSYEQY	2.1	10	7.1	CASSQDVVQETQY	2.5	19
22.1	CASSRDRYYEQY	2.7	8	2.2	CSARIIQGGPNEQGGPNEQF	2.1	15	6.2	CASSQFRGEENQPQY	1.5	7	12.3	CASSVGLASYNEQF	2.1	12
13.4	CASRPDWGRDEQF	2.1	8	22.1	CASSAGNQNTQY	2.4	13	22.1	CASSEGTATNEKLF	1.4	7	22.1	CASSEDLGYEQQY	2.7	8
1.1	CASSLGLGGAIGAQLF	2.2	4	7.1	CASSQNVKGQTQY	2.5	10	7.1	CASSQDVVQETQY	2.5	7	2.2	CSARKVGASVLT	2.6	4
2.2	CSARHYRGGGGNTVY	1.3	4	21.2	CASSSNRRGRTDPQY	2.3	8	6.1	CASSIDRGNEQF	2.1	5	6.5	CASSLGGRGPSGNTVY	1.3	4
22.1	CASSETTGAGNTVY	1.3	4	2.2	CSARVAATDSPLY	1.6	3	7.1	CASSQELGGAGASVLT	2.6	3	22.1	CASSEVTGHQNTQY	2.4	4
6.5	CASSLAAPGNQPQY	1.5	2					12.3	CASSPKETGSNQPQY	1.5	3	13.3	CASSEGGNTVY	1.3	2
14 orphan clonotypes								22.1	CASSEVTGHQNTQY	2.4	3	9 orphan clonotypes			
								6.5	CASSLAAPGNQPQY	1.5	2				
								13.3	CASSEGGNTVY	1.3	2				
								11orphan clonotypes							
RM20296											
7.1	CASSPRPISGNTVY	1.3	41	19.1	CASSYLGRTLQQY	2.7	19	13.3	CASSWGTGGDEQY	2.7	24	7.1	CASSPRPISGNTVY	1.3	26
7.1	CASSPRQISGNTVY	1.3	9	20.1	CAWNRGVYNEQF	2.1	18	13.3	CASSEVGGGETQY	2.5	19	6.5	CASSSDRITEAF	1.1	12
7.1	CASSLERGEKLF	1.4	7	9.2	CASSRTYESSYEQY	2.7	14	1.1	CASSEASAGGRYEQY	2.7	11	13.3	CASSEVGGGETQY	2.5	12
7.1	CASSQDHTAQNTQY	2.4	4	13.3	CASKLDKNTEAF	1.1	14	2.2	CSARWTGKNYDYT	1.2	9	13.3	CASSEGPRYT	1.2	10
2.2	CSARGGWDDYT	1.2	4	8.1	CASSLQTGISAYNEQF	2.1	12	5.1	CASSLTGGTTEAF	1.1	8	5.1	CASSPGQWGDPQY	2.3	9
7.1	CASSQDSWNTEAF	1.1	4	14.1	CASSLSRGEGTEAF	1.1	7	5.1	CASSLLQGENTQY	2.1	5	2.2	CSARDPGDQETQY	2.5	7
2.2	CSARETGTDENTQY	2.4	3	2.2	CSARAGQGDSPLY	1.6	6	7.1	CASSLSGTGGGQNTQY	2.4	5	5.1	CASSLGGGYGEQF	2.1	5
5.1	CASSPGPLTGRTEAF	1.1	3	19.1	CASSQTGSTEAF	1.1	6	7.1	CASSPRPISGNTVY	1.3	3	9.2	CASSLSDQNTQY	2.4	5
5.1	CASSLVFVGDDYT	1.2	3	9.2	CASSQSGTGGSGNTVY	1.3	3	5.3	CASSLEAGRNEKLF	1.4	3	19.1	CASSQDWDNNTAQLF	2.2	5
6.5	CASSLDRERYEQY	2.7	3	9.2	CASSQDRDGEKLF	1.4	3	8.1	CASTLGPNTQY	2.4	3	2.2	CSASTGYEQY	2.7	3
7.1	CASSQDDRGKDEQY	2.7	3					5 orphan clonotypes				3 orphan clonotypes			
13.3	CASSEVGGGETQY	2.5	1												
11 orphan clonotypes															

Four time points were analyzed for the 4 primary infected RM. Two time point post primary infection and two time points post re-infection. The percent frequency of identical clonotypes at each time point are highlighted with the same color. Percent frequency was calculated as follows: (number of clonotype / number of sequences examined) x 100. The clonotypic composition of an emerging RhCMV-specific response during experimental primary infection (n = 4) was strikingly diverse (> 20 sequences per RM) and unstable. Reinfection with RhCMV at post-infection day 224 recruited new CDR3 sequences into the response, further increasing clonotypic complexity.

TABLE 2.3B Determination of TCR BV diversity in the developing CD4$^+$ T cell response against RhCMV after primary infection and reinfection (RM20955 and RM21046)

PRIMARY INFECTION								REINFECTION							
TIMEPOINT #1				TIMEPOINT #2				TIMEPOINT #3				TIMEPOINT #4			
TCRBV	CDR3	TCRBJ	%freq	TCRBV	CDR3	TCRBJ	%freq	TCRBV	CDR3	TCRBJ	%freq	TCRBV	CDR3	TCRBJ	%freq
RM20955															
8.1	CASSLQTGISAYNEQF	2.1	70	2.2	CSARGQRGAPSGNTVY	1.3	17	8.1	CASSLQTGISAYNEQF	2.1	68	8.1	CASSLQTGISAYNEQF	2.1	79
6.5	CASSSQGRDSPLY	1.6	2	1.1	CASSEAYQVTTQY	2.4	16	19.1	CASSQFPRVDPQY	2.3	6	6.5	CASSMDRKTGEQY	2.7	8
6.5	CASSMDRKTGEQY	2.7	2	6.5	CASSLAHRGGNTVY	1.3	10	1.1	CASSEAYQVTTQY	2.4	3	6.1	CASSQTRYEQF	2.1	2
7.1	CASSSEGKMRTEAF	1.1	2	2.2	CSAPQTGPYYDYT	1.2	7	5.3	CASSFNRGRSPLY	1.6	3	6.2	CASSPGRTGQPQY	1.5	2
8.1	CASTEQSNYDYT	1.2	2	2.2	CSAIQGRAYNEQF	2.1	7	6.1	CASSQTRYEQF	2.1	1	19.1	CASSHPQGGNQPQY	1.5	2
6.2	CASSPGRTGQPQY	1.5	1	2.2	CSAPPDRSEVYQETQY	2.5	7	13 orphan clonotypes				5 orphan clonotypes			
18 orphan clonotypes				21.2	CASSLEGTLS	1.3	7								
				7.1	CASSSRPANEQY	2.7	5								
				2.2	CSALGQEKLF	1.4	3								
				6.2	CASSLGNRGAGNTVY	1.3	3								
				6.5	CASSMDRKTGEQY	2.7	3								
				19.1	CASSHPGQGGNQPQY	1.5	3								
				8.1	CASTEQSNYDYT	1.2	2								
				4 orphan clonotypes											
RM21046															
5.3	CASSLGGTATDPQY	2.3	11	9.2	CASSQAPGGADPQY	2.3	17	9.2	CASSQGSGTDPQY	2.3	19	19.1	CASSRRDRAREKLF	1.4	18
8.1	CASSSRDRGALGNQPQY	1.5	11	5.1	CASSFTEPAQLF	2.2	5	19.1	CASSLGEYNSPLY	1.6	8	19.1	CASSPGRGRNPQY	2.3	16
9.2	CASSQGSGTDPQY	2.3	11	5.1	CASSLGGRNYNEQF	2.1	4	5.1	CASSSRGGDEKLF	1.4	6	2.2	CSARSGGTDPQY	2.3	11
2.2	CSARFAAGHGTQY	2.4	6	5.1	CASSLVGEETQY	2.5	4	9.2	CASSQAPGGADPQY	2.3	6	19.1	CASSQWTGGQPQY	1.5	9
6.2	CASSPLFGGAPGAAQLF	2.2	6	7.1	CASSQADRRNDYT	1.2	4	9.2	CASSQAGMETQY	2.5	6	2.2	CSAHGLGGYNEQF	2.1	5
7.1	CASSPWDRGGEQY	2.7	4	7.1	CASSQDPGNNQPQY	1.5	4	5.1	CASSSGTGGNEQF	2.1	4	2.2	CSARDHEVEGWYYDYT	1.2	4
6.5	CASSPDWGYRPQLF	2.2	4	7.1	CASSQAGGSLTDPQY	2.3	4	1.1	CASSSRGGGASGASVLT	2.6	4	2.2	CSARAAGGGGNTVY	1.3	4
6.5	CASSRGGTGGLLNTQY	2.4	4	7.1	CASSQEQETQY	2.5	4	5.3	CASSLGTGFEKLF	1.4	4	2.2	CSAREGRDEKLF	1.4	4
7.1	CASSQEQMNTEAF	1.1	4	9.2	CASSPTGERNTQY	2.4	4	5.1	CASSSLWGAYNEQF	2.1	3	2.2	CSARRAKNTQY	2.4	4
9.2	CASSSGGADPQY	2.3	4	19.1	CASSLGEYNSPLY	1.6	2	7.1	CASSQDAQAEKLF	1.4	3	2.2	CSVGYTGTQVYEQY	2.7	4
19.1	CASSLGEYNSPLY	1.6	4	5.3	CASSLGGTATDPQY	2.3	1	8.1	CASSPDWGRTDPQY	2.3	3	9.2	CASSHGGNTAQLF	2.2	4
17 orphan clonotypes				7.1	CASSQDAQAEKLF	1.4	1	9.2	CASSYRNTEAF	1.1	3	19.1	CASSEQRGDYT	1.2	4
				9.2	CASSQEGGNEKLF	1.4	1	9.2	CASSQEGGNEKLF	1.4	3	19.1	CASSHPRHPGGGFGRNTVY	1.3	4
				38 orphan clonotypes				9.2	CASRQGNFQPQY	1.5	3	19.1	CASSSPTYNEQ	2.1	4
								9.2	CASSLDRVDEQF	2.1	3	6 orphan clonotypes			
								22 orphan clonotypes							

Four time points were analyzed for the 4 primary infected RM. Two time point post primary infection and two time points post re-infection. The percent frequency of identical clonotypes at each time point are highlighted with the same color. Percent frequency was calculated as follows: (number of clonotype / number of sequences examined) x 100. The clonotypic composition of an emerging RhCMV-specific response during experimental primary infection (n = 4) was strikingly diverse (> 20 sequences per RM) and unstable. Reinfection with RhCMV at post-infection day 224 recruited new CDR3 sequences into the response, further increasing clonotypic complexity.

One dominant BV (31%, 41%, and 70%) was present in 3 of 4 RMs. The remaining clonotypes for these 3 RMs were present at lower frequencies. The fourth, RM21046, did not have one dominant RhCMV-responsive BV but rather had 3 RhCMV-responsive clonotypes with frequencies of 11% each and a plethora of low frequency clonotypes. This hierarchy was transient since the observed dominant clonotypes on day 112 pi were not detected during the second time-point (day 182 pi or 203 pi).

I. Using RACE-PCR to determine the diversity of TCR BV expression in the CD4$^+$ T cells after reinfection with RhCMV

Next we examined the clonotypic complexity of the response in the reinfection setting to determine whether the complexity would change and if new clonotypes would be recruited into the response. The RACE-PCR analysis was performed on day 336 pi and day 420 pi for 3 of 4 RMs and the fourth, RM20955, was analyzed on day 336 pi and day 441 pi. Sequence analysis of this cohort on day 336 pi revealed the number of RhCMV-responsive clonotypes had increased for all RMs after reinfection (Table 2.3A & B).

The dominant clonotypes in 3 RMs reappeared after infection (clonotypes highlighted in pink). However, the number of RhCMV-responsive clonotypes in these RMS appeared to first expand from day 182 pi to day 336 pi and then begin to diminish by day 420 or 441 pi, suggesting a waning of the RhCMV-specific

$CD4^+$ clonotypes. The RhCMV-responsive clonotypes from RM21046 also showed signs of waning by day 420 pi even though the responsive clonotypes were more numerous during all days examined in comparison with the other 3 RMs. Given the high level of proliferation as evidenced by Ki-67 staining and increases in the frequencies of $CD4^+$ T cells after reinfection, it is not surprising that the number of clonotypes would increase from day 182 pi to day 336 pi and that new clonotypes would be recruited into the response.

SUMMARY

The goal of this study was to develop assays to study T cell clonotypes in RMs and to characterize the number and frequency of virus-specific $CD4^+$ clonotypes that developed during a primary response. We also compared the clonotypic structure of the primary response to the clonotypic structure of an established memory response. First, we had to develop and optimize new assays to isolate and characterize CMV-specific $CD4^+$ clonotypes that were different from the assays we used in our human studies. We started by confirming surrogate cell surface markers (CD4, CD25, and CD69) that would cluster the antigen-specific clonotypes. Next we modified our stimulation conditions (from 6 hours to 48 hours) to accommodate for the optimal upregulation of CD25 without allowing the uneven proliferation of clonotypes so that their physiologic relative frequencies would remain unchanged. Third, we used RACE-PCR rather than

CDR3 size analysis to identify and sequence the clonotypes because we found that these techniques allowed better coverage of the TCR repertoire. Finally, by confirming the CMV specificity of the $CD4^+$ clonotypes via our standard CFC assay, we were able to validate antigen-specific clonotypes in the RMs.

The evaluation of the clonotypic structure of a primary as well as an established RhCMV infection revealed that the primary $CD4^+$ T cell response against RhCMV is composed of a polyclonal TCR BV repertoire with transient hierarchy followed by recruitment of additional TCR BV sequences after reinfection. Whereas for established RhCMV infection, the $CD4^+$ memory T cell response is oligoclonal with stable hierarchy, the polyclonal and transient hierarchical structure of the primary infection cohort vs. the stable and oligoclonal hierarchy in RMs with long-term established infections implies that the memory clonotypic structure takes months to years to evolve into its current state. Even though we saw some evidence of the waning of the clonotypes, we did not allow the primary infection to mature enough to present clearer evidence for the evolution of a polyclonal viral-specific $CD4^+$ clonotypic structure with transient hierarchy to an oligoclonal clonotypic structure with stable hierarchy.

CHAPTER III

DIRECT EX VIVO ANALYSIS OF HUMAN CD4$^+$ MEMORY T CELL ACTIVATION REQUIREMENTS AT THE SINGLE CLONOTYPE LEVEL

OBJECTIVE

Studies examining the activation of T cell clones suggest that T cells have variable thresholds that may vary within a clone (35, 36, 43). This variability in activation may result in a graded response such that low threshold T cells would respond early with low doses of antigen whereas high threshold T cells would respond only when high doses of antigen are present. Previous studies in our lab have shown that exogenous costimulation with CD28 and CD49d MAbs causes stepwise increases in CMV-responsive CD4$^+$ T cell frequencies without having a stimulatory activity on their own (45). These data suggest that T cells may fall into 3 categories requiring varying degrees of exogenous costimulation to achieve triggering. The differences in triggering thresholds may be due to differences in activation set points that are independent of the TCR and TCR specificity.

Our lab has been investigating primary and memory CD4$^+$ T cell responses to CMV. In particular, we have been characterizing the clonotypic

hierarchies of CMV-specific $CD4^+$ T cells during primary and memory responses. The CMV-specific $CD4^+$ memory T cells have highly skewed clonotypic structures that include dominant clonotypes. We have characterized the CMV epitopes that elicit specific responses from some of the dominant clonotypes. Since we have found large single clonotypes within MAb-defined TCR-Vβ families in our initial studies, we took advantage of this resource to investigate TCR triggering requirements in fresh uncloned $CD4^+$ T cells. To date, T-cell activation studies have been performed using cloned T cells. In order to conduct this investigation we utilized our CFC assay to examine the production of IFN-γ and IL-2 after TCR triggering with and without exogenous costimulation and varying concentrations of antigen.

RESULTS

A. Identification of single clonotypic $CD4^+$ memory T cell responses against defined pp65 epitopes on CMV

CMV-specific $CD4^+$ memory T cells are maintained at high frequencies in CMV-seropositive humans, and we have demonstrated that in some instances single clonotypes are responsible for the CMV response within a particular Vβ family or subfamily (100). Therefore, we postulated that it would be feasible to stimulate PBMCs with the single CMV peptides that could elicit a response within a particular Vβ family, and then to use CFC and Vβ gating to perform

functional analysis of the single clonotypes. We were able to identify two such clonotypes from two different subjects.

Subject 1 had a 7.6% $CD4^+$ T cell response against CMV (Figure 3.1A), 22% of this response (1.7% of $CD4^+$ T cells) was elicited by a single CMV epitope $pp65^{509-523}$, and ~60% (1% of $CD4^+$ T cells) of the response to this epitope was contained within the $V\beta2^+$ subset of $CD4^+$ memory T cells. Subject 2 had a 3.3% $CD4^+$ T cell response against CMV (Figure 3.1A), and 0.7% of this response was elicited by a single CMV epitope $pp65^{45-59}$. >90% of the response against this epitope was contained within the $V\beta17^+$ subset of $CD4^+$ memory T cells. In both of these subjects a proportion of the cells that produced IFN-γ also produced IL-2, but IL-2 production was not observed in the absence of IFN-γ (Figure 3.1A, right panels).

FIGURE 3.1A Identification of single clonotype CD4$^+$ memory T cell responses to defined CMV pp65 epitopes

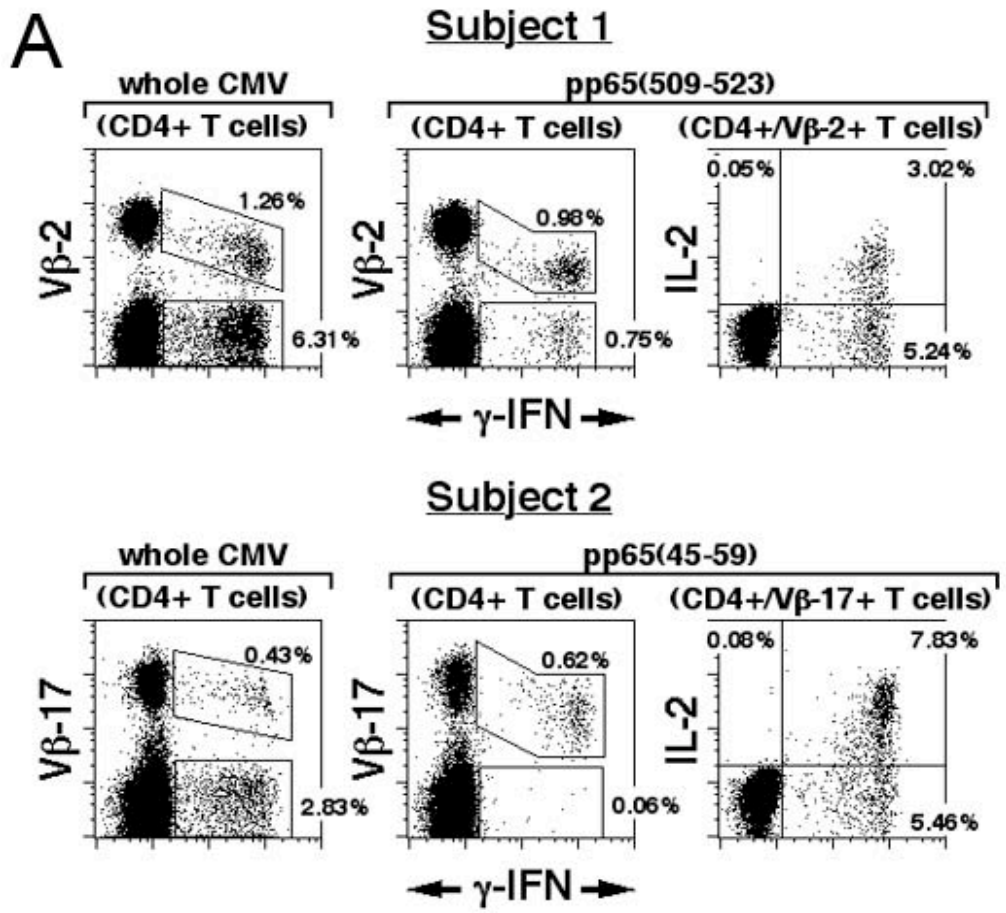

A. PBMCs from two CMV-seropositive subjects were stimulated with CMV or 2μg/ml optimal pp65 15mer for 6 hrs. in the presence of Brefeldin A for the final 5 hrs., and then examined for their correlated expression of cell surface TCR-Vβ-2 or -17 and intracellular IFN-γ, IL-2, and CD4. 50,000 events, gated on CD4$^+$ small lymphocytes, are shown in the left and middle profiles and 10,000 events gated on CD4$^+$, TCR-Vβ-2$^+$ or -17$^+$ small lymphocytes, are shown in the right profiles. The % of events within these gated populations are shown for the designated regions or quadrants. TCR expression is substantially down-regulated on the responding population, but the intensity of staining for TCR remains sufficient to delineate the contribution of each Vβ family/subfamily to these response.

B. Determination of the clonotypic composition of the CD4$^+$ Vβ responses

We next sought to determine the clonotypic composition of the CD4$^+$ Vβ responses against these defined epitopes in each subject. PBMCs were stimulated utilizing the appropriate CMV 15mer epitope and stained with MAbs against CD4, CD69, and IFN-γ. The CD4$^+$ T cells were sorted into two fractions: responsive (CD69$^+$/surface IFN-γ$^+$) and non-responsive (CD69$^-$/surface IFN-γ$^-$) (see Chapter I). We then performed CDR3 size analysis by RT-PCR amplification of the purified RNA from the sorted populations. Figure 3.1B shows the results of this amplification. Subject 1 had a dominant BV2 band in the responsive population, whereas the non-responsive population revealed a smear of bands. Subject 2 had a dominant BV17 band that appeared as a doublet in the responsive population and a series of bands with an apparent Gaussian distribution in the non-responsive population. The bands in the non-responsive populations for both subjects indicated the presence of a polyclonal population of CD4$^+$ T cells. Sequence analysis of the dominant band in the responsive population in both subjects revealed a single CDR3 sequence for both subjects. However, the non-responsive populations contained non-overlapping sequences in the corresponding region of the gel with the dominant band.

FIGURE 3.1B Identification of single clonotype CD4$^+$ memory T cell responses to defined CMV pp65 epitopes

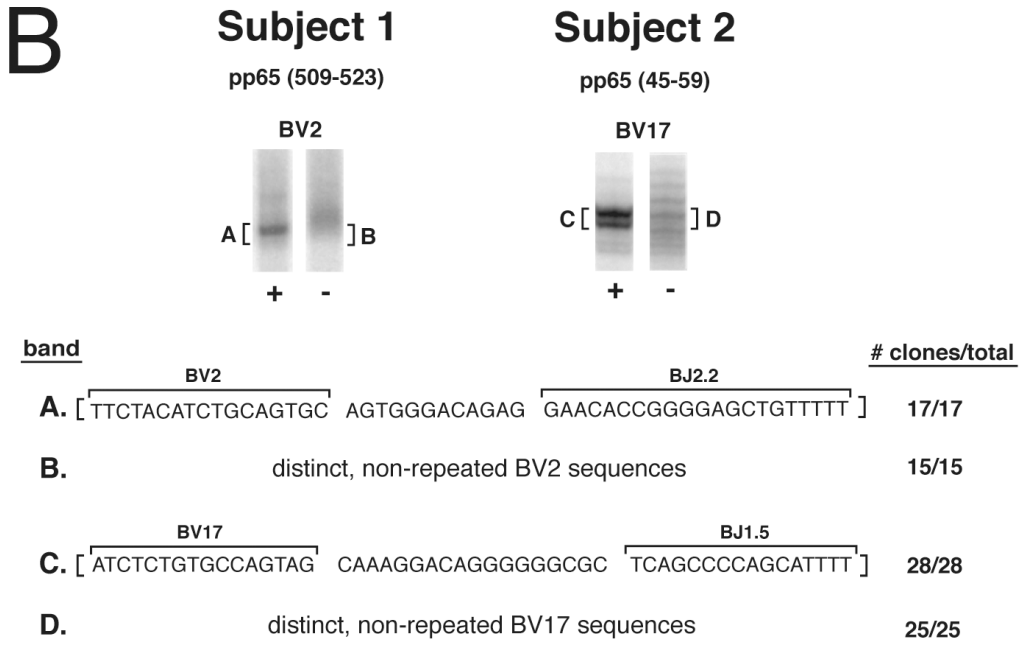

B. PBMCs from these same subjects were stimulated with optimal pp65 15mer and processed for cell sorting on the basis of surface IFN-γ (PE), CD69 (allophycocyanin), and CD4 (FITC). RT-PCR CDR3 size analysis of the sorted peptide responsive (CD69$^+$/IFN-γ$^+$; "+") and non-responsive (CD69-/IFN-γ$^+$; "-") CD4$^+$ small lymphocytes are shown in the figure. Analysis of the responsive population yielded a single dominant band in subject 1 and a dominant doublet in subject 2, whereas the non-responsive populations reveal an indistinct smear of bands (subject 1) or a Gaussian distribution of bands departed by 3 nucleotides. The areas of the gels designated by A-D were excised, cloned, and subjected to sequencing. The dominant band/doublet revealed clonal TCR CDR3 region sequences, whereas the corresponding regions of the gel in the analysis of non-responsive cells revealed distinct, non-repeated TCR sequences.

C. Determination of TCR AV expression in the TCR BV-defined clonotypes

To further characterize the BV-defined clones, we stimulated PBMCs from both subjects by utilizing the appropriate CMV 15 mer epitope and then stained the cells with Vβ2 (subject 1) or Vβ17 (subject 2), CD69, and IFN-γ. The $CD4^+$ T cells were sorted into two fractions: responsive ($CD69^+$/IFN-γ^+) and non-responsive ($CD69^-$/IFN-γ^-) (Figure 3.2A). RNA was purified from the responsive and non-responsive populations and used for RT-PCR amplification of BV2, BV17, and the 29 TCR AV families (Figure 3.2B). The bands from the BV and AV amplification (shown with arrows in Figure 3.2B) were purified, cloned, and sequenced. Sequencing results (Figure 3.2C) confirmed that the BV2 and BV17 sequences were identical to the BV2 and BV17 sequences in the primary experiment, confirming that we had isolated the same clonotypes. The AV amplification revealed two bands for subject 1, AV1 and AV16, and sequence analysis revealed that each band contained one sequence. The AV amplification for subject 2 revealed one band, AV2, and sequence analysis confirmed the presence of one sequence. These results suggest that the BV2 clonotype from subject 1 probably had a productive rearrangement of both TCR α alleles and is among the ~30% of T cells that express mRNA from both TCR α alleles. The BV17 clonotype appears to express mRNA from one rearranged TCR α allele.

FIGURE 3.2 Characterization of *TCRA* gene expression by the TCR BV-defined single clonotypes

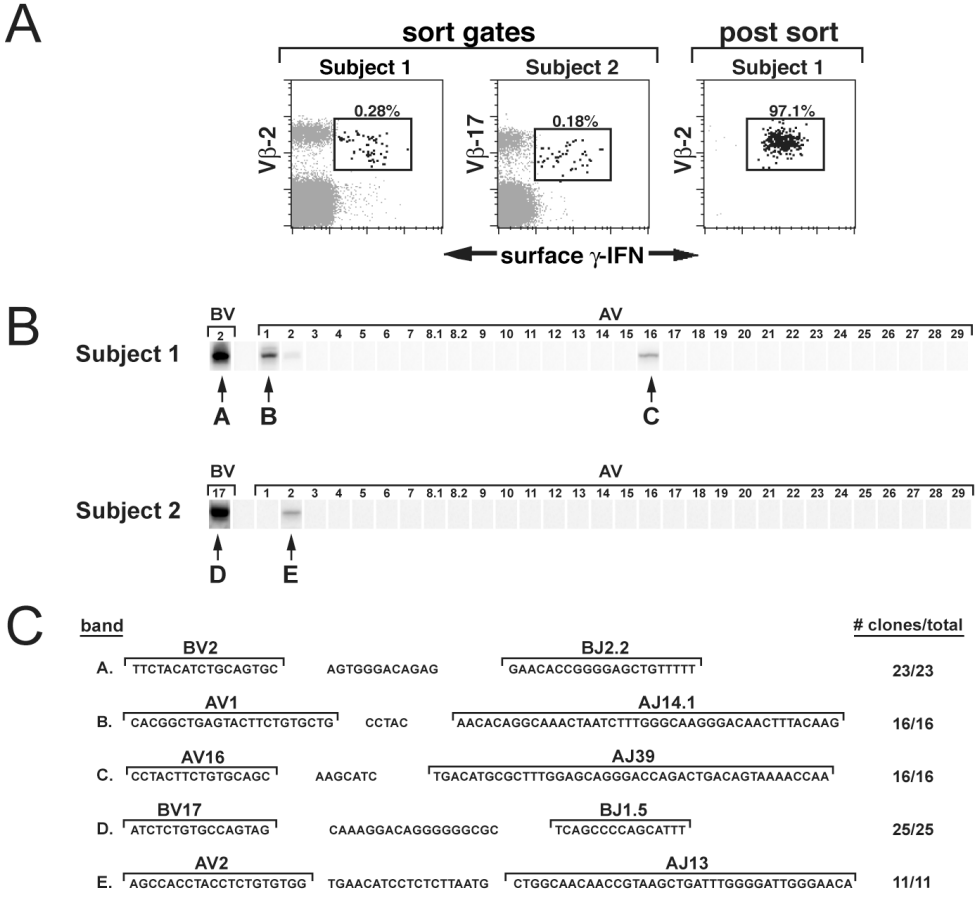

A. PBMCs from subjects 1 and 2 were stimulated with 0.002μg/ml of optimal pp65 15mer with CD28/CD49d and stained for TCR-Vβ2 (subject 1) or TCR-Vβ17 (subject 2), CD4, and IFN-γ surface capture. The cells were sorted and processed for TCRA CDR3 size analysis.

B. TCRA size analysis on TCR-Vβ2$^+$/CD4$^+$/IFN-γ$^+$ (subject 1) and TCR-Vβ17$^+$/CD4$^+$/IFN-γ$^+$ (subject 2) cells. For subject 1, BV2 was amplified as well as AV1 and AV16 and for subject 2, BV17 was amplified as well as AV2.

C. The bands designated A, B, C, D, and E were excised, cloned, and sequenced. Each band yielded one discreet sequence and the BV sequences were identical to the sequences
originally identified.

TABLE 3.1 Determination of BV2BJ2.2 and BV17BJ1.5 frequencies in the CMV-responsive $CD4^+$ T cell fraction using real-time quantitative PCR

						$CD4^+$ T CELLS	
EXP	**SUBJECT**	**VB**	**PEPTIDE**	**PBMC**	**Total**	**peptide +**	**peptide -**
						(INF-γ^+/$CD69^+$)	(INF-γ^- /$CD69^-$)
A	1	2	pp65 (509-523)	1.3%	ND	67%	1.5%
B	1	2	pp65 (511-522)	1.7%	3.9%	59%	0.7%
C	2	17	pp65 (47-58)	2.9%	6.6%	100%	0.6%

footnotes:

1. %$CD4^+CD69^+$IFN-γ^+ cells/total $CD4^+$
2. (# clonotype copies/# input cells)x100

see Table 1 for primers and probes sequences

D. Real-time quantitative PCR quantification of the clonotypes

We next used real-time quantitative PCR to quantify the two clonotypes in peptide-responsive and peptide-non-responsive populations sorted using the CFC assay. The results (Table 3.1) show that BV2/BJ2.2 and BV17/BJ1.5 clonotypes were highly enriched in the peptide-responsive $CD4^+$ T cell population. These constituted 60% and 100% of peptide-responsive cells, respectively. These frequencies correspond to the frequencies determined using the CFC assay (Figure 3.1). Therefore, these results suggest that the two responses from subject 1 and 2 are clonal and could be used to determine functional characteristics in direct *ex vivo* experiments.

E. Characterization of the fine-specificity of the pp65 peptide-specific BV2/BJ2.2 and BV17BJ1.5 single clonotypes

We further defined the specificity of the BV2/BJ2.2 and BV17/BJ1.5 clonotypes against their corresponding 15 mer peptides. A series of consecutive pp65 12 mer peptides (shifted by one amino acid that spanned the sequence of the 15 mer peptide) were synthesized. These 12 mer peptides were used to stimulate PBMCs from each subject in the standard CFC assay in the absence of costimulatory MAbs. The stimulatory effects of each 12 mer peptide were

assessed by both the frequency and degree of TCR down-regulation of the responsive population. The results depicted in Figure 3.3 show that only one 12 mer peptide, $pp65^{511-522}$ for subject 1 and $pp65^{47-58}$ for subject 2, elicited maximal responder frequency and TCR down-regulation. The immediate adjacent peptides did elicit near-maximal responder frequencies and TCR down-regulation, and 5 consecutive 12 mers were capable of eliciting responder frequencies >70% of the optimal 15 mer.

Because the MHC class II cleft is thought to encompass 9 mer peptides (without the overhang ends), we evaluated common 9 mer peptides within the five 12 mer peptides that elicited significant responses. A single 9 mer peptide elicited the best response in each clonotype; however, the optimal 9 mers were not capable of eliciting maximal response frequencies and TCR down-regulation as observed by the optimal 12 mer.

FIGURE 3.3 Consecutive 12 mers and 9 mers reveal essential stimulatory sequences and define optimal and suboptimal epitopes for single clonotype responses

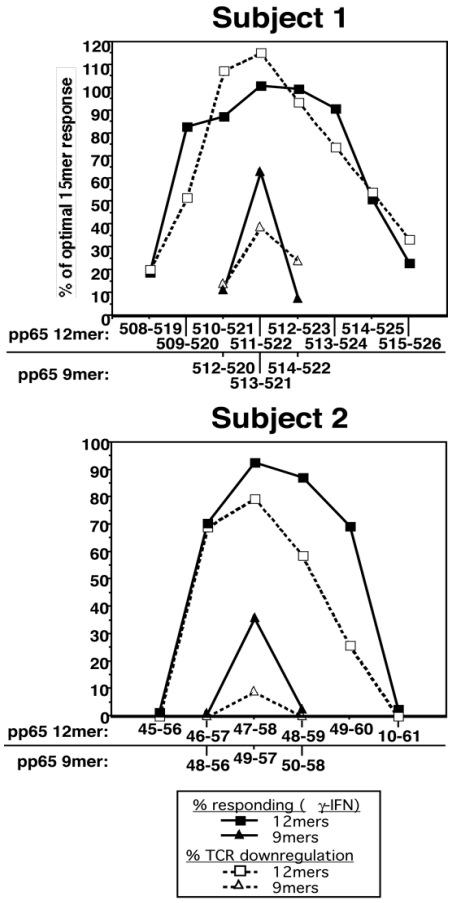

PBMCs from subjects 1 and 2 were stimulated with 1) optimal pp65 15 mer, 2) each of 8 consecutive 12 mers with single amino acid overlaps corresponding to this 15mer, and 3) each of 3 consecutive 9 mers corresponding to the core of the epitope for 6 hrs. in the presence of Brefeldin A for the final 5 hrs., and then examined for their correlated expression of cell surface TCR-Vβ-2 or -17, and intracellular IFN-γ, CD69, and CD4. The % responding ($CD69^+/IFN\text{-}\gamma^+$) and %TCR down-regulation [1-(TCR-Vβ MFI of the responding population/ TCR-Vβ MFI of the non-responding population) x 100] was determined after gating on $CD4^+$/TCR-$V\beta2^+$ or $V\beta17^+$ so that the results reflect the single CMV-specific clonotype found in these TCR-Vβ families. The results in the figure are presented as a % of the response for the parent 15 mer.

F. Single CD4$^+$ T cell clonotypes display broad heterogeneity in their activation thresholds

After characterizing the response frequencies and TCR down-regulation of the two clonotypes using the optimal 15 mer epitope as well as optimal and suboptimal 12 mer epitopes, we investigated the triggering characteristics of these two clonotypes. We evaluated IFN-γ and IL-2 responses against optimal 15 mer and 12 mer, suboptimal 12 mer, and the core 9 mer peptide at ten-fold dose intervals (2 μg/ml to 0.2 pg/ml). These experiments were performed with and without the addition of co-stimulatory antibodies. Figure 3.4 depicts the dose response analysis of optimal 15 mer and 12 mer and suboptimal 12 mer peptides in the presence or absence of exogenous costimulation. For each clonotype the response frequency plateaued for IFN-γ production when higher doses of peptide were used in the presence of costimulation. This frequency plateau was operationally defined as the maximum response for each clonotype, ~6% of Vβ2$^+$CD4$^+$ cells for subject 1 and ~14% of Vβ17$^+$CD4$^+$ cells for subject 2. In the absence of exogenous costimulation, 2-20 pg of optimal peptide elicited detectable IFN-γ responses in these two clonotypes. Each 10-fold increase in optimal peptide concentration over this minimum amount incrementally increased the response. Without exogenous costimulation, maximal IFN-γ response frequencies were not achieved until optimal peptide concentrations were increased 10,000-fold or more. Suboptimal 12 mer peptides elicit similar dose

response patterns for the IFN-γ response with exogenous costimulation. However, without exogenous costimulation the suboptimal 12mer peptides fail to elicit plateau frequencies even at the highest peptide concentration tested (2 μg/ml). The core 9 mer peptide, in the absence of exogenous costimulation, only achieves 50-60% of maximal response frequencies at 2 μg/ml. The response frequency for IL-2 was similar in that ten-fold increases in peptide concentration incrementally increased the responder frequency even at the highest concentration of peptide tested, but without costimulation failed to reach maximal responder frequencies even at the highest concentration of peptide. Interestingly, for all suboptimal 12mer peptide doses, the addition of costimulatory MAbs increased the IFN-γ and IL-2 response frequencies (up to 2- to 3-fold). The effect of costimulatory MAbs was most pronounced for the 9 mer peptide, with response frequency increasing 3- to 6-fold for both IFN-γ and IL-2 (Figure 3.5).

FIGURE 3.4A Dose response analysis of optimal and suboptimal epitopes in the presence or absence of exogenous costimulation demonstrates triggering threshold heterogeneity within single CD4$^+$ memory T cell clonotypes

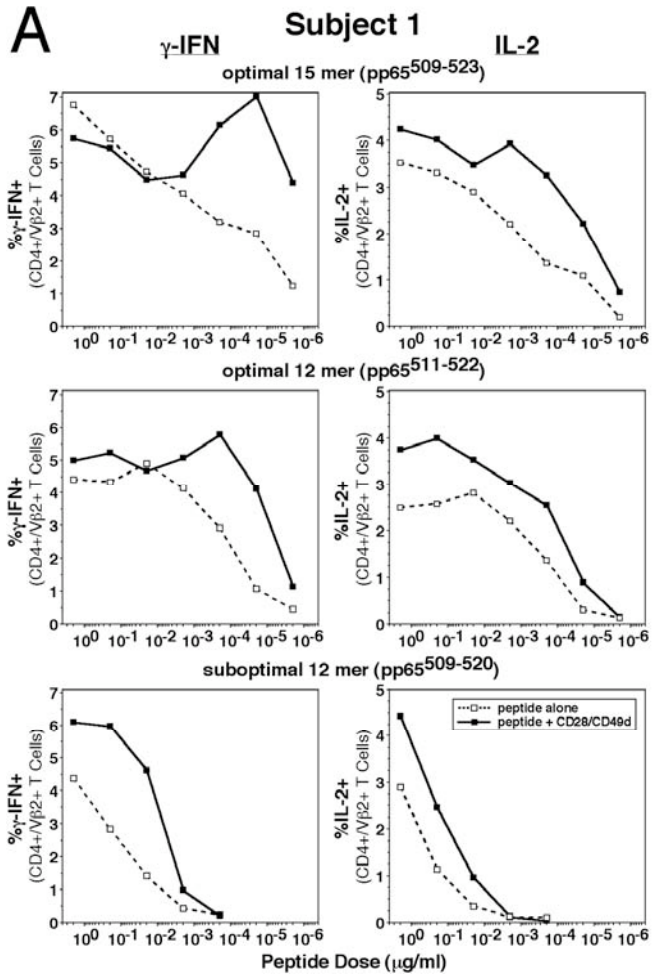

PBMCs from subjects 1 and 2 were stimulated with serial 10 fold dilutions (starting at 2 μg/ml) of selected optimal and sub-optimal epitopes with or without CD28/CD49d for 6 hrs. in the presence of Brefeldin A for the final 5 hrs., and then examined for their correlated expression of cell surface TCR-Vβ-2 or -17, and intracellular IFN-γ, IL-2, and CD4. The % responding for IFN-γ and IL-2 among CD4$^+$, TCR-Vβ2$^+$ (subject 1) or CD4$^+$, TCR-Vβ17$^+$ (subject 2) small lymphocytes are shown in **A** and **B**, respectively.

FIGURE 3.4B Dose response analysis of optimal and suboptimal epitopes in the presence or absence of exogenous costimulation demonstrates triggering threshold heterogeneity within single CD4$^+$ memory T cell clonotypes

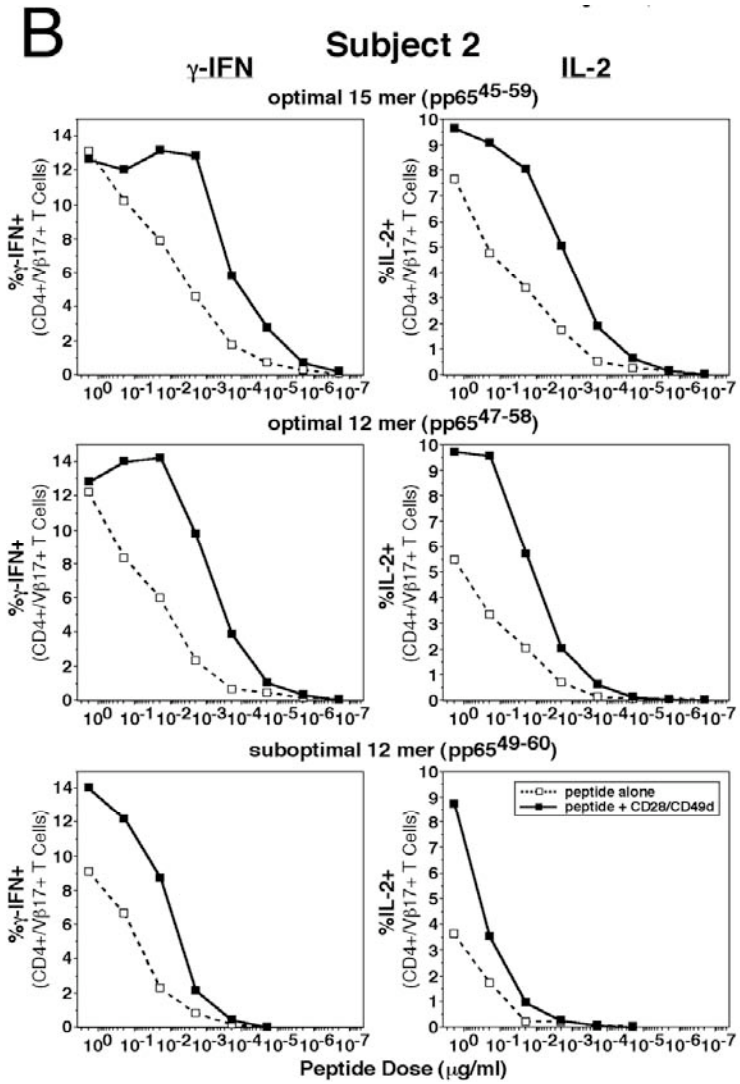

PBMCs from subjects 1 and 2 were stimulated with serial 10 fold dilutions (starting at 2 μg/ml) of selected optimal and sub-optimal epitopes with or without CD28/CD49d for 6 hrs. in the presence of Brefeldin A for the final 5 hrs., and then examined for their correlated expression of cell surface TCR-Vβ-2 or -17, and intracellular IFN-γ, IL-2, and CD4. The % responding for IFN-γ and IL-2 among CD4$^+$, TCR-Vβ2$^+$ (subject 1) or CD4$^+$, TCR-Vβ17$^+$ (subject 2) small lymphocytes are shown in **A** and **B**, respectively.

FIGURE 3.5 Optimal 9 mers can elicit maximal or near-maximal responses from single CD4$^+$ memory T cell clonotypes in the presence of exogenous costimulation

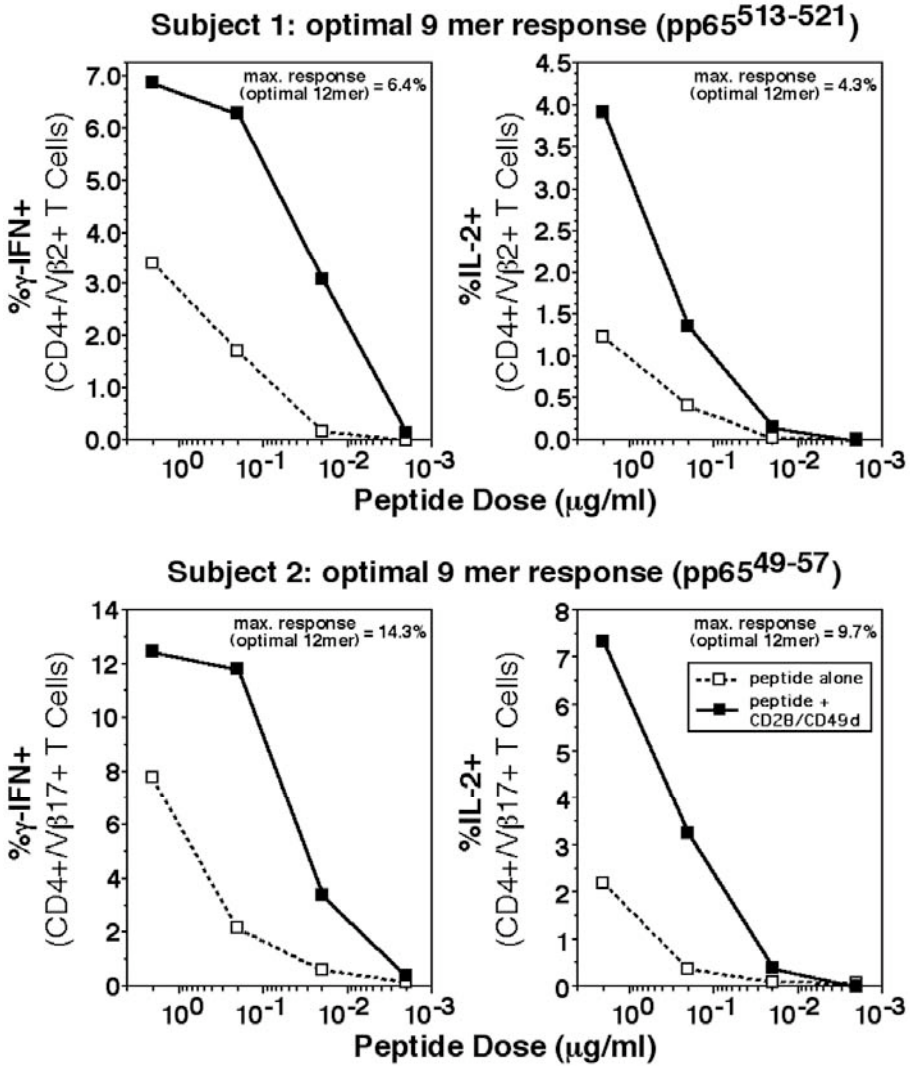

PBMCs from subjects 1 and 2 were stimulated with serial 10 fold dilutions (starting at 2 μg/ml) of the optimal 9 mer peptide for each subject, with or without CD28/CD49d and then examined for their correlated expression of cell surface TCR-Vβ-2 or -17, and intracellular IFN-γ, IL-2, and CD4, as described in detail in Figure 3.4 The maximum response observed to optimal 12 mer in the same experiment is indicated in the upper right corner of each profile.

G. Dissimilar triggering thresholds for IFN-γ and IL-2 results in markedly different functional responses depending on antigen dose and costimulation

Because of the observed non-overlapping response profiles of IFN-γ and IL-2, we further investigated qualitative functional profiles as a function of peptide dose and costimulation. First, we observed that for both clonotypes all of the peptide-responsive cells that synthesized IL-2 also synthesized IFN-γ (Figure 3.1). We compared the fraction of IL-2 producers as a function of peptide dose and costimulation (Figure 3.6A). We found that without CD28 and CD49d costimulation, the fraction of IFN-γ-producing cells that also produce IL-2 doubled from cells that responded to low dose peptides as compared to cells that responded to high dose peptides (Figure 3.6A, dotted line). This difference was more pronounced in the presence of costimulation (Figure 3.6A, solid line). Figure 3.6B depicts the response of the clonotype to a suboptimal 12mer peptide at high dose (2 μg/ml) and low dose (0.002 μg/ml) with CD28 and CD49d costimulation from subject 1. With high dose peptide stimulation a maximal IFN-γ response was observed (~14% of the $V\beta2^+CD4^+$ T cells). Also, ~62% of these responding cells also synthesized IL-2. With low dose peptide stimulation, the IFN-γ responder frequency was nearly identical, with less IFN-γ production per cell. However, only 20.7% of these cells also synthesized IL-2, a 3-fold reduction from the high dose response.

FIGURE 3.6A Triggering thresholds differ for IFN-γ and IL-2 responses, and these differences result in qualitatively distinct cytokine production profiles within a single clonotype, depending on epitope dose and availability of costimulation

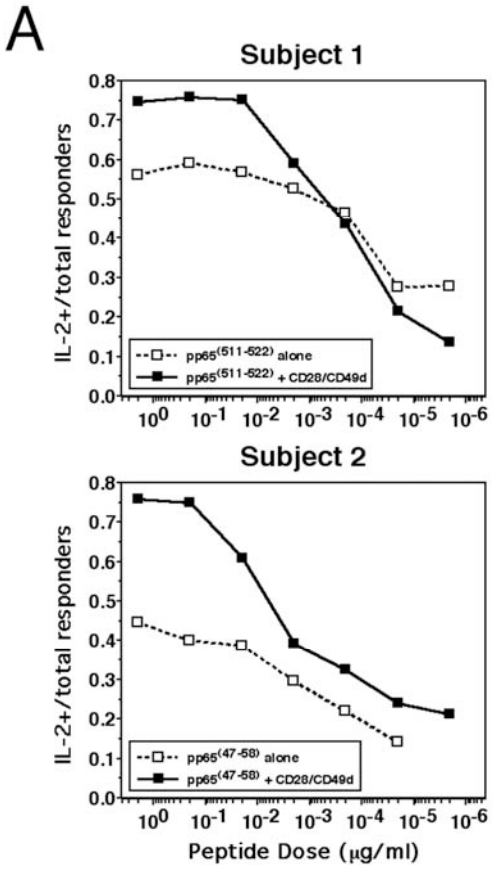

The dose response curves for the optimal 12mer peptide stimulations with and without CD28/CD49d from Figure 3.3 are reconfigured in this figure to demonstrate the fraction of clonotypic $CD4^+$ T cells producing IL-2 in the responding population. Since, as shown in Figure 3.1 and 3.4B, all IL-2 production derives from cells also making IFN-γ, this fractions is simply the $\%IL\text{-}2^+/\%IFN\text{-}\gamma^+$ within the $CD4^+/TCR\text{-}V\beta^+$ gated populations. This fraction declines with dose, most dramatically in the presence of CD28- and CD49d-mediated co-stimulation.

FIGURE 3.6B Triggering thresholds differ for IFN-γ and IL-2 responses, and these differences result in qualitatively distinct cytokine production profiles within a single clonotype, depending on epitope dose and availability of costimulation

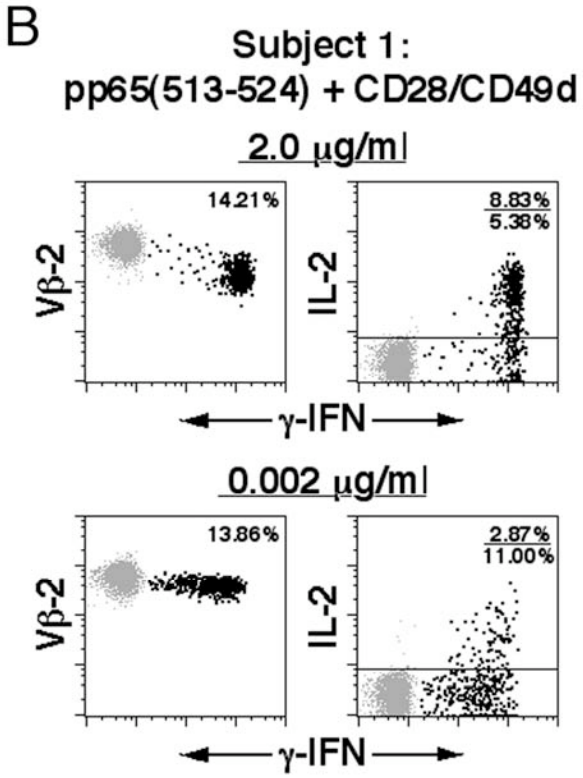

PBMCs from subject 1 was stimulated with 2 μg/ml or 0.002μg/ml of a sub-optimal 12 mer peptide, and analyzed as shown in figure 1. 10,000 events, gated on $CD4^+$/TCR-$V\beta2^+$ small lymphocytes, are shown, with the events in the total responding region (IFN-γ^+) enlarged and colored black and the events in the non-responding region colored gray. The %IFN-γ^+ (total responding) and the %IL-2 positive / IL-2 negative within the gated populations are provided in the left and right profiles, respectively.

Thus, the functional output of a clonally homogeneous memory population is complex due to the spectrum of thresholds present within a single clonotype population and threshold differences between different functional responses (i.e., synthesis of IFN-g and IL-2).

H. CD27$^+$differentiation of CD4$^+$ T cell memory does not correlate with the heterogeneity in activation thresholds

We next determined whether the heterogeneous triggering thresholds of single clonotypes was due to stimulation of cells as they progressed from "central" memory cells to "effector" memory cells as it had been previously suggested (101-103). The phenotypic markers used for the delineation of CD4$^+$ effector memory T cells' differentiation are CD27 and/or CCR7. The most differentiated effector memory population has been characterized as CD27$^-$CCR7$^-$, whereas central memory cells have been characterized as CD27$^+$CCR7$^+$. Because CD27 is stable during short-term activation (data not shown) we investigated the CD27 phenotype of single clonotype CD4$^+$ T cells responding to low- or high-dose peptide concentrations with and without costimulation. Figure 3.7 depicts the results of this analysis where 90% of the responding clonotypes were contained in the CD27$^-$ subset (effector memory) at all concentrations, with and without costimulation.

FIGURE 3.7 The threshold heterogeneity of these clonotypes is independent of the CD27-defined memory T cell differentiation stage

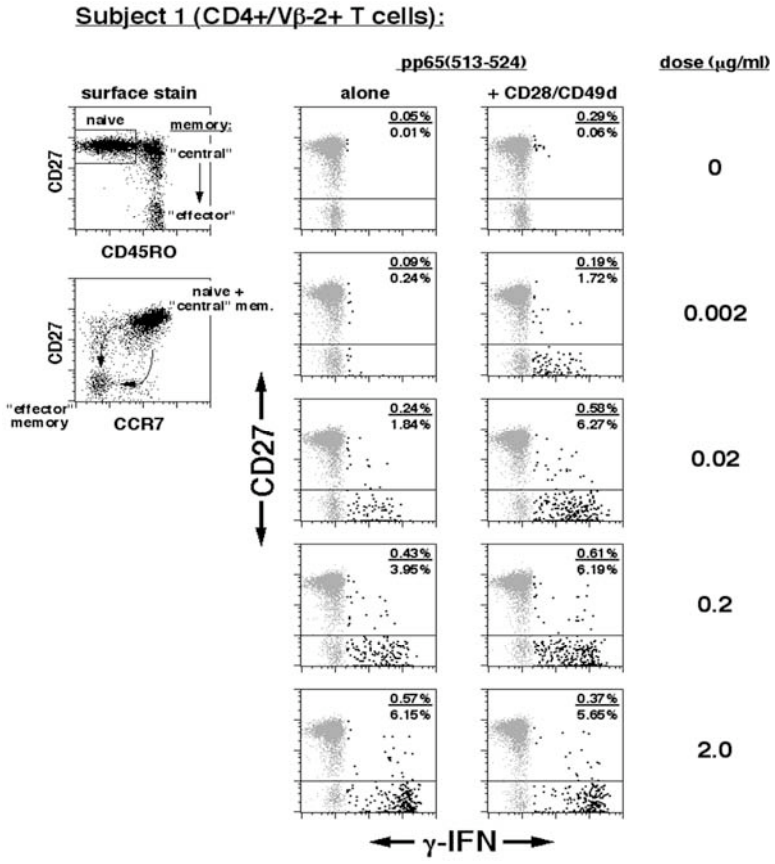

PBMC from subject #1 were examined immediately for cell surface expression of CD4, TCR-Vβ-2, CD27 and CD95 or were stimulated with serial 10 fold dilutions (starting at 2 μg/ml) of the sub-optimal pp65(513-524) peptide with or without exogenous CD28/CD49d, as described in Figure 3.3, and then examined for their correlated expression of cell surface TCR-Vβ-2 and CD27, and intracellular IFN-γ and CD4. 5,000 events are shown in each profile, gated on $CD4^+$, TCR-$V\beta2^+$ T cells. For the cell surface staining, the cell clusters corresponding to the naïve, $CD27^+$ "central memory" and CD27- "effector memory" populations are designated. In the panels showing the functional response of these cells, events corresponding to (IFN-γ^+) responding cells are enlarged and colored black and non-responding cells are colored gray. The % of cells making IFN-γ within the $CD27^+$ and $CD27^-$ subsets (delineated by horizontal line) are indicated in the upper fight hand corner of each profile ($CD27^+/CD27^-$).

A small fraction of the responding cells at all concentrations, with and without costimulation, were $CD27^+$. Therefore, the triggering heterogeneity observed in both subsets of cells cannot be attributed to the differentiation status of the cell.

SUMMARY

We studied triggering thresholds of two single clonotype responses from different subjects. Each clonotype specifically recognized a different HCMV pp65 epitope. The optimal 15 mer and 12 mer peptides for each clonotype were identified along with a series of suboptimal 12 mer peptides and a single core 9 mer peptide (within the optimal 15 mer peptide). The core 9 mer peptides did not elicit optimal responses, even though they were capable of stimulating their cognate clonotype to near maximal IFN-γ response frequencies at high peptide concentrations (0.2-2 μg/ml) and costimulation. The optimal 15 mer and 12 mer peptides were equal in their ability to generate maximal IFN-γ responses, efficient TCR down-regulation, and robust dose-responses. In contrast, the adjacent 12 mers (shifted by 1 or 2 amino acids) had submaximal to relatively low stimulatory potency.

In the absence of costimulation, a 4-log or more increase in optimal 15 mer and 12 mer peptide concentration was required for the responding cells to increase to plateau frequencies. However, for suboptimal 12 mer peptides,

costimulation increased the response frequencies for each subplateau response. This result indicates that exogenous costimulation lowers the triggering threshold of a given antigen-specific response. Finally, the heterogeneity in activation observed in these two clonotypes did not correlate with CD27-defined, $CD4^+$ memory T cell differentiation.

DISCUSSION

When we embarked on this project, little was known about the development and maintenance of $CD4^+$ memory T cell responses against viral pathogens. $CD8^+$ T cells have been the target of most studies that focus on understanding viral immunity (95, 104-106). However, a few studies had begun to establish the importance of $CD4^+$ T cells in viral immunity (57, 59, 81-84). It was apparent from these studies that $CD4^+$ T cells play a role in anti-viral immune responses including elaboration of anti-viral cytokines such as IFN-γ and TNF-α, activation of dendritic cells, maintenance of anti-viral $CD8^+$ CTL, direct CTL activity, and providing help for the production of high-affinity anti-viral antibodies. What remains unclear is whether viral-specific CD4+ memory T cells behave like CD8+ memory T cells. Does the hierarchy of virus-specific clonotypes established after primary infection reflect the hierarchy of an established memory response? Does reinfection introduce new clonotypes into the response? What are the activation requirements for CMV-specific CD4+ memory T cell clonotypes?

We chose CMV as our model viral pathogen because the CD4+ memory T cell response frequencies in human and RM are large (45, 57, 107-109), and this feature would allow us to easily detect and study these cells. To achieve this goal,

it was necessary to start by characterizing the most fundamental unit of memory, a single clone of T cells as defined by the TCR.

The major findings to emerge from this work are: 1) the $CD4^+$ memory T cell response during an established CMV infection is composed of an oligoclonal TCR repertoire with stable hierarchy, 2) the primary $CD4^+$ T cell response against CMV is composed of a polyclonal TCR repertoire with transient hierarchy, 3) reinfection with CMV recruits additional CD4+ T cell clones into the response, and 4) the activation threshold varies within single CD4+ T cell clones.

I. The clonotypic structure of CMV-specific $CD4^+$ T cells

A. T cell repertoire analysis using T cell clones and T cell lines

Prior to the advent of MHC class I and II tetramers and multi-parameter flow cytometry the identification and isolation of antigen-specific T cells required long-term culture of T cell lines and clones and population-based limiting dilution analysis (LDA). Studies examining viral-specific $CD8^+$ memory T cell responses using cloned or long-term cultured $CD8^+$ T cells have variable conclusions regarding the clonality of the viral-specific $CD8^+$ T cells (10, 11, 13-17, 24). One study examined the CTL response against pp65 (HCMV tegument protein) via LDA, which requires the long-term propagation of CTL clones *in vitro*. It was reported that the CTL response to individual HCMV pp65 epitopes was oligoclonal (10). However, another study examining the recall response against

influenza A matrix peptide (58-66) found the responsive BV17 TCR repertoire from a CTL line was polyclonal (17). The cloning process or long-term culture of T cells has the potential to alter physiologic frequencies since some clones may proliferate more rapidly than others in culture. Conclusions regarding antigen-specific T cell clonotypic hierarchies are best made from direct information from *in vivo*-derived viral-specific T cells and their physiologic relative frequencies.

B. Clonotypic complexity assessed using MHC class I and class II tetramers

The development of class I and class II tetramers has enabled the direct *ex vivo* identification and enumeration of antigen-specific T cells. Studies that used MHC class I tetramers to isolate the clonotypes in question to determine antigen-specific $CD8^+$ clonotype evolution had different results. Some studies that evaluated MHC class I tetramer-positive cells found a small number of virus-specific T cell clones present at high frequencies and ever-increasing numbers of clones present at lower and lower frequencies (18-20). Also, these studies found that some of the responsive clonotypes that had identical and/or variable BV and BJ sequences also had conserved CDR3 regions; either the CDR3 region length was conserved and/or there was amino acid homology in the entire CDR3 region or at critical residues in the CDR3 region (i.e., a motif) (24, 110, 111).

Annels and colleagues studied the $CD8^+$ CTL response to an immunodominant EBV epitope in IM patients (24). The primary response to this

epitope was oligoclonal and when these patients were analyzed two years later the rare clonotypes found during the primary infection dominated the $CD8^+$ memory CTL response to this epitope. A separate report in mice examined the primary, memory, and secondary response against three immunodominant LCMV epitopes and reported quantitative changes in epitope-specific T cell hierarchies but few to no changes in Vβ usages or CDR3 length distributions within the epitope-specific populations (110). The limitation of this study was that the investigators only analyzed the CDR3 size distribution without analyzing the CDR3 sequences. Is possible that the CDR3 region length may remain conserved (112) and yet have different sequences. Finally, Maryanski *et al*. did not find any difference between primary and secondary $CD8^+$ T cell responses and clonotypic structures to mouse tumor cell lines expressing HLA-Cw3; the size or composition of the Vβ10-Jβ1.2 TCR repertoire between the primary and secondary response did not change (21). The authors chose to focus on the Vβ10-Jβ1.2 response against this immunodominant epitope and even though the response to one immunodominant epitope was being examined it is unclear if the secondary response included new responses from other Vβ families.

In our studies we examined CMV-specific $CD4^+$ memory T cell responses in direct *ex vivo* experiments with short-term *in vitro* stimulations. Both in humans and RMs we found that long-term $CD4^+$ memory responses against CMV were oligoclonal. The clonotypic hierarchies remained stable over the months

examined (human 20-25 months; RM 4-11 months). In the 4 human subjects examined, we found 1-3 dominant $CD4^+$ clonotypes along with 4-9 subdominant and minor clonotypes. In the 6 RMs with established RhCMV infection we found 1-3 dominant clonotypes along with 1-9 subdominant and minor clonotypes.

By examining the relative frequencies of these clonotypes we were able to discern the clonality of the CMV response. For example, the presence of 11 CMV-responsive clonotypes for RM08919 may be viewed as a polyclonal response. However, the relative frequencies of the clonotypes suggest a highly skewed response with one clonotype providing 43% of the CMV response.

C. Clonotypic complexities of acute viruses (primary response)

Carbone's group (113) examined $CD8^+$ T cell repertoire complexity against Herpes Simplex Virus type I (HSV-1) infection. Analysis of *in vitro*-derived HSV-1-specific CTL lines revealed that 2 Vβ families (Vβ10 60% and Vβ8 20%) dominated the response to envelope glycoprotein B (gB); however, sequence analysis revealed heterogeneous TCR BV transcripts for $V\beta10^+$ cell lines. Sourdive *et al*. (97) studied primary responses against LCMV and reported that the $CD8^+$ T cell response was oligoclonal with 3 Vβ families providing 70% of the response. They also found that the length of the CDR3 region of LCMV-immune $CD8^+$ T cells was conserved. However, they did not examine TCR BV sequences. It is possible that multiple clonotypes comprise the 3 responsive Vβ

families, thus making the response polyclonal. Welsh's group (114) examined the $CD8^+$ $V\beta8^+$ repertoire in the setting of an acute LCMV infection by using the LCMV-ARM strain. The $CD8^+$ $V\beta8^+$ repertoire was chosen because it represented a substantial portion of the $CD8^+$ T cell response with a wide variety of specificities against different LCMV peptides. They found that in the acute infection setting the virus-induced T cell repertoire during primary infection was skewed and changed very little after the virus was cleared.

We examined 4 RMs after primary infection with RhCMV and evaluated the CMV-specific $CD4^+$ T cell clonotypes and their relative frequencies at two time-points after primary infection (pi). At both time-points we found a complex polyclonal $CD4^+$ T cell response to RhCMV. Even though 3 RMs had one dominant clonotype and the fourth RM had 3 co-dominant clonotypes at the first time-point, the hierarchy appeared transient, as these clonotypes were not apparent at the second time-point examined.

D. Clonotypic complexities of acute infections (secondary and memory response)

Some studies have compared the clonotypic hierarchy of primary vs. secondary T cell responses. Maryanski *et al*. (21) did not find any difference between primary and secondary $CD8^+$ T cell responses and clonotypic hierarchies against mouse tumor cell lines expressing HLA-Cw3. However, McHeyzer-

Williams and Davis (22) reported a narrowing in the TCR repertoire during the secondary $CD4^+$ T cell response against pigeon cytochrome C (PCC).

Kedzierska *et al*. (115) examined the complexity of $CD8^+$ T cell response against an immunodominant influenza epitope using CDR3 size analysis and associated Jβ usage. They found the $CD8^+$ T cell response was skewed and the TCRβ that were prominent after the primary response were present and expanded during secondary challenge. They also found "novel" TCRβ after secondary challenge.

E. Clonotypic complexities of chronic/persistent infections

A study examining the clonal composition of an EBV peptide-specific CTL response using CTL clones found the response to be oligoclonal and the clonotypes were preserved over a 5 year period (23). Similarly, Callan *et al*. (13) examined two patients with primary EBV infection with acute IM. CTL clones derived from these PBMCs during primary infection were comprised of clonotypes that dominated the response from the day of diagnosis well into the memory phase 37 months later. A third study (24) examined 3 EBV-infected patients with IM and found oligoclonal receptor usage among *in vitro*-derived clones specific for an immunodominant epitope. However, a 2-year follow-up revealed that the original dominant Vβ were poorly represented, if at all, during the memory phase.

Healthy CMV-seropositive humans have high frequencies of $CD4^+$ and $CD8^+$ CMV-specific T cells (11, 25, 45, 56-59, 116). Wills *et al.* (11) first studied the CTL response against the HCMV structural protein pp65 using LDA and found high frequencies of pp65 CTL in all donors dominated by a single BV gene rearrangement. Weekes *et al.* (10) examined CTL clones from 6 CMV-seropositive subjects and found that the memory CTL response against four pp65 peptides was highly skewed. A recent study utilizing MHC class I tetramers and CDR3 size analysis showed that the CTL response against pp65 in CMV-seropositive subjects was highly skewed and sequence analysis of the tetramer-selected populations revealed a single or very limited number of clones, thus confirming the oligoclonality of the response (25).

F. CMV-specific $CD4^+$ T cell response and clonotypic complexity in RMs

The 4 RMs in our primary infection study were reinfected with RhCMV and the initially dominant clonotypes that were not detected during the second time-point pi re-emerged as dominant clonotypes on one or both time-points after reinfection. Along with the reappearance of some of the dominant clonotypes, we also detected new clonotypes that had been recruited in the response. The recruitment of new clonotypes into the CMV-specific $CD4^+$ T cell response can be explained by our observation of increased CMV-specific $CD4^+$ T cell

frequencies, proliferation, and turnover after secondary infection, as evidenced by the increase in the Ki-67-positive cells. All of the above observations suggest that the antigen-specific T cell repertoire evolves. Some dominant clonotypes appear to be stable, as they remain detectable for months to years while other clonotypes are lost or become undetectable. It is not clear why the antigen-specific repertoire is in this state of flux, but clonal competition and clonal exhaustion may be some of the contributing factors. By performing this analysis we found that the CMV-specific $CD4^+$ T cell response after primary infection is polyclonal with transient hierarchy and it appears to evolve into a memory response that is oligoclonal with a stable hierarchy.

G. $CD4^+$ T cell response focusing

Another characteristic of anti-viral $CD8^+$ memory T cell responses is immunodominance, the focusing of the response to one or a few epitopes (12). However, immunodominance has not been generally considered a common feature of the $CD4^+$ T cell response (16). The $CD4^+$ memory T cell response to CMV is unusually large and we exploited this feature to investigate whether immunodominant pp65 peptide responses existed in two of our human subjects (1 and 4). In subject 4, 31% of the total $CD4^+$ T cell response to HCMV was directed at one pp65 epitope and one clonotype, BV2BJ2.2, was responsible for the majority of the response to this pp65 epitope. However, in subject one, two

immunodominant pp65 epitopes appear to be eliciting ~82% of the total $CD4^+$ T cell response to CMV. One pp65 epitope is recognized by 3 clonotypes with a total of 35% response and an unknown epitope that is recognized by the BV12BJ2.5 clonotype, which constitutes ~47% of the total CMV response. The data from these two subjects show that response focusing may occur in more than one way. First, a few dominant clonotypes recognize different epitopes and second, a large number of smaller clonotypes recognize a single epitope.

This observed response focusing in subjects 1 and 4 shows that CMV-specific $CD4^+$ T cell memory clonotypes behave similarly to $CD8^+$ T cell memory clonotypes. This may not have been apparent in previous studies because the assays that were used to assess the frequency of virus-specific $CD4^+$ memory T cells, namely LDA, have been found to underestimate T cell frequencies by as much as 5-20 times (16). Two reasons as to why our analysis of CMV-specific $CD4^+$ memory T cell responses find highly skewed repertoires may be 1) that the $CD4^+$ T cell structure of the response to this particular persistent virus, CMV, is different than the antigen-specific $CD4^+$ T cell structure of the response to other viruses or 2) that because we examined recall responses to a persistent virus that employs large frequencies of both $CD8^+$ and $CD4^+$ T cells, the hierarchical structure was more readily apparent. Due to the fact that $CD8^+$ T cells traditionally have larger burst sizes in comparison to $CD4^+$ T cells, clonal skewing

is more apparent in $CD8^+$ responses rather than in the smaller $CD4^+$ antigen-specific cohorts.

We have not investigated the mechanisms by which the CMV-specific $CD4^+$ T cell response focusing occurs, but we can postulate that the CMV-specific clonotypes appear to be in competition and, in the end, a handful of these clonotypes out-compete the rest to form the army of long-term memory cells in charge of immune surveillance and control of the virus. The fact that we could not detect the dominant clonotypes during all time-points may be due to the diminution of the clonotype after AICD. The diminution of the clone may cause the clone to fall below detection limits and upon re-infection the clone undergoes an activation burst, thus making it detectable again.

II. CMV-specific $CD4^+$ memory T cell activation requirements

We also investigated the function of single clonotypes taken directly *ex vivo*. Recent data suggest that T cells have variable thresholds that may be tunable and regulated independent of TCR specificity (35, 36, 43). The activation threshold of each clonotype may be a mechanism by which the effector functions of pathogen-specific T cells are controlled. To investigate this issue we decided to characterize the activation requirements of two clonotypes by examining the effect of epitope concentration, exogenous costimulation, and optimal versus suboptimal epitopes.

Having found these large single clonotype responses to CMV, we examined TCR triggering requirements utilizing a novel approach. Traditional analyses of T cell triggering have been performed using cloned T cells. We decided to take advantage of these large single clonotypes within MAb-defined TCR-Vβ families and the CFC assay to perform this investigation on fresh, uncloned T cells.

We found two single clonotypes that responded to different CMV pp65 epitopes from two subjects. Optimal IFN-γ response frequencies were elicited by the optimal 15 mer and 12 mer peptides with high concentration (0.2-2 μg/ml) stimulating peptide or with the addition of exogenous costimulation (CD28/CD49d MAbs) at lower peptide concentrations. Also, for each optimal 15 mer, 12 mer, and suboptimal 12 mer epitopes a stepwise increase in concentration reproducibly increased response frequencies, thus suggesting that a spectrum of triggering thresholds exists within each clonotype population. For subplateau responses, the addition of exogenous costimulation increased response frequencies.

The triggering heterogeneity observed in these two clonotype populations may be due to costimulatory heterogeneity within the APC or due to intrinsic differences in T cell triggering requirements. Costimulatory heterogeneity within the APC population could occur because a broad spectrum of APC may be present when the T cells are sampling peptide-loaded APC. The

activation states of the APC would dictate the level of costimulatory molecules present on the cell surface, which would in turn influence the stability of the interaction between T cells and APC. T cells encountering APC with high levels of costimulatory molecules would be triggered without exogenous costimulation whereas T cells encountering APC deficient in costimulatory molecules would require exogenous costimulation to be triggered. This explanation is not likely because T cell-APC interactions are dynamic and T cells bounce from one APC to another as they sample the peptides being presented by APC, and once they find the cognate peptide-MHC they bind to the APC to engage the costimulatory molecules (117, 118). Experiments from our own lab show that within normal PBMCs, dendritic cells and monocytes (but not B cells) (L. Picker, unpublished observation), equally stimulate T cells and this stimulation is enhanced with the addition of exogenous costimulation. Also, the APC are not limiting in these assays as increasing the APC:T cell ratio did not change the level of response frequency.

Therefore, based on our observations, we can make some inferences regarding differences in T cell triggering requirements responsible for the signaling heterogeneity in these clonotypes. In both clonotypes most of the high- and low-threshold $CD4^+$ T cells were contained within the highly differentiated $CD27^-$ subset, it appears that this threshold heterogeneity is independent of the CD27 differentiation pathway. Since we didn't exhaustively examine

differentiation pathways within these clonotypes, it is possible that a differentiation pathway other than the CD27 pathway is responsible for this triggering heterogeneity.

Another possible explanation for this triggering heterogeneity is that within the clonotypes there are differences in TCR fine specificity. However, since sequence analysis and real-time quantitative PCR analysis revealed a single TCRB CDR3 sequence and a single (subject 2) and a possible dual (subject 1) alpha chain, it is unlikely that the clonotypes would have differences in TCR fine specificity.

A potential explanation for this signaling heterogeneity is that there is differential regulation of components within the downstream T cell signaling apparatus. These components may include a few or all of the signaling or regulatory proteins that are collectively involved in T cell triggering. The differences in triggering heterogeneity may also be explained by the tunable activation threshold (TAT) model (35, 36, 43). The TAT model proposes that the triggering threshold for each T cell is set via the environmental signals it encounters. The cell's recent history, including the number, intensity, and quality of both subthreshold and threshold signals, resets the activation threshold for that cell. Therefore, we could speculate that within a single clonotype, T cells bearing the same TCR having encountered different stimuli will have different triggering thresholds. These memory clonotypes have managed to survive years after

primary infection and since their cognate antigen is a persistent virus it is possible that they are receiving subthreshold or suprathreshold signals, which would lead to a spectrum of triggering thresholds as displayed by these two clonotypes.

We also examined the triggering threshold with respect to IL-2 and found that IL-2 has a higher threshold than IFN-γ, requiring higher concentrations of peptide and/or exogenous costimulation. Therefore, during low-level infection, IL-2 production will be low compared to IFN-γ, thus likely reflecting a higher priority for anti-viral effector activity via IFN-γ rather than effector cell expansion via IL-2. This triggering heterogeneity has also been demonstrated for other cytokines such as IL-4 and TNF-α (119). Therefore, the same T cells can exhibit different responses depending on ligand concentrations and levels of costimulation. These variable responses within a single clonotype may be an efficient way for the immune system to handle various levels of antigen at low or high doses with different levels of costimulation.

III. Summary

CMV is a viral pathogen that has evolutionarily achieved a balance with its host via its mechanisms of persistence and immune evasion (50, 51). The immunological mechanisms that allow the virus to persist without causing disease are not well known. However, the oligoclonal and stable hierarchies of CMV-specific clonotypes we have observed lead us to make some inferences regarding

this balance between virus and host. Oligoclonal and stable clonotypic hierarchies may be an efficient mode of protection against genetically stable and persistent viral pathogens like CMV. The dominant high frequency clonotypes may be charged with immunologic surveillance and hence control of the virus, whereas the subdominant and minor clones may serve as backup to the dominant clones in cases of clonal exhaustion and/or viral escape mutations that may render the dominant clones useless. It is also possible that the dominant and subdominant clonotypes have distinct protective functions such as immune surveillance and immunoregulatory functions that together serve to control the virus. This pronounced hierarchy of clonotypic dominance appears to efficiently keep CMV under immune control, but how the number and relative frequencies of CMV-specific clonotypes render immune protection is unknown. However, since CMV-associated end organ disease (EOD) occurs when $CD4^+$ T cell counts fall below 50 cells per microliter (57, 59, 81, 82), it appears that a threshold of $CD4^+$ T cells is required to keep the virus under immune control and once the $CD4^+$ T cells fall below that threshold the virus can wreak havoc in its host.

Overall, our experiments have not only allowed us to examine some basic features of the complex nature of memory but have also provided us with tools to further investigate physiological aspects of immunity such as clonotype function. Our initial studies demonstrated the oligoclonal nature of the $CD4^+$ memory T cell response to CMV. This oligoclonal response included dominant

clonotypes with large relative frequencies. We capitalized on these large frequencies to examine TCR triggering thresholds in fresh, uncloned $CD4^+$ single clonotypes.

The identification of these clonotypes by CDR3 size analysis followed by sequence analysis allowed us to molecularly track CMV-specific clonotypes. The sequencing data affords us the opportunity to design clonotype specific primers for semiquantitative PCR and primers and probes for real time quantitative PCR. Of course, the sensitivity of these assays places limitations on the scope of such molecular tracking of clonotypes. But with large enough samples these clonotypes can be longitudinally followed and quantified in different compartments such as blood, lung, and other tissues.

IV. Future directions

Our studies have unanswered questions that remain to be addressed in the future. First, the evolution of the $CD4^+$ T cell response to CMV after primary infection needs to be more optimally addressed. In our study we allowed the infection to go 224 days after which we reinfected the RMs. The examination of the primary infected RMs on day 182pi revealed that the number of CMV-responsive $CD4^+$ T cell clonotypes appeared to narrow compared to day 112pi. But reinfection increased the CMV-responsive $CD4^+$ clonotypes on day 336pi. In order to settle this question of memory repertoire narrowing, a new cohort of

primary infected RMs should be analyzed without administering a reinfection. Clonotypic complexity should be analyzed every 100 days post-primary infection for 2 years to determine when the memory repertoire begins to narrow as observed in middle-age and old RMs.

It will also be advantageous if real-time quantitative PCR assays for these clonotypes can be optimized so that these clonotypes can be longitudinally followed over the course of infection. The limitation to this study will be sample size and the reliable detection limit of this assay. Finally, it will be of importance to study the fate of the CMV-specific clonotypes in the context of an HIV/SIV infection. Molecular tracking of viral-specific clonotypes is advantageous as some clones may be anergized and thus unresponsive in our CFC assay. Tracking CMV-specific clonotypes over the course of SIV infection and correlating this data with other parameters such as SIV viremia, $CD4^+$ T cell counts, and CMV disease onset may help us understand how $CD4^+$ memory T cells contribute to protection against CMV disease when this protection is broken down. Having an understanding of how CMV-specific $CD4^+$ memory clonotypes behave in immunocompetent RMs and analyzing these clonotypes in the context of a $CD4^+$ T cell-depleting disease may shed light on the correlates of protection.

REFERENCES

1. Kondo, M., I. L. Weissman, and K. Akashi. 1997. Identification of clonogenic common lymphoid progenitors in mouse bone marrow. *Cell 91:661*.
2. Katsura, Y. 2002. Redefinition of lymphoid progenitors. *Nat Rev Immunol 2:127*.
3. Janeway, C. A. and P. Travers. 1997. *Immunobiology: The immune system in health and disease*. Garland Publishing Inc, New York.
4. Nikolich-Zugich, J., M. K. Slifka, and I. Messaoudi. 2004. The many important facets of T-cell repertoire diversity. *Nat Rev Immunol 4:123*.
5. Elliott, J. I. 1999. Dual Valpha T cells. *Cell Mol Life Sci 56:143*.
6. Sant'Angelo, D. B., P. Cresswell, C. A. Janeway, Jr., and L. K. Denzin. 2001. Maintenance of TCR clonality in T cells expressing genes for two TCR heterodimers. *Proc Natl Acad Sci U S A 98:6824*.
7. Gorski, J., M. Yassai, X. Zhu, B. Kissela, B. Kissella, C. Keever, and N. Flomenberg. 1994. Circulating T cell repertoire complexity in normal individuals and bone marrow recipients analyzed by CDR3 size spectratyping. Correlation with immune status. *J Immunol 152:5109*.

8. Madrenas, J., and R. N. Germain. 1996. Variant TCR ligands: new insights into the molecular basis of antigen-dependent signal transduction and T-cell activation. *Semin Immunol 8:83*.

9. Sercarz, E. E., P. V. Lehmann, A. Ametani, G. Benichou, A. Miller, and K. Moudgil. 1993. Dominance and crypticity of T cell antigenic determinants. *Annu Rev Immunol 11:729.*

10. Weekes, M. P., M. R. Wills, K. Mynard, A. J. Carmichael, and J. G. Sissons. 1999. The memory cytotoxic T-lymphocyte (CTL) response to human cytomegalovirus infection contains individual peptide-specific CTL clones that have undergone extensive expansion in vivo. *J Virol 73:2099*.

11. Wills, M. R., A. J. Carmichael, K. Mynard, X. Jin, M. P. Weekes, B. Plachter, and J. G. Sissons. 1996. The human cytotoxic T-lymphocyte (CTL) response to cytomegalovirus is dominated by structural protein pp65: frequency, specificity, and T- cell receptor usage of pp65-specific CTL. *J Virol 70:7569.*

12. Yewdell, J. W., and J. R. Bennink. 1999. Immunodominance in major histocompatibility complex class I-restricted T lymphocyte responses. *Annu Rev Immunol 17:51*.

13. Callan, M. F., N. Annels, N. Steven, L. Tan, J. Wilson, A. J. McMichael, and A. B. Rickinson. 1998. T cell selection during the evolution of CD8+ T cell memory in vivo. *Eur J Immunol 28:4382*.

14. Ibisch, C., X. Saulquin, G. Gallot, R. Vivien, C. Ferrand, P. Tiberghien, E. Houssaint, and H. Vie. 2000. The T cell repertoire selected in vitro against EBV: diversity, specificity, and improved purification through early IL-2 receptor alpha-chain (CD25)-positive selection. *J Immunol 164:4924*.

15. Kalams, S. A., R. P. Johnson, A. K. Trocha, M. J. Dynan, H. S. Ngo, R. T. D'Aquila, J. T. Kurnick, and B. D. Walker. 1994. Longitudinal analysis of T cell receptor (TCR) gene usage by human immunodeficiency virus 1 envelope-specific cytotoxic T lymphocyte clones reveals a limited TCR repertoire. *J Exp Med 179:1261*.

16. Maini, M. K., G. Casorati, P. Dellabona, A. Wack, and P. C. Beverley. 1999. T-cell clonality in immune responses. *Immunol Today 20:262*.

17. Naumov, Y. N., K. T. Hogan, E. N. Naumova, J. T. Pagel, and J. Gorski. 1998. A class I MHC-restricted recall response to a viral peptide is highly polyclonal despite stringent CDR3 selection: implications for establishing memory T cell repertoires in "real-world" conditions. *J Immunol 160:2842*.

18. Betts, M. R., J. P. Casazza, B. A. Patterson, S. Waldrop, W. Trigona, T. M. Fu, F. Kern, L. J. Picker, and R. A. Koup. 2000. Putative

immunodominant human immunodeficiency virus-specific CD8(+) T-cell responses cannot be predicted by major histocompatibility complex class I haplotype. *J Virol 74:9144.*

19. Naumov, Y. N., E. N. Naumova, K. T. Hogan, L. K. Selin, and J. Gorski. 2003. A fractal clonotype distribution in the CD8+ memory T cell repertoire could optimize potential for immune responses. *J Immunol 170:3994.*

20. Pewe, L., S. B. Heard, C. Bergmann, M. O. Dailey, and S. Perlman. 1999. Selection of CTL escape mutants in mice infected with a neurotropic coronavirus: quantitative estimate of TCR diversity in the infected central nervous system. *J Immunol 163:6106.*

21. Maryanski, J. L., C. V. Jongeneel, P. Bucher, J. L. Casanova, and P. R. Walker. 1996. Single-cell PCR analysis of TCR repertoires selected by antigen in vivo: a high magnitude CD8 response is comprised of very few clones. *Immunity 4:47.*

22. McHeyzer-Williams, M. G., and M. M. Davis. 1995. Antigen-specific development of primary and memory T cells in vivo. *Science 268:106.*

23. Levitsky, V., P. O. de Campos-Lima, T. Frisan, and M. G. Masucci. 1998. The clonal composition of a peptide-specific oligoclonal CTL repertoire selected in response to persistent EBV infection is stable over time. *J Immunol 161:594.*

24. Annels, N. E., M. F. Callan, L. Tan, and A. B. Rickinson. 2000. Changing patterns of dominant TCR usage with maturation of an EBV-specific cytotoxic T cell response. *J Immunol 165:4831.*

25. Peggs, K., S. Verfuerth, A. Pizzey, J. Ainsworth, P. Moss, and S. Mackinnon. 2002. Characterization of human cytomegalovirus peptide-specific CD8(+) T-cell repertoire diversity following in vitro restimulation by antigen-pulsed dendritic cells. *Blood 99:213.*

26. Ploegh, H. L. 1998. Viral strategies of immune evasion. *Science 280:248.*

27. Welsh, R. M., L. K. Selin, and E. Szomolanyi-Tsuda. 2004. Immunological Memory to Viral Infections1. *Annu Rev Immunol 22:711.*

28. Picker, L. J., and M. H. Siegelman. 1998. Lymphoid tissues and organs. In *Fundamental Immunology.* Lippincott-Raven, Philadelphia, p. 479.

29. Sprent, J., and C. D. Surh. 2002. T cell memory. *Annu Rev Immunol 20:551.*

30. Campbell, J. J., K. E. Murphy, E. J. Kunkel, C. E. Brightling, D. Soler, Z. Shen, J. Boisvert, H. B. Greenberg, M. A. Vierra, S. B. Goodman, M. C. Genovese, A. J. Wardlaw, E. C. Butcher, and L. Wu. 2001. CCR7 expression and memory T cell diversity in humans. *J Immunol 166:877.*

31. Unsoeld, H., S. Krautwald, D. Voehringer, U. Kunzendorf, and H. Pircher. 2002. Cutting edge: CCR7+ and CCR7- memory T cells do not differ in immediate effector cell function. *J Immunol 169:638.*

32. Reinhardt, R. L., A. Khoruts, R. Merica, T. Zell, and M. K. Jenkins. 2001. Visualizing the generation of memory CD4 T cells in the whole body. *Nature 410:101*.

33. Blander, J. M., D. B. Sant'Angelo, D. Metz, S. W. Kim, R. A. Flavell, K. Bottomly, and C. A. Janeway, Jr. 2003. A pool of central memory-like CD4 T cells contains effector memory precursors. *J Immunol 170:2940*.

34. Seder, R. A., and R. Ahmed. 2003. Similarities and differences in CD4+ and CD8+ effector and memory T cell generation. *Nat Immunol 4:835*.

35. Grossman, Z., and W. E. Paul. 1992. Adaptive cellular interactions in the immune system: the tunable activation threshold and the significance of subthreshold responses. *Proc Natl Acad Sci U S A 89:10365*.

36. Grossman, Z., and A. Singer. 1996. Tuning of activation thresholds explains flexibility in the selection and development of T cells in the thymus. *Proc Natl Acad Sci U S A 93:14747*.

37. Schluns, K. S., and L. Lefrancois. 2003. Cytokine control of memory T-cell development and survival. *Nat Rev Immunol 3:269*.

38. Northrop, J. K., and H. Shen. 2004. CD8+ T-cell memory: only the good ones last. *Curr Opin Immunol 16:451*.

39. Harari, A., F. Vallelian, and G. Pantaleo. 2004. Phenotypic heterogeneity of antigen-specific CD4 T cells under different conditions of antigen persistence and antigen load. *Eur J Immunol*.

40. Murali-Krishna, K., L. L. Lau, S. Sambhara, F. Lemonnier, J. Altman, and R. Ahmed. 1999. Persistence of memory CD8 T cells in MHC class I-deficient mice. *Science 286:1377*.

41. Swain, S. L., H. Hu, and G. Huston. 1999. Class II-independent generation of CD4 memory T cells from effectors. *Science 286:1381*.

42. Seddon, B., P. Tomlinson, and R. Zamoyska. 2003. Interleukin 7 and T cell receptor signals regulate homeostasis of CD4 memory cells. *Nat Immunol 4:680*.

43. Grossman, Z., B. Min, M. Meier-Schellersheim, and W. E. Paul. 2004. Concomitant regulation of T-cell activation and homeostasis. *Nat Rev Immunol 4:387*.

44. Scherer, A., A. Noest, and R. J. de Boer. 2004. Activation-threshold tuning in an affinity model for the T-cell repertoire. *Proc R Soc Lond B Biol Sci 271:609*.

45. Waldrop, S. L., K. A. Davis, V. C. Maino, and L. J. Picker. 1998. Normal human CD4+ memory T cells display broad heterogeneity in their activation threshold for cytokine synthesis. *J Immunol 161:5284*.

46. Murphy, L. L., M. M. Mazanet, A. C. Taylor, J. Mestas, and C. C. Hughes. 1999. Single-cell analysis of costimulation by B cells, endothelial cells, and fibroblasts demonstrates heterogeneity in responses of CD4(+) memory T cells. *Cell Immunol 194:150*.

47. Hahn, G., R. Jores, and E. S. Mocarski. 1998. Cytomegalovirus remains latent in a common precursor of dendritic and myeloid cells. *Proc Natl Acad Sci U S A 95:3937.*

48. Toro, A. I., and J. Ossa. 1996. PCR activity of CMV in healthy CMV-seropositive individuals: does latency need redefinition? *Res Virol 147:233.*

49. Stinski, M. F. 1990. Cytomegalovirus and its replication. In *Fields Virology*, Vol. 2. B. N. Fields, Knipe, D.M., Chanok, R.M., Hirsch, M.S., Melnick, J.L., Monath, T.P., and Roziman, B., ed. Raven Press, New York, p. 1959.

50. Alford, C. A. a. B., W.J. 1990. CytomegaLovirus. In *Fields Virology*, Vol. 2. B. N. Fields, Knipe, D.M., Chanok, R.M., Hirsch, M.S., Melnick, J.L., Monath, T.P., and Roziman, B., ed. Raven Press, New York, p. 1981.

51. Riddell, S. R. 1995. Pathogenesis of cytomegalovirus pneumonia in immunocompromised hosts. *Semin Respir Infect 10:199.*

52. Lockridge, K. M., G. Sequar, S. S. Zhou, Y. Yue, C. P. Mandell, and P. A. Barry. 1999. Pathogenesis of experimental rhesus cytomegalovirus infection. *J Virol 73:9576.*

53. Kaur, A., N. Kassis, C. L. Hale, M. Simon, M. Elliott, A. Gomez-Yafal, J. D. Lifson, R. C. Desrosiers, F. Wang, P. Barry, M. Mach, and R. P. Johnson. 2003. Direct relationship between suppression of virus-specific

immunity and emergence of cytomegalovirus disease in simian AIDS. *J Virol 77:5749.*

54. Hansen, S. G., L. I. Strelow, D. C. Franchi, D. G. Anders, and S. W. Wong. 2003. Complete sequence and genomic analysis of rhesus cytomegalovirus. *J Virol 77:6620.*

55. Mettenleiter, T. C. 2002. Herpesvirus assembly and egress. *J Virol 76:1537.*

56. Sester, M., U. Sester, B. Gartner, B. Kubuschok, M. Girndt, A. Meyerhans, and H. Kohler. 2002. Sustained high frequencies of specific CD4 T cells restricted to a single persistent virus. *J Virol 76:3748.*

57. Waldrop, S. L., C. J. Pitcher, D. M. Peterson, V. C. Maino, and L. J. Picker. 1997. Determination of antigen-specific memory/effector CD4+ T cell frequencies by flow cytometry: evidence for a novel, antigen-specific homeostatic mechanism in HIV-associated immunodeficiency. *J Clin Invest 99:1739.*

58. Pitcher, C. J., C. Quittner, D. M. Peterson, M. Connors, R. A. Koup, V. C. Maino, and L. J. Picker. 1999. HIV-1-specific CD4+ T cells are detectable in most individuals with active HIV-1 infection, but decline with prolonged viral suppression [see comments]. *Nat Med 5:518.*

59. Komanduri, K. V., M. N. Viswanathan, E. D. Wieder, D. K. Schmidt, B. M. Bredt, M. A. Jacobson, and J. M. McCune. 1998. Restoration of

cytomegalovirus-specific CD4+ T-lymphocyte responses after ganciclovir and highly active antiretroviral therapy in individuals infected with HIV-1. *Nat Med 4:953*.

60. Tyler, K. L. a. F., B.N. 1990. Fields Virology, Vol. 1. B. N. Fields, Knipe, D.M., Chanok, R.M., Hirsch, M.S., Melnick, J.L., Monath, T.P., and Roziman, B., ed. Raven Press, New York, p. 193.

61. Selin, L. K., and R. M. Welsh. 2004. Plasticity of T cell memory responses to viruses. *Immunity 20:5*.

62. Paul, W. 1998. *Fundamental Immunology*. Lippincott-Raven, Philadelphia.

63. Whitmire, J. K., and R. Ahmed. 2000. Costimulation in antiviral immunity: differential requirements for CD4(+) and CD8(+) T cell responses. *Curr Opin Immunol 12:448*.

64. Welsh, R. M., and J. M. McNally. 1999. Immune deficiency, immune silencing, and clonal exhaustion of T cell responses during viral infections. *Curr Opin Microbiol 2:382*.

65. Refaeli, Y., L. Van Parijs, S. I. Alexander, and A. K. Abbas. 2002. Interferon gamma is required for activation-induced death of T lymphocytes. *J Exp Med 196:999*.

66. Sprent, J., and J. F. Miller. 1976. Fate of H2-activated T lymphocytes in syngeneic hosts. II. Residence in recirculating lymphocyte pool and capacity to migrate to allografts. *Cell Immunol 21:303*.

67. Sprent, J., and J. F. Miller. 1976. Fate of H2-activated T lymphocytes in syngeneic hosts. III. Differentiation into long-lived recirculating memory cells. *Cell Immunol 21:314*.

68. Sprent, J. 1976. Fate of H2-activated T lymphocytes in syngeneic hosts. I. Fate in lymphoid tissues and intestines traced with 3H-thymidine, 125I-deoxyuridine and 51chromium. *Cell Immunol 21:278*.

69. Varga, S. M., L. K. Selin, and R. M. Welsh. 2001. Independent regulation of lymphocytic choriomeningitis virus-specific T cell memory pools: relative stability of CD4 memory under conditions of CD8 memory T cell loss. *J Immunol 166:1554*.

70. Hammarlund, E., M. W. Lewis, S. G. Hansen, L. I. Strelow, J. A. Nelson, G. J. Sexton, J. M. Hanifin, and M. K. Slifka. 2003. Duration of antiviral immunity after smallpox vaccination. *Nat Med 9:1131*.

71. Ramsay, A. J., J. Ruby, and I. A. Ramshaw. 1993. A case for cytokines as effector molecules in the resolution of virus infection. *Immunol Today 14:155*.

72. Ahmed, R. a. B., C.A. 1998. Immunity to viruses. In *Fundamental Immunology*. Lippincott-Raven, Philadelphia, p. 1295.

73. Kalams, S. A., and B. D. Walker. 1998. The critical need for CD4 help in maintaining effective cytotoxic T lymphocyte responses [comment]. *J Exp Med 188:2199.*

74. Maloy, K. J., C. Burkhart, G. Freer, T. Rulicke, H. Pircher, D. H. Kono, A. N. Theofilopoulos, B. Ludewig, U. Hoffmann-Rohrer, R. M. Zinkernagel, and H. Hengartner. 1999. Qualitative and quantitative requirements for CD4+ T cell-mediated antiviral protection. *J Immunol 162:2867.*

75. Matloubian, M., R. J. Concepcion, and R. Ahmed. 1994. CD4+ T cells are required to sustain CD8+ cytotoxic T-cell responses during chronic viral infection. *J Virol 68:8056.*

76. Zajac, A. J., J. N. Blattman, K. Murali-Krishna, D. J. Sourdive, M. Suresh, J. D. Altman, and R. Ahmed. 1998. Viral immune evasion due to persistence of activated T cells without effector function [see comments]. *J Exp Med 188:2205.*

77. Muller, D., B. H. Koller, J. L. Whitton, K. E. LaPan, K. K. Brigman, and J. A. Frelinger. 1992. LCMV-specific, class II-restricted cytotoxic T cells in beta 2-microglobulin-deficient mice. *Science 255:1576.*

78. Williams, N. S., and V. H. Engelhard. 1996. Identification of a population of CD4+ CTL that utilizes a perforin- rather than a Fas ligand-dependent cytotoxic mechanism. *J Immunol 156:153.*

79. Jonjic, S., W. Mutter, F. Weiland, M. J. Reddehase, and U. H. Koszinowski. 1989. Site-restricted persistent cytomegalovirus infection after selective long-term depletion of CD4+ T lymphocytes. *J Exp Med 169:1199.*

80. Jonjic, S., I. Pavic, B. Polic, I. Crnkovic, P. Lucin, and U. H. Koszinowski. 1994. Antibodies are not essential for the resolution of primary cytomegalovirus infection but limit dissemination of recurrent virus. *J Exp Med 179:1713.*

81. MacGregor, R. R., S. J. Pakola, A. L. Graziani, D. P. Montzka, R. L. Hodinka, C. W. Nichols, and H. M. Friedman. 1995. Evidence of active cytomegalovirus infection in clinically stable HIV-infected individuals with CD4+ lymphocyte counts below 100/microliters of blood: features and relation to risk of subsequent CMV retinitis. *J Acquir Immune Defic Syndr Hum Retrovirol 10:324.*

82. Spector, S. A., G. F. McKinley, J. P. Lalezari, T. Samo, R. Andruczk, S. Follansbee, P. D. Sparti, D. V. Havlir, G. Simpson, W. Buhles, R. Wong, and M. Stempien. 1996. Oral ganciclovir for the prevention of cytomegalovirus disease in persons with AIDS. Roche Cooperative Oral Ganciclovir Study Group. *N Engl J Med 334:1491.*

83. Riddell, S. R., K. S. Watanabe, J. M. Goodrich, C. R. Li, M. E. Agha, and P. D. Greenberg. 1992. Restoration of viral immunity in immunodeficient humans by the adoptive transfer of T cell clones. *Science 257:238.*

84. Walter, E. A., P. D. Greenberg, M. J. Gilbert, R. J. Finch, K. S. Watanabe, E. D. Thomas, and S. R. Riddell. 1995. Reconstitution of cellular immunity against cytomegalovirus in recipients of allogeneic bone marrow by transfer of T-cell clones from the donor. *N Engl J Med 333:1038.*

85. Einsele, H., E. Roosnek, N. Rufer, C. Sinzger, S. Riegler, J. Loffler, U. Grigoleit, A. Moris, H. G. Rammensee, L. Kanz, A. Kleihauer, F. Frank, G. Jahn, and H. Hebart. 2002. Infusion of cytomegalovirus (CMV)-specific T cells for the treatment of CMV infection not responding to antiviral chemotherapy. *Blood 99:3916.*

86. McGeoch, D. J., S. Cook, A. Dolan, F. E. Jamieson, and E. A. Telford. 1995. Molecular phylogeny and evolutionary timescale for the family of mammalian herpesviruses. *J Mol Biol 247:443.*

87. Murphey-Corb, M., L. N. Martin, S. R. Rangan, G. B. Baskin, B. J. Gormus, R. H. Wolf, W. A. Andes, M. West, and R. C. Montelaro. 1986. Isolation of an HTLV-III-related retrovirus from macaques with simian AIDS and its possible origin in asymptomatic mangabeys. *Nature 321:435.*

88. Baskin, G. B. 1987. Disseminated cytomegalovirus infection in immunodeficient rhesus monkeys. *Am J Pathol 129:345*.

89. Kuhn, E. M., N. Stolte, K. Matz-Rensing, M. Mach, C. Stahl-Henning, G. Hunsmann, and F. J. Kaup. 1999. Immunohistochemical studies of productive rhesus cytomegalovirus infection in rhesus monkeys (Macaca mulatta) infected with simian immunodeficiency virus. *Vet Pathol 36:51*.

90. Pitcher, C. J., S. I. Hagen, J. M. Walker, R. Lum, B. L. Mitchell, V. C. Maino, M. K. Axthelm, and L. J. Picker. 2002. Development and homeostasis of T cell memory in rhesus macaque. *J Immunol 168:29*.

91. Manfras, B. J., W. A. Rudert, M. Trucco, and B. O. Boehm. 1997. Analysis of the alpha/beta T-cell receptor repertoire by competitive and quantitative family-specific PCR with exogenous standards and high resolution fluorescence based CDR3 size imaging. *J Immunol Methods 210:235*.

92. Chen, Z. W., Z. C. Kou, L. Shen, K. A. Reimann, and N. L. Letvin. 1993. Conserved T-cell receptor repertoire in simian immunodeficiency virus-infected rhesus monkeys. *J Immunol 151:2177*.

93. LeMaoult, J., I. Messaoudi, J. S. Manavalan, H. Potvin, D. Nikolich-Zugich, R. Dyall, P. Szabo, M. E. Weksler, and J. Nikolich-Zugich. 2000. Age-related dysregulation in CD8 T cell homeostasis: kinetics of a diversity loss. *J Immunol 165:2367*.

94. Douek, D. C., M. R. Betts, J. M. Brenchley, B. J. Hill, D. R. Ambrozak, K. L. Ngai, N. J. Karandikar, J. P. Casazza, and R. A. Koup. 2002. A novel approach to the analysis of specificity, clonality, and frequency of HIV-specific T cell responses reveals a potential mechanism for control of viral escape. *J Immunol 168:3099.*

95. Lin, M. Y., L. K. Selin, and R. M. Welsh. 2000. Evolution of the CD8 T-cell repertoire during infections. *Microbes Infect 2:1025.*

96. Chen, Z. W., Y. Li, X. Zeng, M. J. Kuroda, J. E. Schmitz, Y. Shen, X. Lai, L. Shen, and N. L. Letvin. 2001. The TCR repertoire of an immunodominant CD8+ T lymphocyte population. *J Immunol 166:4525.*

97. Sourdive, D. J., K. Murali-Krishna, J. D. Altman, A. J. Zajac, J. K. Whitmire, C. Pannetier, P. Kourilsky, B. Evavold, A. Sette, and R. Ahmed. 1998. Conserved T cell receptor repertoire in primary and memory CD8 T cell responses to an acute viral infection. *J Exp Med 188:71.*

98. Picker, L. J., M. K. Singh, Z. Zdraveski, J. R. Treer, S. L. Waldrop, P. R. Bergstresser, and V. C. Maino. 1995. Direct demonstration of cytokine synthesis heterogeneity among human memory/effector T cells by flow cytometry. *Blood 86:1408.*

99. Klimecki, W. T., B. W. Futscher, and W. S. Dalton. 1994. Effects of ethanol and paraformaldehyde on RNA yield and quality. *Biotechniques 16:1021.*

100. Bitmansour, A. D., S. L. Waldrop, C. J. Pitcher, E. Khatamzas, F. Kern, V. C. Maino, and L. J. Picker. 2001. Clonotypic structure of the human CD4+ memory T cell response to cytomegalovirus. *J Immunol 167:1151.*

101. Lanzavecchia, A., and F. Sallusto. 2000. Dynamics of T lymphocyte responses: intermediates, effectors, and memory cells. *Science 290:92.*

102. Sallusto, F., D. Lenig, R. Forster, M. Lipp, and A. Lanzavecchia. 1999. Two subsets of memory T lymphocytes with distinct homing potentials and effector functions [see comments]. *Nature 401:708.*

103. Iezzi, G., D. Scheidegger, and A. Lanzavecchia. 2001. Migration and function of antigen-primed nonpolarized T lymphocytes in vivo. *J Exp Med 193:987.*

104. Chen, H. D., A. E. Fraire, I. Joris, M. A. Brehm, R. M. Welsh, and L. K. Selin. 2001. Memory CD8+ T cells in heterologous antiviral immunity and immunopathology in the lung. *Nat Immunol 2:1067.*

105. Liu, F., J. L. Whitton, and M. K. Slifka. 2004. The rapidity with which virus-specific CD8+ T cells initiate IFN-gamma synthesis increases markedly over the course of infection and correlates with immunodominance. *J Immunol 173:456.*

106. Selin, L. K., and R. M. Welsh. 1997. Cytolytically active memory CTL present in lymphocytic choriomeningitis virus-immune mice after clearance of virus infection. *J Immunol 158:5366*.

107. Gamadia, L. E., E. B. Remmerswaal, J. F. Weel, F. Bemelman, R. A. van Lier, and I. J. Ten Berge. 2003. Primary immune responses to human CMV: a critical role for IFN-gamma-producing CD4+ T cells in protection against CMV disease. *Blood 101:2686.*

108. Gamadia, L. E., R. J. Rentenaar, R. A. Van Lier, and I. J. Ten Berge. 2004. Properties of CD4(+) T cells in human cytomegalovirus infection. *Hum Immunol 65:486.*

109. Harari, A., S. C. Zimmerli, and G. Pantaleo. 2004. Cytomegalovirus (CMV)-Specific cellular immune responses. *Hum Immunol 65:500.*

110. Blattman, J. N., D. J. Sourdive, K. Murali-Krishna, R. Ahmed, and J. D. Altman. 2000. Evolution of the T cell repertoire during primary, memory, and recall responses to viral infection. *J Immunol 165:6081.*

111. Turner, S. J., G. Diaz, R. Cross, and P. C. Doherty. 2003. Analysis of clonotype distribution and persistence for an influenza virus-specific CD8+ T cell response. *Immunity 18:549.*

112. McHeyzer-Williams, L. J., J. F. Panus, J. A. Mikszta, and M. G. McHeyzer-Williams. 1999. Evolution of antigen-specific T cell receptors in vivo: preimmune and antigen-driven selection of preferred

complementarity-determining region 3 (CDR3) motifs. *J Exp Med 189:1823*.

113. Cose, S. C., J. M. Kelly, and F. R. Carbone. 1995. Characterization of diverse primary herpes simplex virus type 1 gB-specific cytotoxic T-cell response showing a preferential V beta bias. *J Virol 69:5849*.

114. Lin, M. Y., and R. M. Welsh. 1998. Stability and diversity of T cell receptor repertoire usage during lymphocytic choriomeningitis virus infection of mice. *J Exp Med 188:1993*.

115. Kedzierska, K., S. J. Turner, and P. C. Doherty. 2004. Conserved T cell receptor usage in primary and recall responses to an immunodominant influenza virus nucleoprotein epitope. *Proc Natl Acad Sci U S A 101:4942*.

116. Khan, N., N. Shariff, M. Cobbold, R. Bruton, J. A. Ainsworth, A. J. Sinclair, L. Nayak, and P. A. Moss. 2002. Cytomegalovirus seropositivity drives the CD8 T cell repertoire toward greater clonality in healthy elderly individuals. *J Immunol 169:1984*.

117. Gunzer, M., A. Schafer, S. Borgmann, S. Grabbe, K. S. Zanker, E. B. Brocker, E. Kampgen, and P. Friedl. 2000. Antigen presentation in extracellular matrix: interactions of T cells with dendritic cells are dynamic, short lived, and sequential. *Immunity 13:323*.

118. Lanzavecchia, A., and F. Sallusto. 2001. Regulation of T cell immunity by dendritic cells. *Cell 106:263*.

119. Itoh, Y., and R. N. Germain. 1997. Single cell analysis reveals regulated hierarchical T cell antigen receptor signaling thresholds and intraclonal heterogeneity for individual cytokine responses of CD4+ T cells. *J Exp Med 186:757.*

VITAE

Arlene Diana Bitmansour was born in Tehran, Iran (with an Assyrian heritage) on September 19, 1967 to Elda Sargon and William Bitmansour. She has one sibling, Andrew Bitmansour. After graduating from Blackford High School, she attended San Jose State University, where she received a Bachelor of Science degree in General Biology with a Minor in Chemistry in 1993. She then completed a Master of Science degree in Biological Sciences in 1997. She was admitted to the Graduate School of Biomedical Sciences at the University of Texas Southwestern Medical Center at Dallas in August 1997 and entered the laboratory of Dr. Louis J. Picker in January 1998.

Permanent address: 27 Chicory Lane
San Carlos, CA 94070